ปฏิสัมพันธ์ระหว่างดินและโครงสร้างโบราณสถานจังหวัดเชียงใหม่ภายใต้สภาวะการกระทำของแรงแผ่นดินไหว

นาย รณนภา พจนา

# SOIL-STRUCTURE INTERACTION OF ANCIENT MASONRY STRUCTURE IN CHIANGMAI
## UNDER SEISMIC EXCITATION

Mr. Ronnapa Photchana

A Dissertation Submitted in Partial Fulfillment of the Requirements

for the Degree of Doctor of Philosophy Program in Civil Engineering

Department of Civil Engineering

Faculty of Engineering Chulalongkorn University
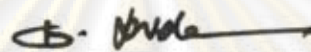
Academic year 2007

501298

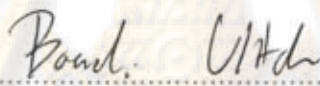| Thesis Title | SOIL-STRUCTURE INTERACTION OF ANCIENT MASONRY STRUCTURE IN CHIANGMAI UNDER SEISMIC EXCITATION |
| By | Mr. Ronnapa Photchana |
| Filed of study | Civil Engineering |
| Thesis Advisor | Associate Professor Supot Teachavorasinskun, D.Eng. |

Accepted by the Faculty of Engineering, Chulalongkorn University in Partial Fulfillment of the Requirements for the Doctor's Degree
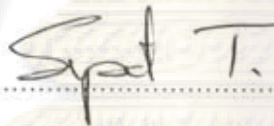
.................................................... Dean of Faculty of Engineering

(Associate Professor Boonsom Lerdhirunwong, Dr.Ing.)
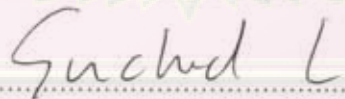
THESIS COMMITTEE

.................................................... Chairman

(Associate Professor Boonchai Ukritchon, Sc.D.)

.................................................... Thesis Advisor

(Associate Professor Supot Teachavorasinskun, D.Eng.)

.................................................... Member

(Assistant Professor Suched Likitlersuang, D.Phil.)

.................................................... Member

(Assistant Professor Siam Yimsiri, Ph.D.)

.................................................... Member

( Pipat Thongchim, Ph.D.)

นาย รณนภา พจนา : ปฏิสัมพันธ์ระหว่างดินและโครงสร้างโบราณสถานจังหวัดเชียงใหม่ภายใต้
สภาวะการกระทำของแรงแผ่นดินไหว. (SOIL-STRUCTURE INTERACTION OF ANCIENT
MASONRY STRUCTURE IN CHIANGMAI UNDER SEISMIC EXCITATION) อ. ที่ปรึกษา:
รศ.ดร. สุพจน์ เตชวรสินสกุล, จำนวนหน้า 123 หน้า.

นักวิจัยหลายท่านได้ค้นคว้าและวิจัยวิธีการคำนวณปฏิสัมพันธ์ระหว่างดินกับโครงสร้างภายใต้แรง
กระทำจากแผ่นดินไหว การหาผลเฉลยที่ถูกต้องใกล้เคียงในการตอบสนองแต่ละกรณี ปัจจัยสำคัญขึ้นอยู่
กับคุณสมบัติทางพลศาสตร์ของดินที่ทำการวิจัย ได้แก่ค่าโมดูลัสเฉือนและอัตราส่วนการกระจายตัว
พลังงานของดิน ซึ่งการหาคุณสมบัติของดินทางพลศาสตร์นั้นสามารถหาได้จากการทดสอบภาคสนาม
และการทดสอบในห้องปฏิบัติการ

เจดีย์หลวงตั้งอยู่ในจังหวัดเชียงใหม่ทางภาคเหนือของประเทศไทยซึ่งอยู่ในบริเวณที่มีความเสี่ยง
ของการเกิดแผ่นดินไหว โครงสร้างหลักของเจดีย์ทำจากอิฐที่มีอายุหลายร้อยปี วัตถุประสงค์หลักของ
งานวิจัยนี้คือการประเมินความสามารถในการต้านทานรับแรงแผ่นดินไหวของโครงสร้างเจดีย์หลวงซึ่งถูก
แรงกระทำจากแผ่นดินไหวในอดีตทำให้โครงสร้างบางส่วนได้รับความเสียหาย โดยคำนึงถึงปฏิกิริยาของ
ดินต่อโครงสร้างนี้ วิธีไฟไนต์อิลิเมนต์ได้ถูกนำมาใช้ในการวิเคราะห์ทางพลศาสตร์ของโครงสร้างนี้ ข้อมูล
ต่างๆที่ใช้เช่น อัตราส่วนปัวซง ความสามารถในการรับแรงอัดและแรงดึงของอิฐที่นำมาสร้างเจดีย์ โมดูลัส
เฉือนและความเร็วคลื่นเฉือนมาจากผลการทดลองในห้องปฏิบัติการและผลการทดลองภาคสนาม
ความสัมพันธ์ระหว่างความเร่งกับเวลา และความเค้นของโครงสร้างที่จุดต่างๆได้ถูกวิเคราะห์

จากการวิเคราะห์พบว่าโครงสร้างของเจดีย์ที่ทำจากอิฐนี้มีความสามารถเพียงพอในการรับแรงอัด
ขณะที่ความสามารถในการรับแรงดึงนั้นไม่เพียงพอในบางส่วนของโครงสร้าง ซึ่งเป็นบริเวณที่ควรจะต้อง
เสริมความแข็งแรงในการซ่อมแซมครั้งต่อไป

ภาควิชา ..........วิศวกรรมโยธา.......... ลายมือชื่อนิสิต...........Ronnapa P.

สาขาวิชา ..........วิศวกรรมโยธา.......... ลายมือชื่ออาจารย์ที่ปรึกษา...........

ปีการศึกษา 2550

# # 4871841021    : MAJOR  CIVIL ENGINEERING

KEY WORD:  SEISMIC / SOIL-STRUCTURE INTERACTION / MASONRY / FAULT

RONNAPA  PHOTCHANA:  SOIL-STRUCTURE  INTERACTION  OF  ANCIENT  MASONRY STRUCTURE IN CHIANGMAI UNDER SEISMIC EXCITATION.  THESIS ADVISOR: ASSOC. PROF. SUPOT TEACHAVORASINSKUN, D.Eng., 123 pp.

There are several researchers developed the analytical procedures for evaluating the response of soil-structure interaction under seismic loading. To obtain the good result for determining ground response in specific cases, it is essentially dependent on the correct representative soil properties in the analysis. Consideration effort has also been directed toward the determination of soil properties for use in these analytical procedures. The response is determined mainly by shear modulus and damping characteristics of soil.

Chediluang (Pagoda), located in Chiangmai province in the northern part of Thailand. The structure made from ancient masonry in several hundred years ago. The main purpose of the research is to investigate the seismic resistance capacity of the Chediluang, which was partly torn down by past earthquake with the soil-structure interaction under seismic excitation. The finite element method is used for dynamic analysis. The input parameters such as Poisson's ratio, compressive and tensile strength, shear modulus and shear wave velocity are selected from the report and in-situ testing. The stress of the structure under dynamic condition is considered. In addition, the time-history of acceleration plots and stress contour used for determining the weak zones of the structure are also reported for further restoration solutions.

From the analysis, the structure is able to resist the compressive stress but some part of the structure is unable to resist the tensile stress. Some reinforcement is required for next restoration.

| | | |
|---|---|---|
| Department.........Civil Engineering.......... | Student's signature..... | Ronnapa P. |
| Field of study........Civil Engineering........... | Advisor's signature...... | |
| Academic year...........2007....... | | |

# ACKNOWLEDGMENTS

A number of individuals and organizations contributed greatly to this study by providing structural and geotechnical data for the sites which were considered. They are far too numerous to completely acknowledge here, however, I would like to express my sincere appreciation to Assoc. Prof. Supot Teachavorasinskun, D. Eng., who is my thesis advisor and Asst. Prof. Anat Ruangratsamee, D. Eng., for valuable suggestion concern this study.

Next, I would like to thank all of my family members who have continuous supported during my study in graduate school.

The gathering of strong motion data for this study would not have been possible without the help of Mr.Pulpong P., Lecturer at Kasetsart University. Gratefully acknowledged are also extended to Mr.Burin Vechbantheng at the Department of Meteorological for providing access to seismograph digitization data.

Gratefully acknowledge the support and encouragement received from our colleagues and all members at Earthquake Engineering Research Center at Chulalongkorn University in the processing of seismic data.

ศูนย์วิทยทรัพยากร

จุฬาลงกรณ์มหาวิทยาลัย

# TABLE OF CONTENTS

# LIST OF TABLE

LIST OF FIGURE

FIGURE

# LIST OF ABBREVIATION

| | | |
|---|---|---|
| $M_s$ | = | Surface Wave Magnitude |
| $M_w$ | = | Moment Magnitude |
| $S$ | = | Standard Error |
| $L$ | = | Length |
| $A$ | = | Area of the Fault Rupture |
| $D$ | = | Maximum Surface Displacement |
| $\upsilon$ | = | Number of Degree of Freedom |
| $\delta$ | = | Dip Angle |
| $W$ | = | Fault Width |
| $\phi$ | = | Strike Angle |
| $E$ | = | Compressive Modulus |
| $E_u$ | = | Undrained Modulus |
| $V_s$ | = | S-Wave Velocity |
| $V_p$ | = | P-Wave Velocity |
| $\rho$ | = | Density |
| $G$ | = | Shear Modulus |
| $\sigma_m'$ | = | Mean Principle Effective Stress |
| $\sigma_v'$ | = | Effective Vertical Stress |
| $e$ | = | Void Ratio |
| $N$ | = | Number of Cycles of Loading |
| $S$ | = | Degree of Saturation for cohesive soil |
| $\gamma$ | = | Strain Amplitude |
| ASTM | | American Society for Testing and Material |

# CHAPTER I

## INTRODUCTION

### 1.1 Introduction

Earthquakes have been recognized as one of the most damaging natural hazard. Earthquakes typically strike without warning any after only a few seconds leave damage behind. Although earthquakes cannot be prevented, the current technology in science and engineering provides new tools that can be used to reduce their damaging effects. Many earthquake disasters have occurred during the present decade. An earthquake causes a disaster depends on

1. The magnitude of the event

2. The distance of the active fault from the city

3. The characteristics of soil profile.

If the earthquake is small magnitude will not sufficiently violent to cause extensive damage. If the large magnitude earthquake is distant far away from the city, the ground shaking will not be strong. If the city is well-prepared even the magnitude is large, those close distance will not cause disaster.

Seismic hazard in northern part of Thailand areas became a subject of detailed study during the last few decades. The northern part of Thailand located in an active region wherein several active faults have been detected. As the historical data prove, a large number of earthquakes have occurred in this area. The magnitudes of these earthquakes are normally less than 5 of the Richter scale. However, northern part of Thailand is likely to experience strong earthquake frequently in the future. Recent studies on active faults in this area indicate that earthquake with magnitude greater than 6 of the Richter scale might be possible occur. This study evaluates the seismic hazard of Thailand, especially on the basis of the latest earthquake record and geological active fault studies.

Wat Chediluang (1411 A.D.) is located in Chiangmai province of Thailand. This is one of the most important ancient temples in Chiangmai since. The main structure

systems made from brick and stone masonry. Chediluang (Grand pagoda) is the highest pagoda in Chiangmai. The foundation is in square shape with the 60x60 meters and height of 74 meters before it was partly destroyed by an earthquake in the past. It was to remain one of the tallest structures in Chiangmai. The present restored pagoda is approximately 40 meters height as shown in Figure1.
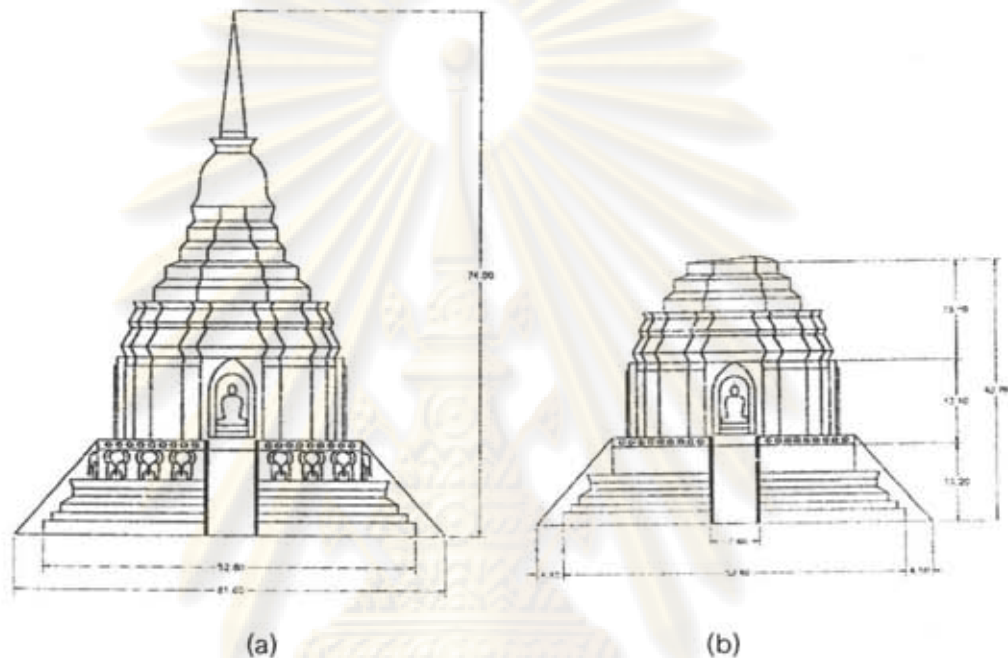


Figure 1 (a) Chediluang after completed the construction in 1411 AD. (b) Chediluang was partly destroyed in an earthquake in 1545 A.D.

Although the brick masonry is one of the oldest forms of structural material, the study of its behavior under earthquake load started late in comparison with other materials like concrete and steel. Masonry is a composite structural material which in its basic form consists of masonry units and mortar. Although masonry can carry substantial loads in compression, its load bearing capacity for tension and shear developed when subjected to seismic load is relatively low.

The dynamic behavior of masonry structures is too complicated to be interpreted by simple model. It is quite difficult to perform reliable quantitative strength evaluations due to the difficulty of gathering experimental data on the resistance of structural elements and even on the properties of the material on site. The analytical model of

temples needs to be validated by the real structural characteristics that are normally obtained from the lab tests. Also structural resistance decreases in time due to deterioration and aging effect is frequently accelerated by neglect or carelessness. The most appropriate method to investigate seismic effects on masonry structure would be the measurement of real structure response during earthquake or intensive artificial seismic excitation. As for many reasons this is difficult and time consuming, therefore, the seismic analysis was performed in FLUSH program. The real dynamic characteristics of the temples are also the most important issue to evaluate their seismic load capacity for future earthquakes.

The past strong earthquakes have already destroyed many ancient masonry structures. To determine the dynamic capacity of masonry structures from seismic excitation has become very important to protect these heritages from the possible earthquakes in the future.

## 1.2 Objectives of work

1. To investigate active faults in Northern Thailand and determine waveform of maximum credible earthquake magnitude based on existing data from previous faults studies.
2. To determine appropriate value of soil and material properties using in this analysis such as soil density, shear modulus, damping ratio etc.
3. To estimate dynamic capacity of masonry structure subjected to seismic excitation.

## 1.3 Scope of work

1. Maerim and Maetha fault's characteristics which are 23 and 38 kilometers away from Chiangmai city will be investigated base on existing geological data.
2. Maximum credible earthquake magnitude will be considered, based on previous studied, by empirical formulas.
3. Simulation of ground motion will be generated by stochastic method.
4. The behavior of masonry structure in various distances from the active faults will be considered to evaluate their seismic resistance using FLUSH program.

# CHAPTER II
## FAULTS INVESTIGATION AND WAVEFORM DETERMINATION

### 2.1 Faults Investigation

The seismic hazard at any given site obviously depends on the seismic activity of the region. Background information can be obtained from many sources. Regional seismic activity is seen to include source mechanism, distribution of sources, magnitudes, intensity of shaking, attenuation of intensity with distance and rates of activity.

As most earthquakes arise from stress build-up due to deformation of the earth's crust, understanding of seismic activity depends heavily on geological condition, which is the science of the earth's crust, and also calls upon knowledge of the physics of the earth as a whole, i.e. geophysics. Faults are usually the seat of damaging earthquakes. It is widely held that virtually all large earthquakes are caused by sudden displacements on faults at varying depths.

In some cases faults may reach the surface but are difficult to be recognized, and it may not be possible to identify as an active fault from surface traces prior to its next major movement. Apart from the presence of weak superficial deposits, other factors contribute to the difficulty of identifying faults, such as low degree of fault activity, thus creating less evidence and erosion and sediment deposition rates that are higher than the fault slip rates.

Some tectonic processes result in dispersed fault zones at the surfaces so that individual features are less pronounced. Fault zones vary in width from a few meters to as much as kilometer or more. It appears that the characteristics of strong ground motion in the general vicinity of the causative fault can be strongly influenced by the type of faulting. Housner suggests that four types of fault should be considered in the study of destructive earthquakes;

(1) Low-angle, compressive, underthrust faults: These result from tectonic sea-bed plates spreading apart and thrusting under the adjacent continental plates, a phenomenon common to much of the circum-Pacific earthquake belt;

(2) Compressive, overthrust faults: compressive forces cause shearing failure forcing the upper portion upwards, as occurred in San Fernando California, in 1971 (also called reverse faults);
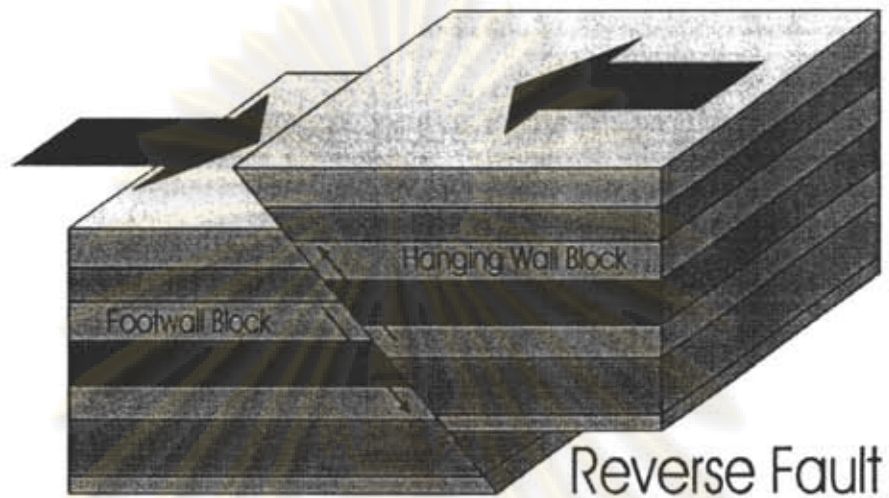


Reverse Fault

Figure 2 Reverse Fault

(3) Extensional faults: this is the inverse of the previous type, extensional strains pulling the upper block down the sloping fault plane (also called normal faults);
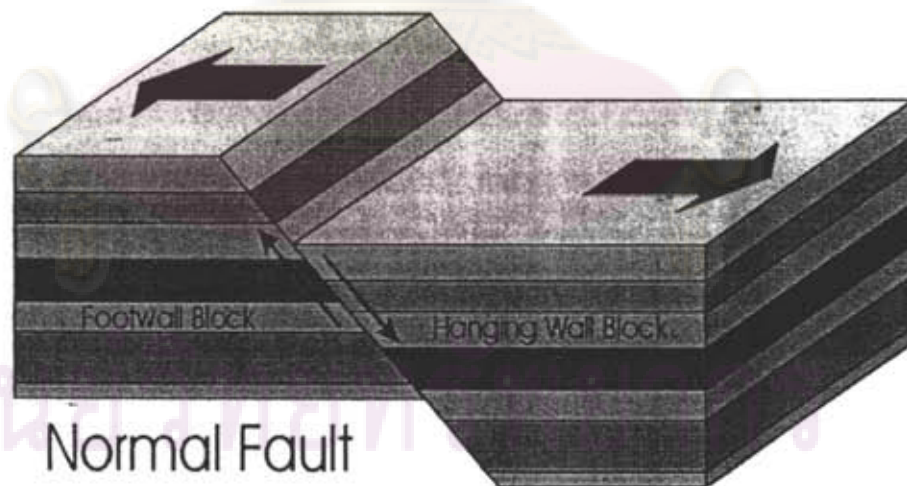


Normal Fault

Figure 3 Normal Fault

(4) Strike-slip faults: relative horizontal displacement of the two sides of the fault takes place along an essentially vertical fault plane, such as occurred at San Francisco in 1906 on the San Andreas fault (also called wrench or transcurrent faults).

Left Lateral Strike-Slip Fault
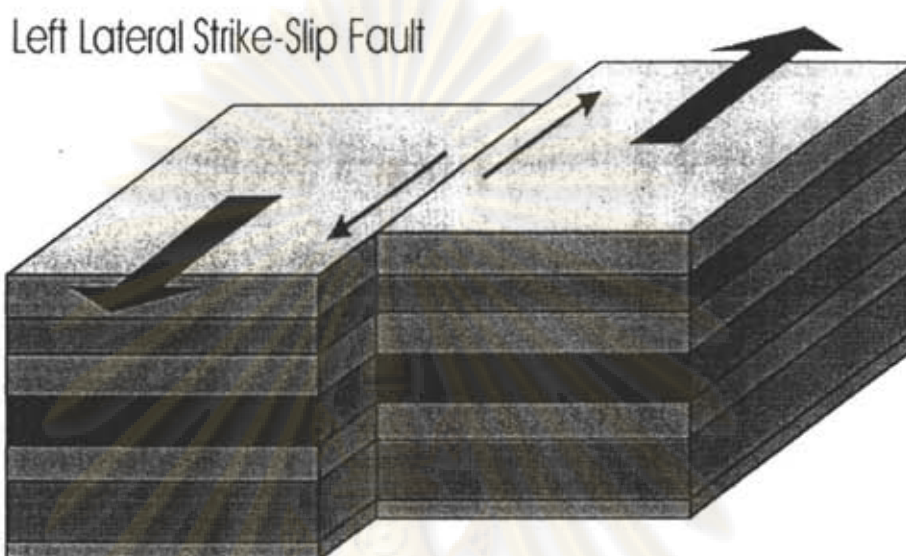


Figure 4 Strike-Slip Fault

Active faults include any faults which are considered capable of moving in the future. Because the amount and frequency of movement can vary enormously, it is important to be able to estimate the degree of activity likely to be exhibited by any fault in the region of interest, and various schemes have been devised for doing this. To this rating of likelihood of movement should be added estimates of the associated magnitudes of events. With the growing understanding of source mechanisms and the use of the concept of seismic moment, a compressive system of fault activity classification has been proposed by Cluff et al. as set out in Table 1, based on an analysis of 150 active faults on a worldwide basis. The classification uses all the parameters of interest in fault behavior, in six general classes of active fault and five sub-classes. Cluff et al. gave the following examples of different classes of faults.

Table 1 Comprehensive activity criteria for fault classification

| Class | Slip rate (mm/yr) | Slip per event (m) | Rupture length (km) | Seismic moment (dyne-cm) | Magnitude $M_s$ | Recurrence interval (yr) |
|---|---|---|---|---|---|---|
| 1 | $\geq 10$ | $\geq 1$ | $\geq 100$ | $\geq 10^{26}$ | $\geq 7.5$ | $\leq 500$ |
| 1A | $\geq 5$ | $\geq 1$ | $\geq 100$ | $\geq 10^{26}$ | $\geq 7.5$ | $\leq 1000$ |
| 1B | $\geq 10$ | $< 1$ | $\geq 100$ | $\geq 10^{26}$ | $\geq 7.0$ | $\leq 100$ |
| 2 | $1-10$ | $\geq 1$ | $\geq 50-200$ | $\geq 10^{25}$ | $\geq 7.0$ | $100-1000$ |
| 2A | $1-10$ | $< 1$ | $\geq 50-200$ | $\geq 10^{25}$ | $< 7.0$ | $< 100$ |
| 2B | $1-10$ | $\geq 5$ | $\geq 100$ | $\geq 10^{25}$ | $\geq 7.0$ | $1000$ |
| 3 | $0.5-5$ | $0.1-3$ | $10-100$ | $\geq 10^{25}$ | $\geq 6.5$ | $50-5000$ |
| 4 | $0.1-1$ | $0.01-1$ | $1-50$ | $\geq 10^{24}$ | $\geq 5.5$ | $1000-10000$ |
| 4A | $0.1-1$ | $\geq 0.5$ | $\geq 10$ | $10^{25}$ | $\geq 6.5$ | $1000-10000$ |
| 5 | $\leq 1$ | | | | | $\geq 10000$ |
| 6 | $\leq 0.1$ | | | | | $\geq 100000$ |

The classification system of Table 1, by incorporating the full range of possible fault behavior, avoids the over rigidity of active-inactive descriptions which considered a fault active if it had moved repeatedly in the past. However, in many cases it may be impossible to obtain enough information about the dates and rates of movement to use Table 1.

## 2.2 The nature and attenuation of ground motions

In order to obtain a complete predictive model for the ground motion at a given site, it is necessary to describe fully the ground motion at the source and to describe the modifications to the ground motion as it propagates from source to site, i.e. the attenuation. The nature of the sources and the attenuation are not the same for all regions, and hence the appropriate regional descriptions need to be determined from assessing the seismic hazard at a given site.

### 2.2.1 Earthquake source models

The subject of source models is an area of study for seismologists, the results of which are fundamental to our understanding of the nature of ground motion. From amidst the complexities of this major study area a number of key parameters are evident as being of interest to earthquake engineers, some of which have already been introduced, such as fault length, fault width, fault displacement (or slip), stress drop on a fault, and earthquake magnitude.

An earthquake is the product of a displacement discontinuity sweeping across a fault surface. The shape of the rupture surface and the resistance across it are variable, such that mathematical modeling of the source process, while often qualitatively plausible, remains quantitatively promising rather than convincing. Nevertheless, various simplified models are useful predictors of gross features of ground motion and can be helpful for extrapolations in predicting design ground motions in regions with few data at the appropriate magnitudes and focal distances

Early work on source models concentrated on what could be learned from the kinematics only, while more recently studies have been carried out based on the fracture mechanics of cracks initiated in pre-existing stress fields on a fault plane. In this approach, called the dynamic model, components of the model such as fault slip and rupture velocity are obtained by solving a mixed boundary problem. The local stress drop inside the circular crack areas is relatively constant, ranging from 50 to 400 bars for all the events studied. Thus the maximum value of stress drop that is likely to occur in any earthquake is uncertain, but values higher than several hundred bars do not seem likely. Rupture velocity, the velocity at which fault rupture propagates, is a basic

parameter of source modeling, with estimates typically varying from about half to about equal to the shear wave velocity of the ruptured material, yielding rupture velocities $v_r$ approximately 2 to 3 km/s.

### 2.2.2 Peak ground motions and attenuation

The most obvious piece of information to be gained from earthquake record is the maximum acceleration, or peak ground acceleration, partly because it is so easy to obtain, and partly because earthquake forces are proportional to acceleration, in the past this parameter has received most attention by engineers. Peak ground velocity and displacement also have their uses, with growing interest in velocity in recent years. The characteristics of ground motion vary with the nature and size of the event at source and with the distance from the source. Traditionally the peak ground motions have been described as a function of magnitude and distance from the source.

### 2.2.3 Upper bounds to peak ground motion

Brune gives two arguments for an upper bound of about 2g for horizontal acceleration in solid rock near to the source. An elaboration of these results comes from considering the ground motion at the surface due to an S-wave radiated vertically during the failure of the most heavily loaded asperity on a fault. The upper bound for a can lie anywhere between 0.4 and 2.0g, depending on the ratio of horizontal to vertical principal stress.

A method of estimating peak horizontal accelerations which is independent of source mechanism and location comes from considering the maximum acceleration that can be transmitted according to the strength of the soil. Consider a seismic shear wave being transmitted upwards through an elementary column of soil with forces and motions.

### 2.2.4 Duration of strong motion

This variable is important because the amount of cumulative damage incurred by structures increases with number of cycles of loading, and also because the duration of strong motion is used in evaluating one of the measures of strength of shaking, namely

the root-mean-square acceleration. Duration of strong motion is usually defined in relation to ground accelerations and several different definitions exist. The direct approach is to equate duration to the time between the first and last accelerations on the record which exceed some arbitrary minimum value, typically taken as 0.05g for stronger events. Duration of strong motion tends to increase with both magnitude and distance from the source and may also increase from rock to soil sites.

Unfortunately, widely varying expressions for such correlations exist, partly because of the inherent scatter in the data and partly because of the use of varying definitions for duration of strong motion. As with all earthquake variables, durations should be calculated from data for the region concerned, but at present the regional dependence of duration of strong.

## 2.3 Active Faults in Northern Thailand

Recent investigations have identified a number of active faults in Northern Thailand. The normal faults are marked by steep, linear range fronts with triangular facets and wineglass canyons and have slip rates of 0.1 to 0.8 mm/year. Based on limited data, the average vertical displacement-per-event is about 1.0 to 1.5 m. These faults are characterized by recurrence intervals of thousands to tens thousands of years and are capable of generating earthquakes up to moment magnitude M7, and larger (Clark H. Fenton, Punya Charusiri and Spencer H. Wood, 2003).

Due to lack of large damaging earthquakes during historical time, Thailand has not been considered to be a seismically active country. Although there are number of accounts of historical earthquake damage, the locations and sizes of most of these events are not well defined. Recent seismic in Thailand has been confined to low to moderate levels with no clear association with existing mapped faults (Bott et al., 1997). In areas like Thailand, where there is no reliable, long-term earthquake record and an absence of historical faults surface ruptures, it is necessary to examine the geologic and geomorphic record, in order to quantify the activity on suspected active faults, and thereby determine their contribution to the seismic hazards of the region. List of earthquake suspected from Maerim and Maetha faults from 1978-2007 is shown in Table 2.

In this research, the results of several recent investigations of active faults in Northern Thailand are summarized. The evidence for active faulting, illustrated by examples of Maerim and Maetha faults, and characteristics of these faults are discussed.

Table 2 List of earthquake suspected from Maerim and Maetha faults from 1978-2007

| Year | Month | Day. | Time | Lattitude | Longtitude | Magnitude | Depth |
|------|-------|------|------|-----------|------------|-----------|-------|
| 1978 | 5 | 25 | 232229.1 | 19.28 | 99.07 | 4.8 | 8 |
| 1980 | 2 | 10 | 21752.8 | 19.35 | 99.23 | 4.1 | 10 |
| 1985 | 8 | 23 | 152300.3 | 19.15 | 99.28 | | 33 |
| 1986 | 1 | 5 | 161632.8 | 18.77 | 99.03 | | 30 |
| 1987 | 1 | 29 | 220903 | 18.98 | 98.96 | | 33 |
| 1988 | 2 | 18 | 183842.4 | 18.87 | 99.17 | 4.2 | 5 |
| 1989 | 10 | 7 | 112028.8 | 19.18 | 98.78 | | 32 |
| 1989 | 9 | 29 | 144051.9 | 19.22 | 99.23 | | 33 |
| 1989 | 10 | 9 | 91421.29 | 19.32 | 99.00 | | 64 |
| 1989 | 11 | 11 | 64102.87 | 19.46 | 98.51 | | 10 |
| 1990 | 9 | 1 | 24344.81 | 19.29 | 99.26 | 3.7 | 33 |
| 1991 | 8 | 4 | 122133.8 | 18.59 | 98.83 | | 10 |
| 1995 | 12 | 21 | 162957.9 | 19.46 | 99.07 | 4.5 | 41 |
| - 1998 | 5 | 23 | 44320.28 | 19.38 | 98.76 | 4.0 | 33 |
| 2002 | 12 | 18 | 134712.7 | 19.19 | 98.96 | 4.3 | 40 |
| 2006 | 8 | 6 | 51525.13 | 19.43 | 98.65 | | 10 |
| 2006 | 12 | 12 | 170229.7 | 18.90 | 98.92 | 4.6 | 9 |
| 2007 | 6 | 19 | 50642.69 | 18.90 | 99.00 | | 10 |

2.4 Historical seismic activity in Thailand

Contemporary seismic activity in the Northern Thailand is diffusely distributed, of low to moderate levels, does not appear to be associated with currently mapped faults (Figure 5), and is probably confined to the upper 10 to 20 km of the crust (Bott et al., 1997). Although the historical earthquake record extends back to at least 1300 A.D., the

largest known earthquake in Thailand has probably not exceeded Richter magnitude M6.5. Associating seismic activity with specific geologic structures, particularly mapped faults, is extremely difficult in northern Thailand because large location uncertainties of individual earthquakes (Bott et al., 1997).
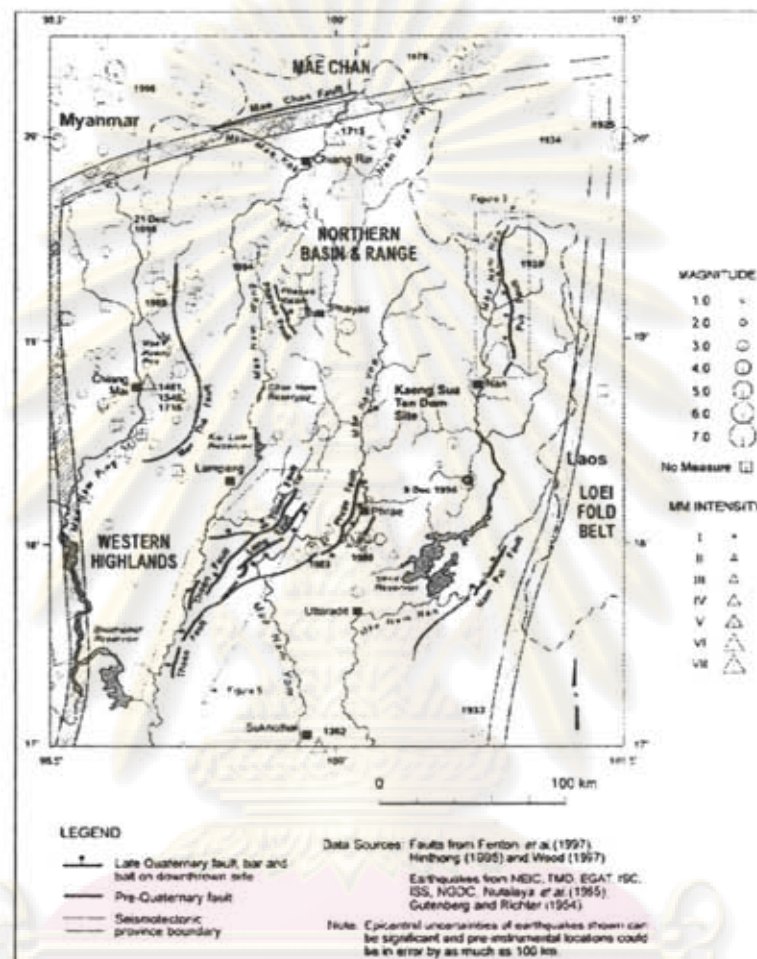


Figure 5 Faults and historical seismic activity (1362 to 1996) of the Northern Thailand modified from Bott et al. (1997).

## 2.5 Previous fault studies in Thailand

Seismic source zones for Thailand was first introduced by Nutalaya et al. (1985), based upon both seismological and geological evidences. Subsequently, Shrestha (1990) identified 9 active faults in the country on the basis of only seismological data analysis. Recently Department of Mineral Resources put an enormous effort to produce the active fault map of Thailand with the co-operative research studies of Chulalongkorn

University (Thailand) and Akita University (Japan) on the bases of all the relevant geotectonic, digitally - enhanced satellite-borne image, geochronological, historical and seismological data along with the earlier published works (e.g., Hinthong, 1995; Nutalaya et al., 1985). Nutalaya (1994) and Hinthong (1995, 1997) initially complied data on active faults in Thailand, identifying 23 active, potentially active, or suspected active faults, based primarily on geomorphic expression obtained from fault gouges. Subsequent investigations have added to the inventory of active and suspected active faults in Thailand (Figure 6).



| | | | |
|---|---|---|---|
| 1 | Mae Chan Fault | 13 | Three Pagodas Fault Zone |
| 2 | Fang Fault | 14 | Ranong Fault Zone |
| 3 | Mae Saraing Fault Zone | 15 | Klong Mauri Fault Zone |
| 4 | Mae Rim Fault | 16 | Ao Luk Fault Zone |
| 5 | Mae Tha Fault Zone | 17 | Khlong Thom Fault Zone |
| 6 | Wang Nua Fault | 18 | Kantang Fault |
| 7 | Mae Chang Fault | 19 | Saba Yoi Fault |
| 8 | Thoen Fault Zone | 20 | Khok Pho Fault |
| 9 | Phrae Fault Zone | 21 | Yala Fault |
| 10 | Hot Fault | 22 | Betong Fault |
| 11 | Moei Fault Zone | 23 | Bang Pakong Fault |
| 12 | Si Sawat Fault Zone | | |

Figure 6 Active and suspected active faults in Thailand modified from Hinthong (1995).

### 2.5.1 Maerim Fault

Maerim fault northwest to southeast strike which is approximately 23 kilometers away from Chaingmai city. Due to limited studies, so Maerim fault is not well defined. But numerous events have been identified that the epicenter of many earthquake during past 10 years lied on this fault as shown in Figure 7.

### 2.5.2 Maetha Fault

Maetha Fault Zone forms approximately 140 km-long, roughly NW-trending to the east of the Chiangmai basin. The fault plane has a moderate dipping angle to west and northwest. Along the northern part of its fault trace it sharply truncates the Maekuang River, with the offset of about 4.5 km in the right lateral slip. Small earthquakes with mostly less than M3.0 and shallow depth occurred abundantly in the northwestern part of the fault. However, our geomorphologic investigations show poorly-defined morphotectonic features during Quaternary. Hot spring locations are mainly in the southern part of the fault. No dating data have been done along this fault yet.



Figure 7 Local map of Chiangmai showing location of Chediluang and selected earthquake epicenter generated by Maerim and Maetha fault (USGS data)

2.6 Determination maximum credible earthquake magnitude

### 2.6.1 Magnitude versus fault rupture length

This is the most common method of estimating magnitude from a fault. As seismic moment is a function of fault area. It may be expected that the magnitude is related to rupture length. From data on worldwide historical events, Slemmons found rough correlations for different fault types as follow;

Normal faults: $\qquad M_s = 0.809 + 1.341 \log L$ (1)

Reverse faults: $\qquad M_s = 2.021 + 1.142 \log L$ (2)

Strike-slip faults: $\qquad M_s = 1.404 + 1.169 \log L$ (3)

where, $L$ is the rupture length in meters. Because of the inherent large variance in the above relationship, Bonilla carefully reworked the worldwide data, examining five different fault types and carefully studying the variance. They found,

$$M_S(L) = 6.04 + 0.708 \log L \quad S = 0.306$$ (4)

and the 95 percentile magnitude

$$M_{0.95} \approx M_S(L) + t_{0.05} S \left[ \frac{1}{\upsilon} + 1 \right]^{\frac{1}{2}}$$ (5)

where, $L$ is the rupture length in kilometers, $S$ is the standard error, $v$ is the number of degree of freedom, and $t$ is the statistic t-test parameter.

Alternatively, Moment magnitude, $M_w$, calculated from the formula of Well and Coppersmith (1994) can be used

$$M_w = 5.81.16 \log L$$ (6)

where $L$ = Length of active segment.

### 2.6.2 Magnitude versus fault rupture area

Because of the relationship between fault rupture area and seismic moment, a stronger relationship may be expected using rupture area rather than rupture length. Indeed,

even with errors in rupture area up to a factor of two, estimates of magnitudes vary only by 0.3 magnitude units. according to Wyss, who gives the following expression:

$$M_S^{\bullet} = 4.15 + \log A \tag{7}$$

where, $A$ is the area of the fault rupture surface in square kilometers.

### 2.6.3 Magnitude versus fault displacement

Various empirical relationships have been developed between magnitude and maximum observed surface displacements for historical events. and those derived by Slemmons are

$$\begin{array}{llr} \text{Normal faults:} & M_S = 6.668 + 0.75 \log D & (8) \\ \text{Reverse faults:} & M_S = 6.793 + 1.306 \log D & (9) \\ \text{Strike-slip faults:} & M_S = 6.974 + 0.804 \log D & (10) \end{array}$$

where, $D$ is the maximum surface displacement in meters. As well as difficulties experienced in finding and measuring the true maximum displacement in the field, the large variance in the data used to derive these expressions needs to be recognized. A special problem with earthquake in the magnitude of 5 to 6 range is that many such events have been associated with no observed displacement, but regression analyses have not usually allowed for this and are thus biased in this magnitude range.

### 2.7 Determination of waveform

Determination of waveform is one of the most important parameters in conducting dynamic analysis of any kind of structures. In case where seismometer has been widely installed, waveform of a particular site can be directly obtained from the recorded strong ground motion of the nearby instrument station. Without network of reliable seismometer, generation of strong motion waveform from reliable numerical method must be adopted.

Waveform can be more reliable generated based on the existing recorded of small earthquakes in the targeted area. However, the proposed Chediluang site is a remote area. There is no existing earthquake record nearby the site. To overcome this

disability, small earthquake waveform will be first estimated from the statistical simulation. The existing of soft soil can attenuate and alternate frequency content of the vibration.

For most design purposes it can be assumed that ground motion is a random vibratory process, and that accelerograms can be mathematically simulated with random vibration theory. This will be most true at distances from the causative fault sufficient to ensure that the details of the fault displacement are not significant in the ground shaking. Because of the scarcity of actual bedrock recordings, at present the modeling of simulated earthquake is necessarily based on the more numerous accelerograms recorded on softer soils. This is considered reasonable, as there is much to suggest that the main difference between bedrock and soft-soil motions is one of frequency content;

To predict ground motions from future large earthquakes, the most important factors are the source characterizations for complex rupture processes to formulate the source characterizations based on recent results of the waveform source inversion. There are two important aspects of characterizing the earthquake sources, outer and inner source parameters. The outer source parameters such as total fault length, width, seismic moment and so on are obtainable based on geological investigations of capable earthquake faults and seismological studies of source models. The inner source parameters are parameters related to slip heterogeneity on fault plane from the waveform inversion of strong motion records. To examine the procedure comparing between observed records and synthetic ground motions from the characterized sources based on kinematic models for the recent large earthquakes. The validity of the procedures for characterizing the earthquake sources and calculating ground motions have to be confirmed.

High-quality ground motion records have been obtained from those recent earthquakes. Peak ground acceleration and velocity and response spectrum for earthquake-resistant design are given by empirical methods as a function of magnitude, fault distance, ground condition. There are two important factors for predicting strong ground motion, one is source characterization based on geological features for active

faults and statistical analysis of source processes from the waveform inversion of strong motion records, the other is the estimation of the Green's functions from source to site. To estimate strong ground motions in a deterministic approach, we need to have two kinds of source parameters, outer and inner ones.

### 2.7.1 Outer Source Parameters

The outer source parameters are total fault length and width, average slip and slip duration, rupture velocity and so on, which are to characterize the macroscopic pictures of given source faults. They are inferred, based on geological investigations of capable earthquake faults and seismological studies of source models.

Total fault lengths ( $L$ ) of scenario earthquakes would be evaluated as one of the long-term seismic hazard evaluation. Some attempts have been making to estimate segmentation and grouping of active faults based on branching features of seismic surface ruptures (e.g. Matsuda, 1998; Nakada, 1998). Such surveys give us strike ( $\phi$ ) and slip type of every segment consisting of the fault system. Dip angle ( $\delta$ ) is inferred from seismic reflection profile.

Fault width ( $W$ ) cannot be directly determined from the geological survey but mostly from source modeling for waveform simulations compared with observed records. The saturation of the width yields for events larger than M6.8, correspond to the thickness of seismogenic zones. The seismogenic zones are inferred from the depth-frequency distribution of small earthquakes (Ito, 1990). Recent study by Ito (1999) shows that the seismogenic zones seem to have upper cutoff depth as well as lower cutoff depth derived from the seimic-aseismic boundary in the mid-crust dependent on regions.

The seismic moment of the capable faults are estimated by the empirical relationship between the source areas and seismic sources ( $A = LW$ ), then average slips are automatically constrained by the seismic moment and source area (e.g. Somerville et al. 1999).

### 2.7.2 Inner Source Parameters – Fault Heterogeneity or Roughness –

The slip and slip velocity have been found not to be uniform in the source areas, in particular for large earthquakes more than 7 as clarified from the waveform inversion of rupture process (e.g. Wald, 1996). We need to know slip and slip velocity distribution in the source area as well as the average slip to estimate strong ground motions. We call here such source parameters inner source parameters that express fault heterogeneity or roughness. So far slip models have been derived from longer period ground motions using the waveform inversion. Direct application of such long-period 4 source models to strong ground motion estimation is not always available because higher ground motions than 1 Hz cannot be generated. Nevertheless, we found that the asperity models derived from the heterogeneous slip distribution using the waveform inversion of longer-period ground motion recordings are available for estimating broad-band ground motions of engineering interest (e.g. Kamae and Irikura, 1998).

Somerville et al. (1999) analyzed the characteristics of slip models of totally fifteen crustal earthquakes ranging from about 6 to 7 in moment magnitude ($M_w$) for use in the prediction of strong ground motion. They used two approaches, deterministic and stochastic, in characterizing the slip models. First they define fault asperities in a deterministic manner to quantify the properties of heterogeneous slip models. The asperities are areas on the fault rupture surface that have large slip relative to the average slip on the fault. An asperity is defined to enclose fault elements whose slip is 1.5 or more times larger than the average slip in the fault (in detail refer to Somerville et al.1999).

A simple and powerful method for simulating ground motions is to combine parametric or functional descriptions of the ground motion's amplitude spectrum with a random phase spectrum modified such that the motion is distributed over a duration related to the earthquake magnitude and to the distance from the source. This method of simulating ground motions often goes by the name "the stochastic method." It is particularly useful for simulating the higher-frequency ground motions of most interest to engineers (generally, $f > 0.1$ Hz), and it is widely used to predict ground motions for regions of the world in which recordings of motion from potentially damaging earthquakes are not available. This simple method has been successful in matching a

variety of ground-motion measures for earthquakes with seismic moments spanning more than 12 orders of magnitude and in diverse tectonic environments. One of the essential characteristics of the method is that it distills what is known about the various factors affecting ground motions (source, path, and site) into simple functional forms. This provides a means by which the results of the rigorous studies reported in other papers in this volume can be incorporated into practical predictions of ground motion.

### 2.8 Literature Review

Comgrit (1997) investigated the behavior of a masonry structure without considering the soil-structure interaction during earthquake by using STRAP program. The basic assumption was based on the structure are thin shell structure which vary depth from base to top of the structure. He found that under medium earthquake, the structure were not able to resist the seismic load.

Juhasova (2002) analyzed the seismic response of the masonry structure and describes experiences with modeling of boundary conditions during the test of large heavy model on shaking table. The main purpose of the research was how to increase dynamic resistance capacity of old masonry buildings including the medium and strong seismic effects.

Jaishi (2003) investigated the dynamic properties of multi-tiered temples by using finite element method. Those temples are test by ambient vibration methods under wind-induced excitation to obtain real dynamic properties. Seismic capacity evaluation was performed using seismic coefficient method. The results show that the failure modes of masonry temple are associated with tensile and compressive stresses.

Soneji (2006) attempted to assess the influence of dynamic soil-structure interaction on the behavior of seismically isolated structure. The emphasis has been placed on assessing the significance of nonlinear behavior of soil that affects the response of the system and identify the circumstances under which it is necessary to include the soil-structure-interaction effects in the design of the structure. He found the essential for effective design of the structure especially when the structures are very rigid and the soil condition is soft to medium. He also found that the linear soil model

does not lead to accurate prediction of structure base shear response, and nonlinear soil modeling is essential to reflect dynamic behavior of soil-structure system.

Livaoglu (2006) was also analytically investigated the foundation interaction. He found that the tank roof displacements were affected significantly by the embedment in soft soil. However, this effect was smaller for stiff soil types.

# CHAPTER III
## SOILS CHARACTERISTIC AND MATERIAL PROPERTIES

### 3.1 Determination of site characteristics

In seismic regions geotechnical site investigations obviously should including the gathering of information about the physical nature of the site and its environment that will allow an adequate evaluation of seismic hazard to be made. In many earthquakes the local geology and soil conditions have had a profound influence on site response. On the assumption that the gross bedrock vibration will be similar at two adjacent sites, local differences in geology and soil produce different surface ground motions at the two sites. Factors influencing the local modifications to the underlying motion are the topography and nature of the bedrock and the nature and geometry of the depositional soils.

Soil conditions and local geological features affecting site response are numerous. The greater the horizontal extent of the softer soils, the less the boundary effects of the bedrock on the site response. The depth of soil overlying bedrock affects the dynamic response, the natural period of vibration of the ground increasing with increasing depth. This helps to determine the frequency of the waves amplified or filtered out by the soils and is also related to the amount of soil-structure interaction that will occur in an earthquake.

The slope of the bedding planes of the soils overlying bedrock obviously affects the dynamic response; but it is less easy to deal rigorously with non-horizontal strata. Changes of soil types horizontally across a site affect the response locally within that site, and may profoundly affect the safety of a structure straddling the two soil types.

The water content of the soil is an important factor in site response. This applies not only to sloping soils as mentioned above, but liquefaction may also occur in flat terrain composed of saturated cohesionless soils.

Faults of varying degrees of potential activity sometimes cross the site of proposed or existing construction and cases of damage have been recorded. The recurrence interval of given levels of fault displacement both horizontal and vertical, and

the structure's ability to tolerate the design displacement, sometimes need to be evaluated.

## 3.2 Site investigations and soil tests

It is normal to carry out some investigations of the site, generally using fairly standardized operations in the field and in the laboratory such as drilling boreholes.

### 3.2.1 Soil distribution and layer depth

Standard borehole drilling and sampling procedures are satisfactory for determining layer thicknesses for most seismic response analysis purposes as well as for normal foundation design. In the upper 15m of soil, sampling is usually carried out at about 0.75 or 1.5 m intervals; from 15-30 m depth, a 1.5 m interval may be desirable; while below 30m depth, 1.5 or 3.0 m may be adequate, depending on the soil complexity. If the site may be prone to liquefaction or slope instabilities, thin layers of weak materials enclosed in more reliable material may need to be identified, requiring more frequent or continuous sampling in some cases.

### 3.2.2 Depth to bedrock

For use in response calculation, knowledge of the depth to bedrock or rock-like material is essential. Beyond the ordinary borehole depth of 50-100 m, bedrock may be determined from geophysical refraction surveys, preferably checked by reference to information from geological records. In areas of deep overburden, for seismic response purposes the depth at which bedrock or equivalent bedrock is reached may have to be defined fairly arbitrarily. For example, on some sites it may be reasonable to say that equivalent bedrock is material for which the shear wave velocity at low strains (0.0001 percent) is 760 m/s, where such material is not underlain by materials having significantly lower shear wave velocities.

### 3.2.3 Groundwater conditions

Adequate standard borehole installations are available for accurately measuring groundwater conditions at any site. For response calculations this information is used

indirectly through effective confining pressures as they affect both shear modulus and damping of the soil. Those sites which are most susceptible to liquefaction have their water table within 3 m of the surface, while sites with water tables within about 8 m of ground level may also be potentially liquefiable, depending on other soil parameter.

### 3.2.4 Penetration resistance tests

The penetration resistance test is really an indirect means of determining the relative density or degree of compaction of granular deposits. It is therefore an important factor in the study of settlement and liquefaction of soils in earthquake. It may also be used to estimate shear modulus of the soil. Because it can be carried out simply, frequently, and cheaply as part of routine subsoil investigations, it is probably preferable to the direct laboratory test for determining relative density.

Two basic types of penetrometer are in common use for peneration tests, namely hollow tube samplers and cone penetrometers. Both types may be either driven by a falling weight or by a static load into the undisturbed soil at the bottom of the borehole as drilling proceeds. When using the results of penetration tests for assessing the condition of granular soils they may in some cases be used directly or else indirectly. It is particularly important to bear in mind the large scatter of results obtained using all penetration tests; therefore penetrometer readings should be used to establish trends of soil compaction rather than be considered as absolute values.

### 3.2.5 Field determination of shear wave velocity

Although the shear wave velocity is often used directly in response analyses, it may be thought of mainly as a means of determining the shear modulus $G$ of a soil from the empirical relationship. Determining shear wave velocity are the most applicable field procedures because they involve a large mass of soil, they can be carried out in most soil types, and they permit shear wave velocity to be determined as a function of depth. Because these tests are only feasible at low levels of soil strain of $10^{-5} - 10^{-3}$ percent, compared with design earthquake strains of about $10^{-3} - 10^{-1}$ percent, values of shear modulus calculated from the values of shear wave velocity will be scaled down for

seismic response purposes. It is also wise to compare values $G$ computed in this manner with values determined from laboratory tests.

### 3.2.5.1 Downhole method

Down hole surveys are performed by monitoring longitudinal and shear wave propagation vertically in soil deposits in the vicinity of a borehole. A geophone or hydrophone is clamped to the wall of borehole as illustrate in Figure 8, to monitor the arrival of wave front propagating downward from the source on the ground surface. As the source, a wooden plate clamped on the surface is hit manually by a hammer. If the plate is hit horizontally, it generates a shear wave polarized in the horizontal direction. The longitudinal wave (P-wave) is generated by hitting the plate vertically or by dropping a weight onto it. In the downhole method, the geophone is lowered to the desired depth successively while generating the wave each time on the surface. The downhole survey can be conducted effectively in place where space is limited. Shear wave velocities from down-hole seismic test at site is shown in Figure 9.
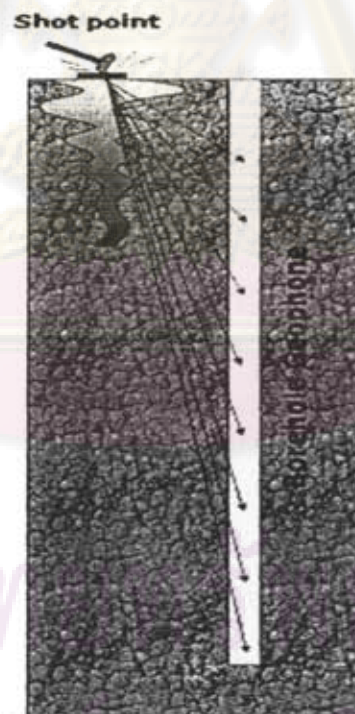


Figure 8 Downhole test method
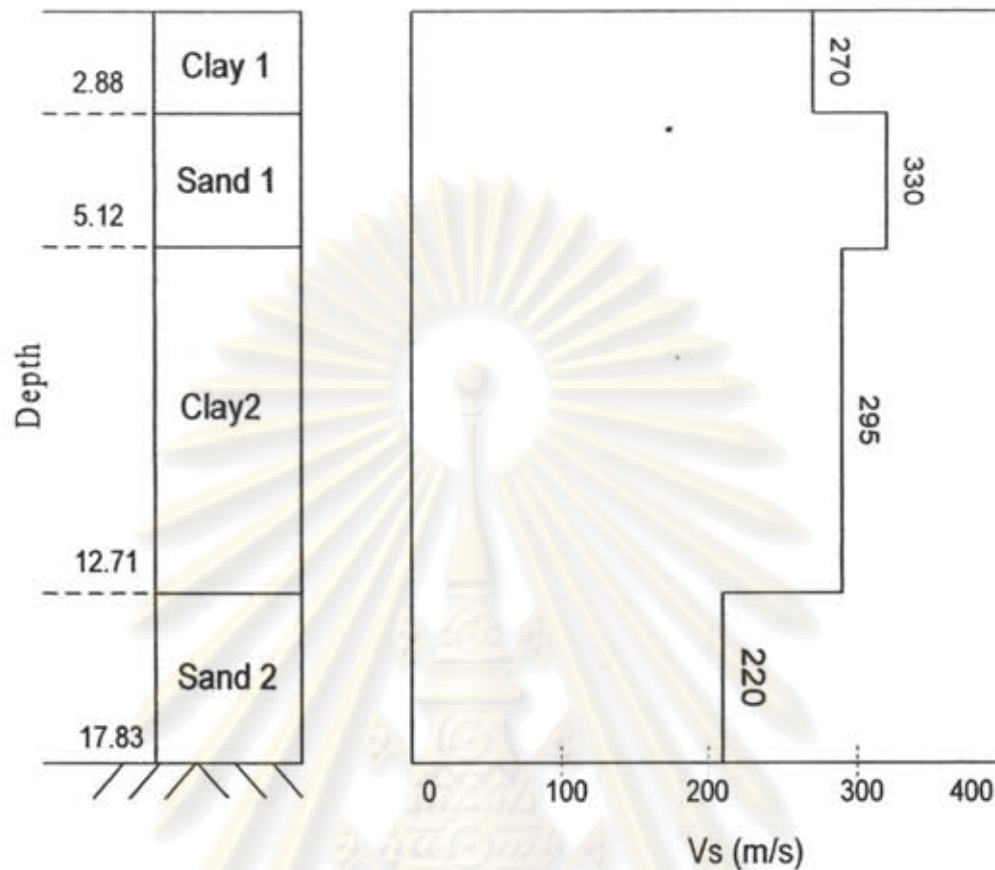
Figure 9 Shear wave velocities from down-hole seismic test at site.

### 3.2.6 Field determination of fundamental period of soil

Knowledge of the predominant period of vibration of a given site is helpful in assessing a design earthquake motion and the vulnerability of the proposed construction to earthquakes. Many attempts have been made to measure the natural period of vibration of different sites; the vibrations measured have generally been micro tremors, some arising from small earthquakes or those induced artificially such as by explosive charges, pile driving, passing trains or nuclear test explosions. It should be noted that the fundamental period of the soil will generally be between about 0.2 and 4.0 s, depending on the stiffness and depth of the soils overlying bedrock

Those investigating techniques related to the seismic response of soils are discussed and summarized in Table 3.

Table 3 List of main seismic soil factors with the most suitable test used in their evaluation

| General Procedure | Test Condition | Approx. Strain Range | Properties Determine |
|---|---|---|---|
| Determination of hysteretic stress-strain relationships | Triaxial compression | $10^{-2}$ to 5% | Modulus, Damping |
| | Simple shear | $10^{-2}$ to 5% | Modulus, Damping |
| | Torsional shear | $10^{-2}$ to 5% | Modulus, Damping |
| Forced vibration | Longitudinal vibration | $10^{-4}$ to $10^{-2}$ % | Modulus, Damping |
| | Torsional vibration | $10^{-4}$ to $10^{-2}$ % | Modulus, Damping |
| | Shear vibration lab | $10^{-4}$ to $10^{-2}$ % | Modulus, Damping |
| | Shear vibration field | $10^{-4}$ to $10^{-2}$ % | Modulus |
| Free vibration tests | Longitudinal vibration | $10^{-3}$ to 1 % | Modulus, Damping |
| | Torsional vibration | $10^{-3}$ to 1 % | Modulus, Damping |
| | Shear vibration lab | $10^{-3}$ to 1 % | Modulus, Damping |
| | Shear vibration field | $10^{-3}$ to 1 % | Modulus |
| Field wave velocity | Compression waves | $\approx 5 \times 10^{-4}$ % | Modulus |
| | Shear waves | $\approx 5 \times 10^{-4}$ % | Modulus |
| | Rayleigh waves | $\approx 5 \times 10^{-4}$ % | Modulus |
| Field seismic response | Measurement of motions at different levels in deposit | | Modulus, Damping |

3.3 Laboratory tests relating to dynamic behavior of soils

3.3.1 Cyclic triaxial test

This test is one of the laboratory methods at present available for determining the shear modulus and damping of cohesive and cohesionless soils for use in dynamic response analyses. In this test cyclically varying axial compression stress-strain characteristics are measured directly. The compressive modulus $E$ so obtained is converted to the shear modulus $G$ using the relationship.

$$G = \frac{E}{2(1+v)} \tag{11}$$

where $v$ is Poisson's ratio. The damping ratio may also be obtained from this test from the resulting hysteresis diagram as illustrated in Figure 10. Depending on the range of strains produced in the test, any desired level of strain may be chosen for plotting the hysteresis loops.
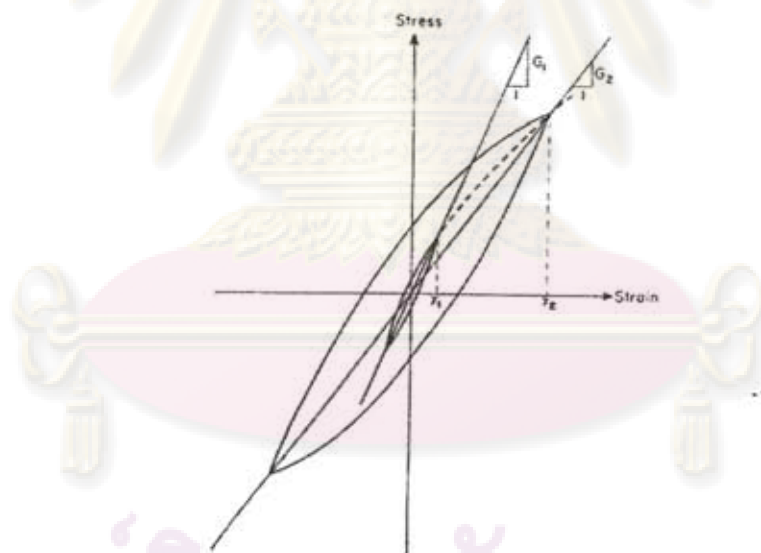


Figure 10 Hysteretic stress-stain relationships at different strain amplitudes

As well as having the facility for applying a variety of stress conditions, the cyclic triaxial test has the advantages that it can be applied to all types of soils except gravel. The disadvantages of this test are related to its inability to reproduce the stress

conditions found in the field, i.e. that the cyclic shear stresses are not applied symmetrically in the test, that zero shear stresses are applied in the laboratory with isotropic rather than, anisotropic consolidation, and also that the test involves deformations in the three principal stress directions, whereas in earthquakes the soil in many cases is thought to be deformed mainly unidirectionally in simple shear.

Cyclic shear tests are carried out at high strains ($10^{-2}$ – 5 percent) equal to and larger than the strains occurring in strong earthquakes; since geophysical test involve low strains, values of $G$ at intermediate strains may be determined by interpolating between $G$ values found from these different methods, but as there is no overlap between the strains occurring in these two tests cross-checking between the field and laboratory method is not possible. It is also to be noted that in the use of this test to determine soil damping characteristics, no field method of evaluating damping is as yet available for comparison, and hence any values of damping coefficient obtained should be treated with appropriate caution.

## 3.4 Dynamic properties of soils

Soil behavior under dynamic loading depends on many factors, including the nature of the soil, the environment of the soil (static stress state and water content) and the nature of the dynamic loading (strain magnitude, strain rate, and number of cycles of loading). Some soils increase in strength under rapid cyclic loading, while others such as saturated sands or sensitive clays may lose strength with vibration.

To provides background information on soil and rock properties required for dynamic response analysis of soil or soil-structure systems, ways of estimating the basic parameters of shear modulus, damping, and shear wave velocity are suggested, and typical values of these and other parameter are given. In order to obtain appropriate design values of these parameters for a given site, suitable field and laboratory tests may be necessary.

### 3.4.1 Shear modulus

For soils the stress-strain behavior of most interest in earthquakes is that involving shear. For small strains the shear modulus of a soil can be taken as the mean

slope of the stress-strain curve. At large strains the stress-strain curve becomes markedly non-linear so that the shear modulus is far from constant but is dependent on the magnitude of the shear strain (Figure 11). There are various field and laboratory methods available for finding the shear modulus $G$ of soils. Field tests may be used for finding the shear wave velocity, $v_s$ and calculating the shear modulus from the relationship

$$G = \rho v_s^2 \qquad (12)$$

where $\rho$ is the mass density of the soil.
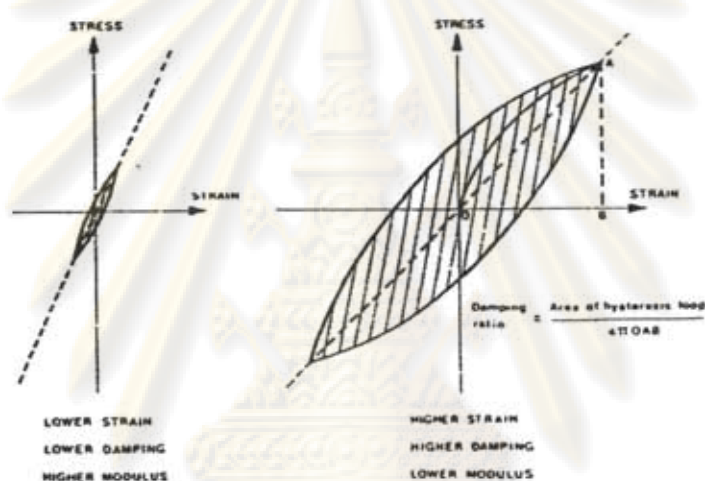


Figure 11 Illustration defining the effect of shear strain on damping and shear modulus of soils (Seed and Idriss)

### 3.4.1.1 Shear modulus values for sands

All investigations have been that modulus values for sands are strongly influenced by the confining pressure, the strain amplitude and the void ratio (or relative density) but not significantly by variations in grain size characteristics. It has been found that in general, the shear modulus and confining pressure are related by the equation

$$G = 1000 K_2 (\sigma'_m)^{\frac{1}{2}} \qquad (13)$$

so that the influence of void ration and strain amplitude can be expressed through their influence on the parameter $K_2$

The influence of other factors on $K_2$, may be illustrated by the results in Figure 12 which were computed using the relationships suggested by Hardin and Drnevich.
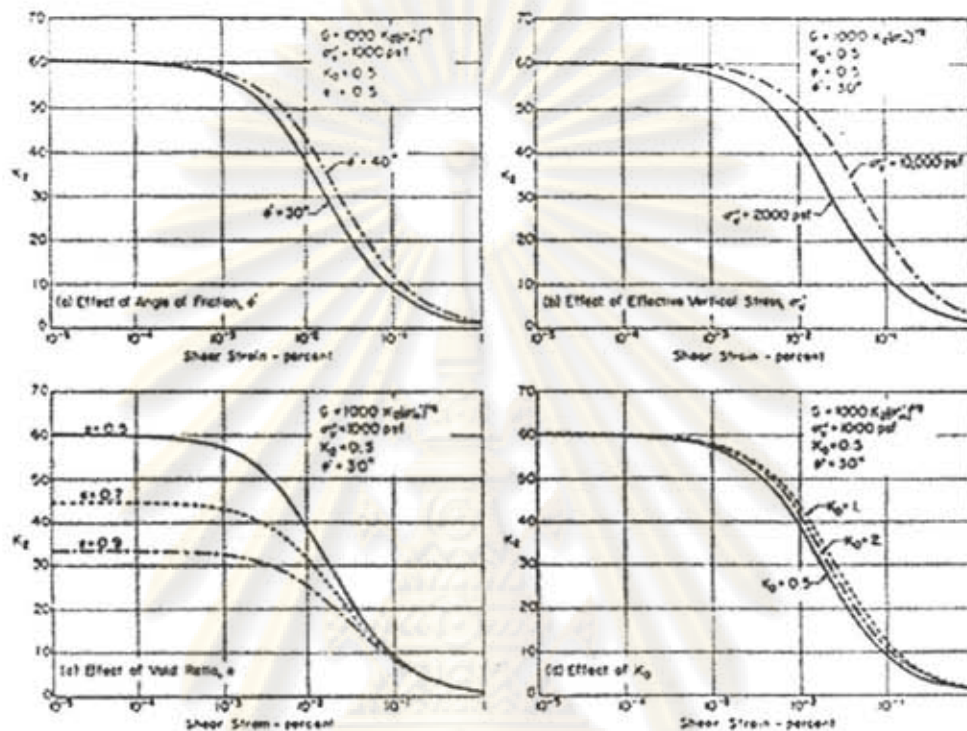


Figure 12 Influence of various factors on the shear modulus of sands (Seed and Idriss)

Plots are presented to show the influence of $\phi'$, effective vertical stress $(\sigma'_v)$, $K_0$, and void ratio on the computed relationships between $K_2$ and strain amplitude From Figure 12, It may be seen that:

(a) At very low strains ($\gamma \leq 10^{-3}$ percent), $K_2$ depends only on the void ratio, $e$

(b) At intermediate strains ($10^{-3} \leq \gamma \leq 10^{-1}$ percent) the variation of $K_2$ with strain is only slightly influenced by the vertical stress, and very slightly by variations in $\phi'$ and $K_0$. The values of $K_2$ are still influenced strongly by the void ratio however.

(c) At very high strains ($\gamma \geq 10^{-1}$ percent), the values of $K_2$ are slightly influenced by the vertical stress but they are essentially independent of $K_0$, $\phi'$ and $e$.

Thus for practical purposes, values of $K_2$ may be considered to be determined mainly by the void ratio or relative density and the strain amplitude of the motions.

A number of investigators, using different laboratory testing procedures, have presented data on the relationships between these factors. The test conditions used in these investigations and the results are presented in Figure 13, for samples having a relative density of about 75 percent, and in Figure 14 for samples having a relative density of about 40%.
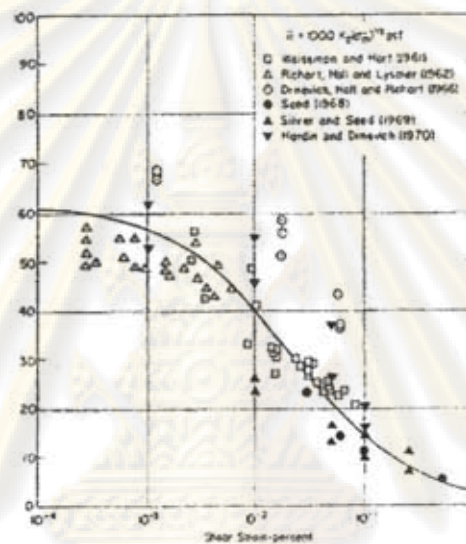


Figure 13 Shear modulus of sand at relative density of about 75%
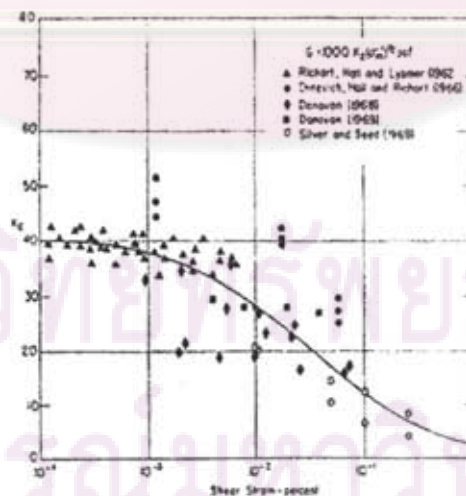


Figure 14 Shear modulus of sands at relative density of about 40%

Average relationships between $K_2$ and strain for these two relative density conditions are shown in Figure 13 and 14, and they are compared in Figure 15. Values of $K_2$ at other relative densities can be estimated by interpolation, as shown in Figure 15.
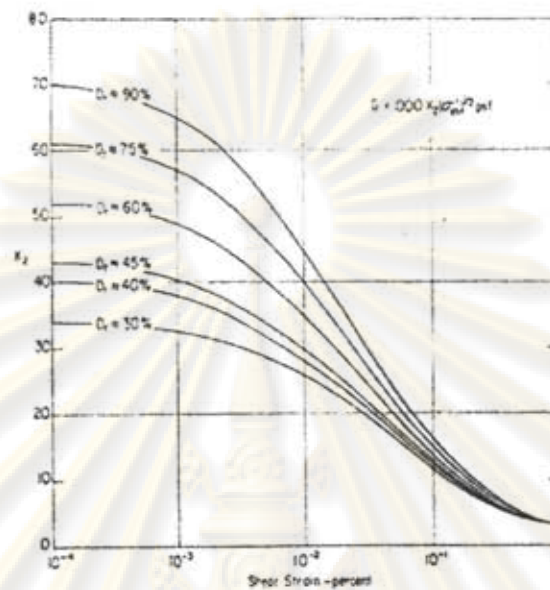


Figure 15 Shear modulus of sands at different relative densities

It may be seen that for relatively dense samples, the values of $K_2$ determined at very low strains for laboratory test specimens are typically in the range of 50 to 75. The results of a number of determinations of shear modulus of sands at very low strain levels by means of in-situ shear wave velocity measurements are summarized in Table 4; the six investigations for dense to extremely dense sands (excluding clayey and partly cemented sands) give values for $K_2$ ranging from 44 to 86. Thus there appears to be good general agreement between the results of laboratory and in-situ investigations.

For purposes of comparison, representative values of the relationship between $K_2$ and strain at different void ratios determined by the Hardin-Drnevich relationship for an effective vertical stress of 3000 psf, $K_0 = 0.5$ and $\phi' = 36°$ are plotted in Figure 12.

The good agreement between the results in Figure 11 and 12 indicates that reasonable values for the shear modulus of sands may be obtained either by use of the curves in Figure 15 or by use of the Hardin-Drnevich equations where field data is obtained in terms of the standard penetration resistance.

Table 4 Shear modulus of sands based on in-situ shear wave velocity measurements

| Soil | Depth (ft) | $K_2$ |
|---|---|---|
| Loose moist sand | 10 | 34 |
| Dense dry sand | 10 | 44 |
| Dense saturated sand | 50-300 | 58-72 |
| Dense saturated silty sand | 60 | 65 |
| Extremely dense silty sand | 125 | 86 |
| Dense dry sand (slightly cemented) | 65 | 166 |
| Moist clayey sand | 30 | 119 |

It may be noted that if each of the relationships shown in Figure 15 and 16 is replotted to show the variation with shear strain of the ratio of shear modulus at strain $\gamma$ to shear modulus at a shear strain of $10^{-4}$ percent, the results fall within the relatively narrow band shown in Figure 17. Thus a close approximation to the modulus vs shear strain relationship for any sand can be obtained by determining the modulus at a very low strain level, say by wave propagation methods in the field, and then reducing this value for other strain levels in accordance with the results indicated by the average (dashed) line in Figure 17.
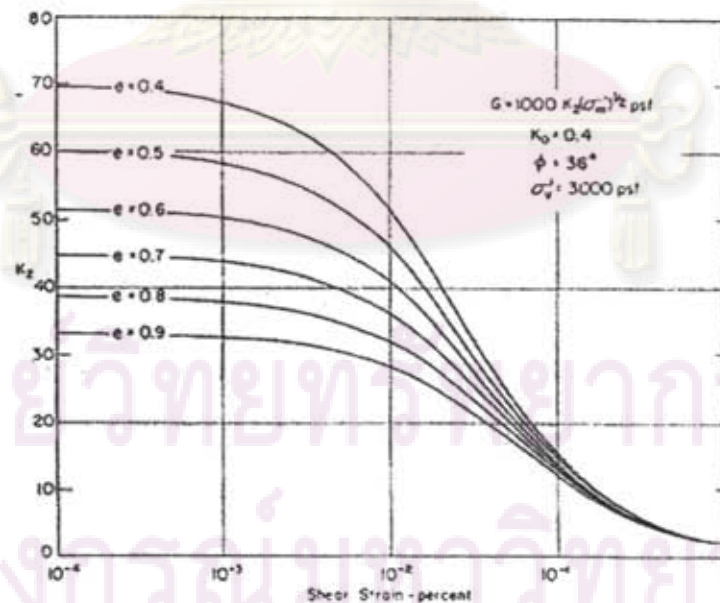


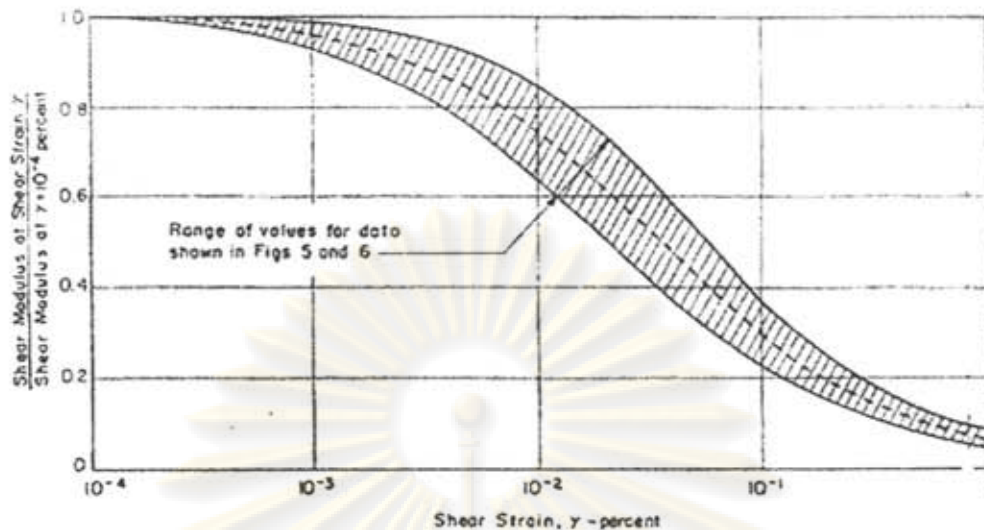Figure 16 Shear modulus of sand at different void ratio

Figure 17 Variation of shear modulus with shear strain for sand

### 3.4.1.2 Shear modulus values for saturated clays

Accurate determination of the shear modulus of saturated clays is enormously complicated by the large effects of strain amplitude and sample disturbance on modulus values. In-situ measurements eliminate the problems raised by sample disturbance, but to date no techniques have been developed for inducing large controlled strain amplitude in natural deposits and thus modulus can only be determined at very small strain levels. In the laboratory, on the other hand, samples may be tested under a wide range of strains but for test specimens from natural deposits, the modulus determined will inevitably be influenced by the effects of sample disturbance.

The joint influence of these effects is illustrated by the data presented in Figure 18 and 19. Figure 18 shows values of shear modulus for mud at a depth of about 25 ft determined by in-situ shear wave velocity measurements by Aisiks andTarshansky (1968) and values determined by cyclic loading simple shear tests on undisturbed samples by Thiers (1965) Projecting the laboratory test data to the strain level corresponding to the field test conditions, it may be seen that the laboratory test values are only about 40 percent of those for the in-situ clay. This result is not surprising in the light of previous studies of the influence of disturbance on the modulus of natural clays (Ladd, 1964) and it emphasizes the magnitude of the correction which may have to be made for this effect.

The influence of strain amplitude on shear modulus is also apparent from the data in Figure 18, the values at strains of about 0.5 percent being only about 12 percent of those corresponding to strains of the order to $10^{-3}$ or $10^{-4}$ percent.
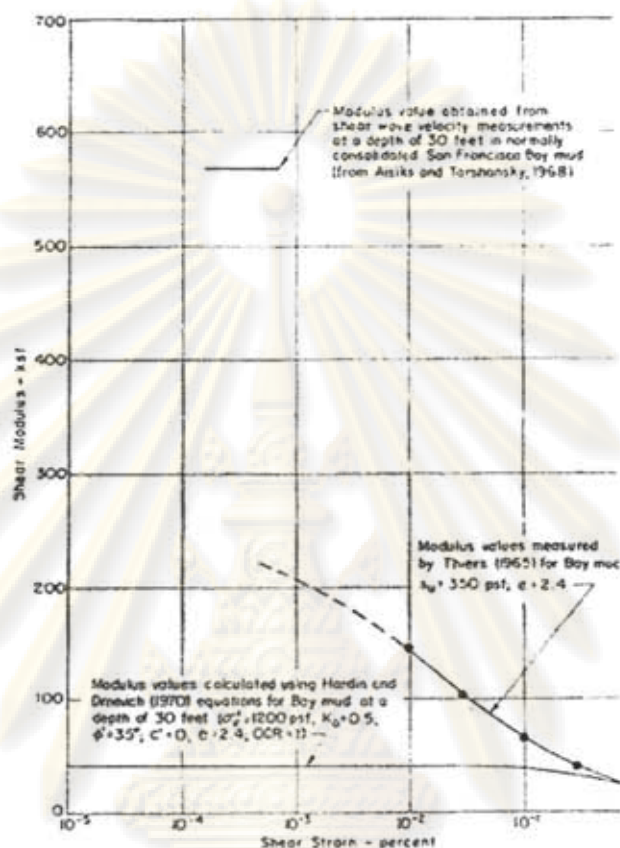


Figure 18 Shear modulus determination for clay

Figure 19 shows similar data for Union Bay clay. In this case values of shear modulus for in-situ conditions were determined from seismic wave velocity measurements and from observations of the response of the clay during an earthquake; modulus values for undisturbed samples were determined by resonant frequency tests and cyclic loading tests in the laboratory. Again the in-situ modulus is two or three times greater than the laboratory test values at comparable strains, and the modulus decreases enormously with increasing strain amplitude.

In addition to the effects of strain amplitude and disturbance, the shear modulus of different clays will clearly depend on their relative strengths and stiffness. Hardin and Drnevich express these effects in terms of the effective mean principal stress, void ratio,

overconsolidation ratio and effective stress strength parameters, but the resulting relationships do not always provide reasonable evaluations of shear modulus for in-situ conditions, as evidenced by the results shown in Figure 18 and 19.
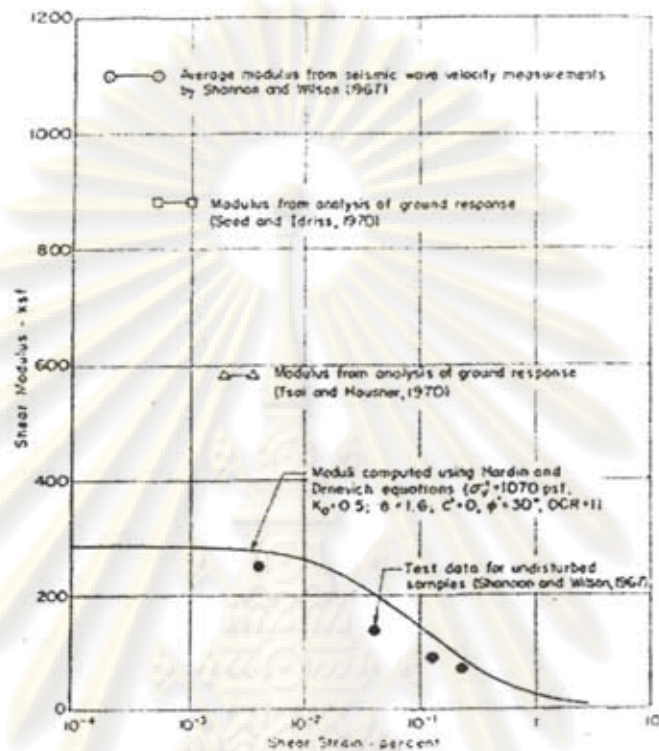


Figure 19 Shear modulus determination for clay at higher depth

However in view of the facts that

(1) Stiffness increases in general with soil strength,

(2) For static load conditions, the ratio $\dfrac{E}{S_u}$ for saturated clays does not vary widely from one soil to another, and

(3) Test data at very low strain levels indicates an approximately linear relationship between the shear modulus and shear strength for a number of clays (Wilson and Dietrich, 1960), it seems reasonable to expect that variation in clay characteristics might be taken into account with a reasonable degree of accuracy by normalizing the shear modulus, $G$, with respect to the undrained shear strength, $S_u$, and expressing the relationship $\dfrac{G}{S_u}$ as a function of shear strain.

Test data obtained by a number of investigators and expressed in this form are summarized in and plotted in Figure 20. For test data obtained in laboratory tests under unconsolidated-undrained test conditions, the measured modulus were multiplied by a factor of 2.5 to make an approximate allowance for sample disturbance. Clearly the effects of disturbance will vary from one study to another but in the absence of detailed information on sampling and testing conditions it was considered that a factor of 2.5 would represent a reasonable average correction factor for these effects. For in-situ and laboratory consolidated-undrained test conditions, no correction was applied to the test results.
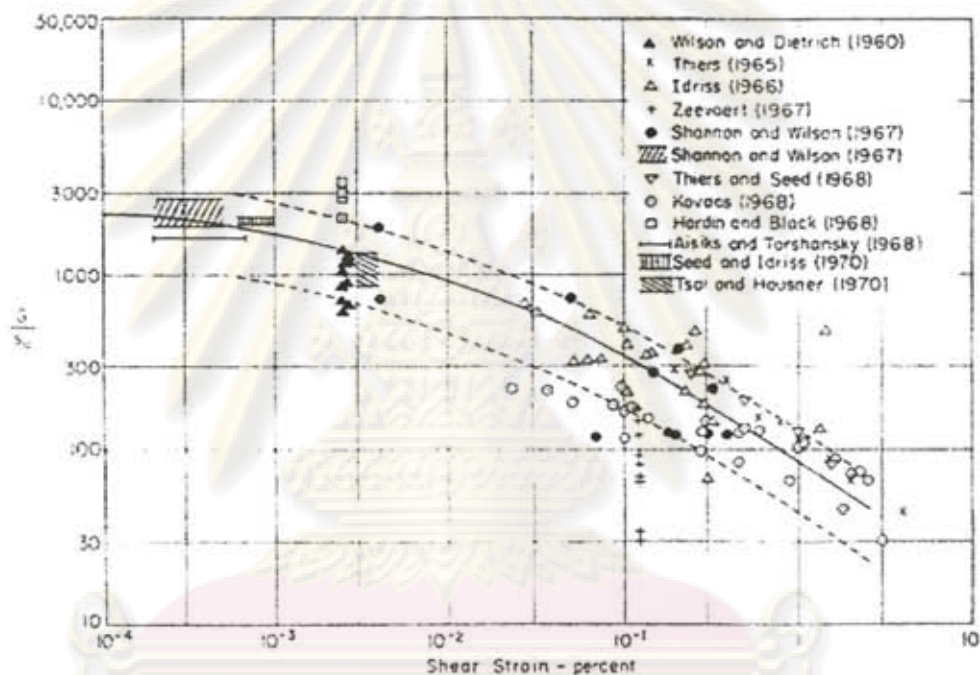


Figure 20 Shear modulus for saturated clay

While there is considerable scatter in the data, most of the test results fall within the dashed lines in Figure 20; that is, within ±50% of the average values shown by the solid line in the figure. Thus the average values are likely to provide reasonable estimates of the in-situ modulus for clay.

Alternatively the data in Figure 16 might be used to assess the influence of strain amplitude on the shear modulus of natural clays, by expressing the ordinates in terms of the ratio of shear modulus at shear strain $\gamma$ to shear modulus at a shear strain of $3 \times 10^{-4}$

percent. This ratio for the average values shown in Figure 20, is plotted as a function of shear strain in Figure 17. Reasonable estimates of the shear modulus of clay at any strain amplitude can be obtained by determining the in-situ value at strains of the order of $3 \times 10^{-4}$ percent by means of shear wave velocity measurements and applying the reduction factors shown in Figure 21 to determine values at other shear strains.
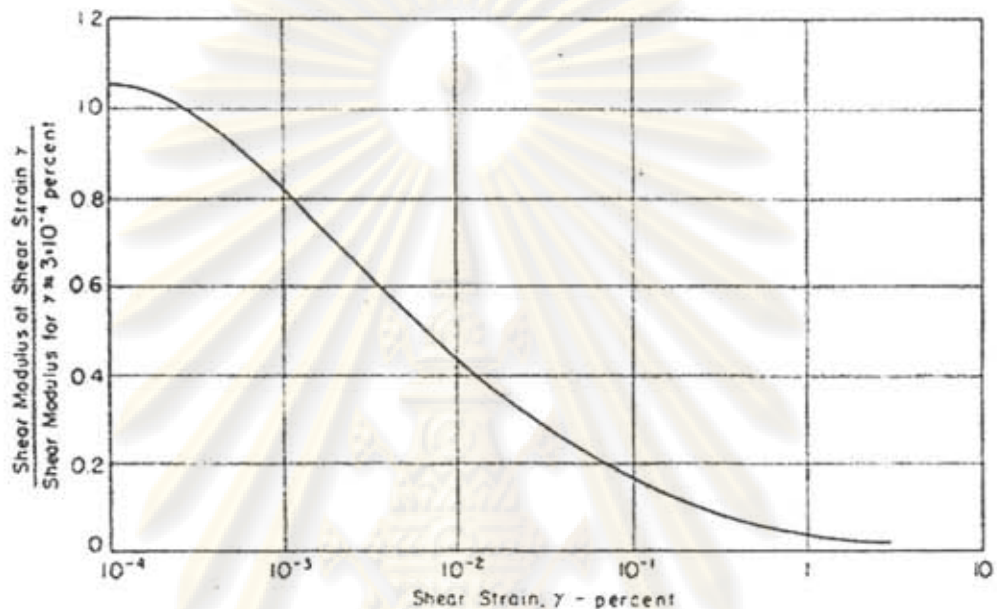


Figure21 Typical reduction of shear modulus with shear strain for saturated clay

### 3.4.2 Damping

The second key dynamic parameter for soils is damping. Two fundamentally different damping phenomena are associated with soils, namely material damping and radiation damping.

### 3.4.2.1 Damping ratios for sands

From their study of factors influencing the damping ratios of sands, Hardin and Drnevich concluded that shear strain, effective mean principal stress (or $\sigma_v'$ and $K_0$), void ratio and number of cycles were very important, while octahedral shear stress, angle of friction and degree of saturation had lesser effects. As in the case of modulus, the effects of variations in grain size characteristics were considered to be relatively insignificant.

Computations of the effects of the above factors on the relationship between damping ratio and shear strain amplitude, as determined by the Hardin-Drnevich relationships are shown in Figure 22. It is apparent that the effects of $\phi'$, $K_0$, void ratio and degree of saturation are relatively minor, and it can readily be seen from the equation for maximum damping ratio

$$\lambda_{max} \approx 30 - 1.5\log_{10} N \qquad (14)$$

that if values of $\lambda$ are determined for about $N = 5$ cycles, values for other numbers of cycles in the range of interest (say 5 to 30) will not be significantly different.
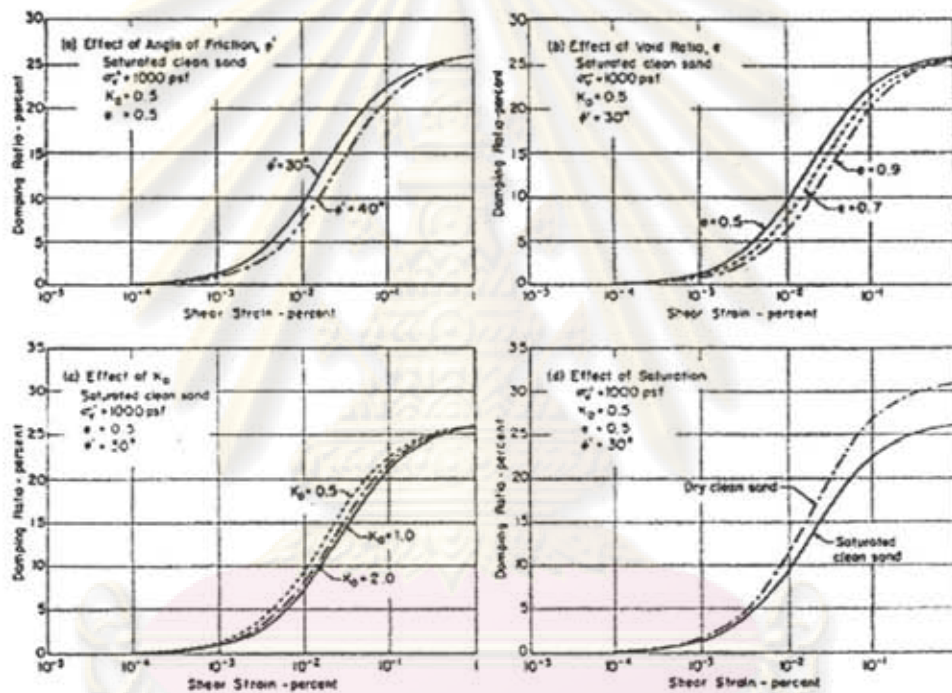


Figure 22 Influence of various factors on the damping ratio for sand

Thus the main factor affecting the relationship between damping ratio and shear strain is the vertical confining pressure $\sigma'_v$. The influence of this factor, as determined by two studies is shown in Figure 23. For pressures less than about 500 psf, the effect of pressure changes may be significant but excluding these very low pressure, which represent conditions in the top few feet of soils, the effect of variations in pressure is very small compared with the effect of shear strain, and an average damping ratio vs shear strain relationship determined for an effective vertical stress of 2000 to 3000 psf

would appear to be adequate for many practical purposes. Considering the potential scatter of test data for damping ratios, even those obtained by the same investigator using the same test procedure, the adoption of such an average relationship may be even more justified.
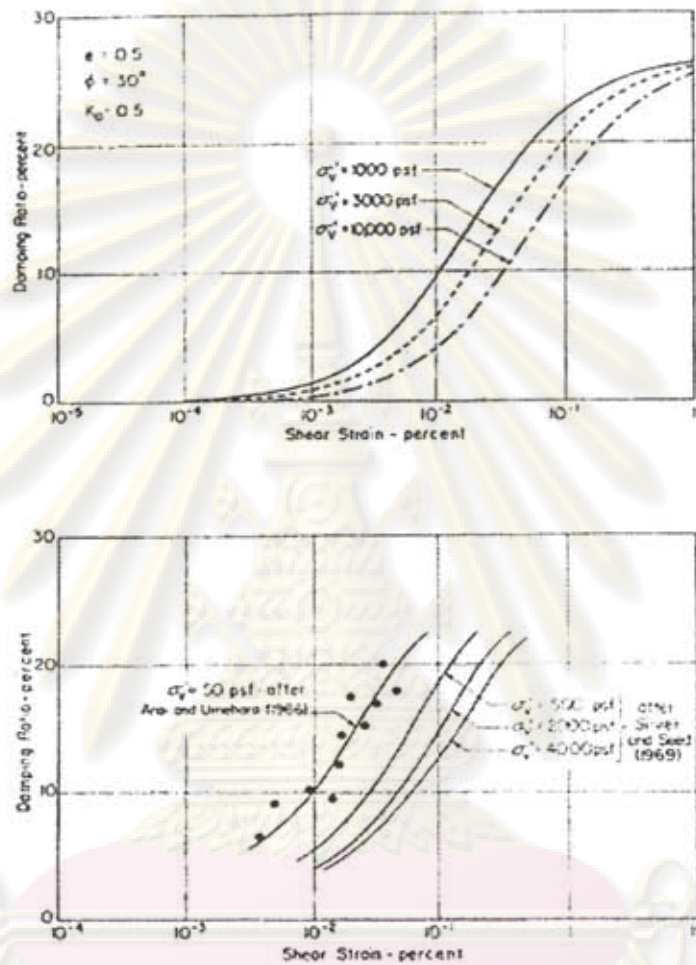


Figure 23 Influence of confining pressure on damping ratio of dry sand

Approximate upper and lower bound relationships are shown by dashed lines and a representative average relationship for all of the test data is shown by the solid line. This average relationship is likely to provide values of damping ratio with sufficient accuracy for many practical purposes.

The curves in Figure 24 also provide a basis for evaluating the relationship between damping ratio and strain of particular sands for which limited test data is available. If the value of damping ratio at a strain level of 0.1 to 0.5 percent is

determined, the probable damping ratios at other strains can be closely approximated by drawing a line through the known data point parallel to the curves shown in Figure 24.



Figure 24 Damping ratio for sand

### 3.4.2.2 Damping values for saturated clays

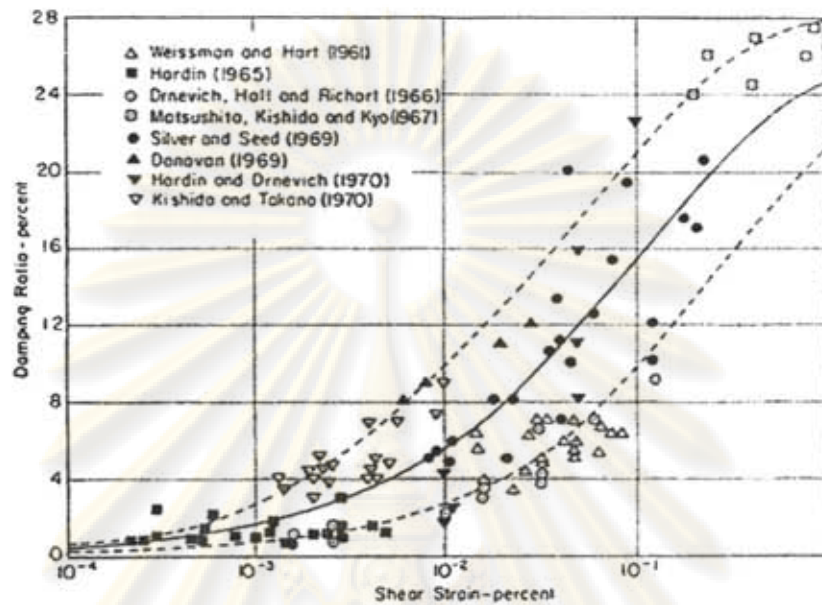Test data for damping ratios for saturated clays are so limited and the results vary to such an extent that it is difficult to determine the main factors influencing the damping ratios of these soils. The results of these studies are summarized in Figure 21. Approximate upper and lower bound relationships between damping ratio and shear strain are shown by the dashed lines and a representative average relationship for all of the test data is shown by the solid line. This average relationship may well provide values of damping ratio with sufficient accuracy for many practical purposes.

The curves in Figure 25 also provide a basis for evaluating the relationship between damping ratio at a strain for any particular clay. If the value of damping ratio at a strain level of 0.1 to 0.5 percent is determined, the probable damping ratios at other strains can be estimated by drawing a line through the known data point parallel to the curves shown in Figure 25.
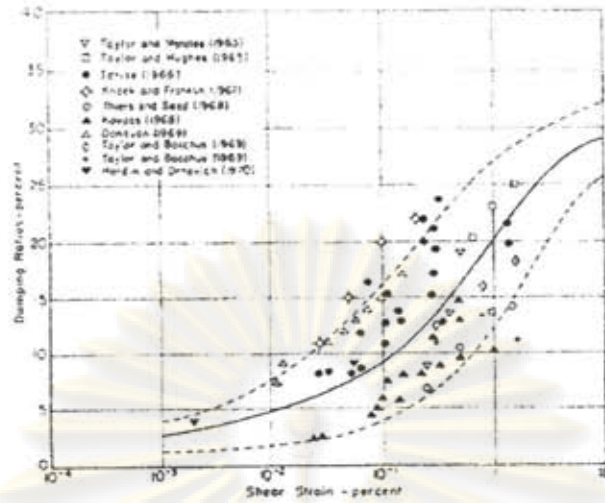
Figure 25 Damping ratio for saturated clay

Laboratory methods generally measure $G$ more directly from stress-strain tests. It is clear that the level of strain at which $G$ is measured must be known. Average relationships of shear modulus to strain are shown for clay and sand in Figure 26 as produced by Seed et al. The shear modulus for clays, while always having the general form shown in Figure 26, appears to vary as a function of the plasticity index.



Figure 26 Average relationships of shear modus to shear strain for sand and saturated clays (Seed et al.)

Shear strains developed during earthquakes may increase form about $10^{-3}$ percent in small earthquakes to $10^{-1}$ percent for large motions, and the maximum strain in each cycle will be different. Whitman suggests that for earthquake design purposes a

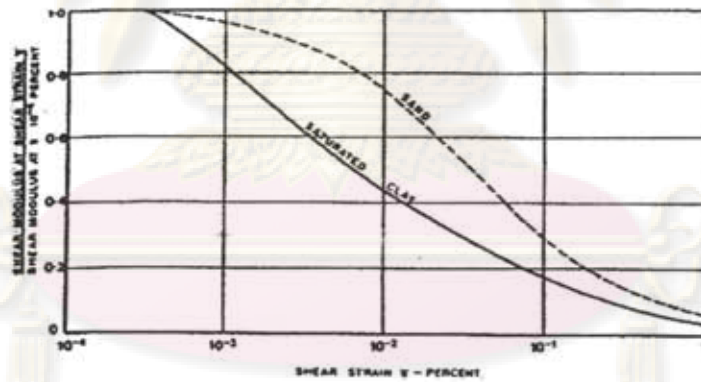value of two thirds $G$ measured at the maximum strain developed may be used. Alternatively, an appropriate value of $G$ can be calculated from the relationship.

$$G = \frac{E}{2(1+\upsilon)} \tag{15}$$

where $E$ is Young's modulus and $\upsilon$ is Poisson's ratio. In the absence of any more specific data, low strain values of $E$ may be taken from Table 5 values of Poisson's ratio from Table 6 may be used in the above formula.

Table 5 Typical modulus of elasticity values for soils and rocks

| Soil Type | E (MN/m2) | E/cu |
|---|---|---|
| Soft clay | up to 15 | 300 |
| Firm, stiff clay | 10 to 50 | 300 |
| Very stiff, hard clay | 25 to 200 | 300 |
| Silty sand | 7 to 70 | |
| Loose sand | 15 to 50 | |
| Dense sand | 50 to 120 | |
| Dense sand and gravel | 90 to 200 | |
| Sandstone | up to 50,000 | 400 |
| Chalk | 5,000 to 20,000 | 2000 |
| Limestone | 25,000 to 100,000 | 600 |
| Basalt | 15,000 to 100,000 | 600 |

Table 6 Typical values of Poisson's ratio for soils

| Soil type | Poisson's ratio |
|---|---|
| Clean sands and gravels | 0.33 |
| Stiff clay | 0.40 |
| Soft clay | 0.45 |

Further studies are required of the factors influencing the damping ratios of saturated clays to permit more detailed assessments of this characteristic for analysis purposes.

Published data on damping ratios are sparse, and consist only of values deduced from tests on small samples, or theoretical estimates. It should be appreciated that to date no in situ determinations of material damping have been made, and that damping ratios may only be used in analyses in a comparative sense. As dynamic soils analyses are required for some projects, at least for its qualitative information, a means of choosing values of material damping is required. Some material damping values are therefore given in Figure 27. These represent average values of laboratory test results on sands and saturated clays as presented elsewhere. In the absence of any other information it may be reasonable to take the damping of gravels as for sand.
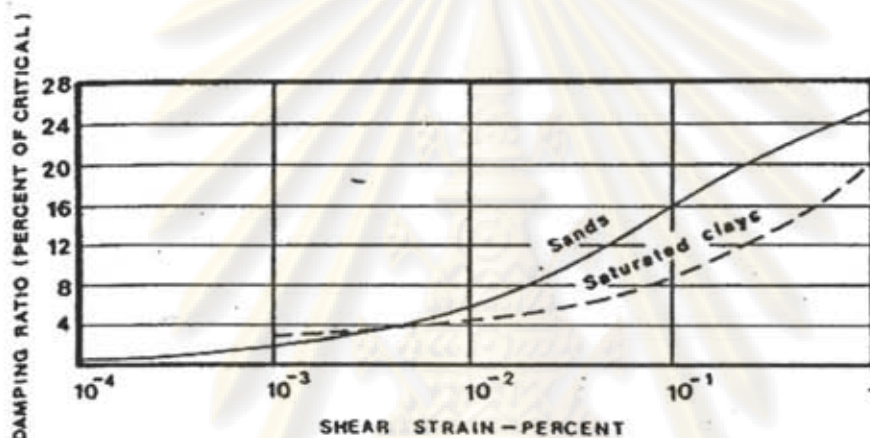


Figure 27 Average relationship of internal damping to shear strain for sands and saturated clay (Seed et al.)

## 3.5 Masonry Structure

The brick masonry is one of the oldest forms of structural material. Masonry has also lagged behind other materials in the adoption of strength. There are numerous studies concerning about behavior of masonry structure under seismic load. It also has reasonable resistance to horizontal forces. However, masonry has a number of serious drawbacks for earthquake resistance. It is naturally brittle; it has high mass and hence has high inertial response to earthquakes; and relatively little research has been done into its seismic response characteristics compared with steel and concrete. The tendency to fail in a brittle fashion is the central problem with masonry. While

unreinforced masonry may be categorically labeled as brittle, uncertainty exists as to degree of ductility which should be sought in reinforced masonry.

Subsequent research in various countries has examined various masonry products and wall-reinforcing layouts, sometimes under slow cyclic reversed loading and shake-table dynamic tests. The value of having vertical and horizontal reinforcement only at the perimeter of wall panels is surprisingly effective for both in-plane and out-of-plane loading. The latter is more true for masonry of higher tensile strength (i.e. concrete blocks) and also is probably more true for stiff structures with low lateral displacements. Perimeter-only reinforcement is very cost-effective as a minimum provision for low-cost construction and for strengthening of existing buildings.

For obtaining reliable seismic response behavior the principles concerning choice of form, materials, and failure mode control discussed apply to masonry structures, while further factors specific to masonry are discussed below.

The wide range of masonry products, of clay and concrete types, means a wide range of material behavior and hence of seismic reliability. Probably the most reliable type is reinforced hollow concrete blocks, which have been more studied than other masonry materials. However, with the growing research interest in reinforced clay bricks[6] and other masonry products the full reliability potential and relative merits of the various masonry materials are becoming better understood. Where a choice between relatively unresearched masonry materials has to be made, those which are weaker in compression and tension will obviously tend to be less reliable in earthquakes.

In considering reliability of seismic behavior of masonry structures through structural forms and failure mode control fewer alternatives need be considered than for other structural materials. Masonry is best suited to forming walls and less suited to columns and lintel beams, and is constructionally and a seismically ill-suited for forming other structural members. Thus this discussion mainly relates to the reliable seismic behavior of walls.

While quite high repeatable ductility can be achieved in masonry walls and columns by using thin steel plates between block courses[4] the constructional complications and cost of such measures suggest that seeking high ductility for masonry structures is another example of seeking high ductility. The more pragmatic

traditional approach of seeking limited ductility, so well demonstrated as successful (at least for single-storey buildings) by the EERC tests, seems likely to remain appropriate for most masonry structures, namely:

(1) Suppress the more brittle failure modes (e.g. shear);
(2) Design for limited ductility and adequate strength (e.g. the UBC approach);
(3) Use sound structural forms (as discussed below).

Masonry is a term covering a very wide range of materials such as brick, stone and concrete blocks. Each of these materials varies widely in form and mechanical properties. The variety available in form, color and texture makes masonry a popular construction material. Masonry has reasonable resistance to horizontal forces. However, masonry has a number of serious drawbacks for earthquake resistance. It is naturally brittle, high mass and has high inertial response to earthquakes. Relatively little research has been done into its seismic response characteristics compared with steel and concrete.

The tendency to fail in a brittle is a major problem with masonry. Subsequent research in various countries has examined various masonry products and wall-reinforcing layouts, sometimes under low cyclic reversed loading and shake-table dynamic tests. The value of having vertical and horizontal reinforcement distributed throughout walls is apparent, but the use of reinforcement only at the perimeter of wall panels is surprisingly effective for both in-plane and out-of-plane loading.

For obtaining reliable seismic response behavior the principles concerning choice of form, materials, and failure mode control apply to masonry structures. The wide range of masonry products, of clay and concrete type, means a wide range of material behavior and seismic reliability. Probably the most reliable type is reinforced hollow concrete blocks, which have been more studied than other masonry materials. However, with the growing research interest in reinforced clay bricks and other masonry products the full reliability potential and relative merits of the various masonry materials are becoming better understood. Where the choice between relatively unresearched masonry materials has been made, those which are weaker in compression and tension will obviously tend to be less reliable in earthquakes.

In considering reliable of seismic behavior of masonry structures through structural forms and failure mode control fewer alternatives need be considered than for other structural materials.   .

Masonry is one of the most widely used building materials in the world. Since masonry is brittle, if construction does not accommodate this expansion and contraction, cracking can result. Masonry can be used as a structural system, as a veneer, and can be used to build fireplaces and retaining wall. Masonry is strong in compression but require the incorporation of reinforcing steel to resist tensile and bending stresses. Masonry veneers can be constructed over many types of structural frames and backing walls. Masonry also provides fire resistance, energy efficiency and durability.

The International Building Code (IBC2000) defines masonry as "a built-up construction or combination of building units or materials of clay, shale, concrete, glass, gypsum, stone or other approved units bonded together with or without mortar or grout or other accepted methods of joining". ASTM (The American Society for Testing and Materials) E631 defined masonry as "construction usually in mortar, of natural building stone or manufactured units such as brick, concrete block, adobe, glass, block tile, manufacture stone, or gypsum block."

From structural engineering perspective, masonry is classified as plain masonry and reinforced masonry. Plain masonry or masonry unit refers to natural or manufactured building units of burned clay, concrete, stone, glass, gypsum, or other similar building units or combination made to be bonded together by a cement agent. Plain masonry refers to a form of construction that depends on high compressive strength of masonry units. Like plain concrete, plain masonry possesses little tensile strength. Therefore, it cannot be used as an efficient building material for structures or structural elements that must resist tensile forces.

The term masonry includes many different materials and types of construction. Natural stone as well as manufactured unit of clay brick, concrete block, cast stone, structural clay tile are all masonry materials. Brick, concrete block, and stone are the most popular and most widely used. Brick and concrete block are usually laid with mortar, but some block can be dry-stacked without mortar if the units have an

interlocking shape or if a special surface-bonding mortar is applied to hold the unit together.

Brick can be made of several different materials, but the most common type of brick is made from ordinary clay oil. Clay brick is the oldest manufactured building material in the world, and it is still one of the most widely used. Sun-dried bricks are a traditional residential construction material in dry climates and are still used in many countries.

Brick are rectangular in shape but come in many different sizes. The easiest size to work with is called modular brick because its height and length are based on a 4 inches module. Colors and textures vary depending on the clay and the methods used to form the brick. Reds, browns, tans and pinks colors are common.

Brick has many properties which make it a good building material. It is strong, hard, fireproof, abrasion resistance and provides some degree of thermal and acoustical resistance. Three of the most important properties of brick are strength, absorption and freeze-thaw resistance.

Brick are much stronger than they need to be for simple one and two story construction. Compressive strength can range from 1,500 to 22,500 psi. Mortar is not as strong as brick, so when mortar and brick are combined, the compressive strength of the masonry drops to about 1,000-2,000 psi depending on the mortar mix and the exact brick strength. A brick wall could theoretically support its own weight for a height of more than 100 meters without crushing. To resist the bending stress of wind loads, the wall also needs flexural strength. Flexural strength requires good bond between the mortar and the units. Good bond is a function of brick texture and absorption, mortar quality and workmanship.

Unreinforced masonry has been in use in many countries for many years. The inherent weakness of unreinforced masonry structures to resist lateral loads was clearly exposed during the 1933 Long Beach earthquake (M6.3). Although strong enough to resist gravity loads, these structures proved incapable of providing the required lateral resistance to seismic forces. Thus, in the ensuring period, reinforcing of masonry construction was codified, resulting in modern engineered reinforced masonry construction, most numerous examples of which are to be found in California. Poor

performance of unreinforced masonry was again evident during October 1, 1987 Whittier Narrows earthquake (M6.3), and the October 17, 1989 Loma Prieta earthquake (M7.1). In The January 17, 1994 Northridge earthquake (Mw=6.7), hundreds of unreinforced masonry structures were severely damaged and some simply collapsed. Many reinforced masonry structures and retrofitted unreinforced masonry structures also were severely damaged during this earthquake, presumably because of poor engineering design, detailing or poor workmanship and quality control. Extensive destruction of unreinforced masonry structures during these earthquakes called attention to poor tension and shear resistance of unreinforced masonry. This is not to say that unreinforced masonry structures do not posses any strength or stiffness. On the contrary, numerous studies have proved unreinforced masonry walls to be stronger than their cracking strength, and that they do posses substantial deformation capacity. Sufficient evidence of this inherent strength was found during the Loma Prieta earthquake in the historic two-story firehouse in Gilroy, California (approximately 15 km southeast of the epicenter at Loma Prieta), which had been instrumented with six accelerometers before the earthquake. Unreinforced masonry brick walls form the envelope of this building, joined by wood floor and roof systems. In spite of the roof accelerations as large as 0.79g, this structure was undamaged, with the exception of two isolated cracks.

### 3.5.1 Standard Test Methods for Sampling and Testing Brick and Structural Clay Tile (ASTM C67-99a)

These test methods cover procedures for the sampling and testing of brick and structural clay tile. Although not necessarily applicable to all types of units, tests include modulus of rupture, compressive strength, absorption, saturation coefficient, effect of freezing and thawing, efflorescence, initial rate of absorption and determination of weight, size, length change, and void area. (Additional methods of test pertinent to ceramic glazed facing tile are included in Specification C 126.)

### 3.5.1.1 Compressive Strength

Test Specimens:

Brick—The test specimens shall consist of dry half brick, the full height and width of the unit, with a length equal to one half the full length of the unit 61 in. (25.4 mm), except as described below. If the test specimen, described above, exceeds the testing machine capacity, the test specimens shall consist of dry pieces of brick, the full height and width of the unit, with a length not less than one quarter of the full length of the unit, and with a gross cross-sectional area perpendicular to bearing not less than 14 in.$^2$ (90.3 cm$^2$). Test specimens shall be obtained by any method that will produce, without shattering or cracking, a specimen with approximately plane and parallel ends. Five specimens shall be tested.

Capping Test Specimens:

All specimens shall be dry and cool before any portion of the capping procedure is carried out. If the surface which will become bearing surfaces during the compression test are recessed or paneled, fill the depressions with a mortar composed of 1 part by weight of quick-hardening cement conforming to the requirements for Type III cement of Specification C 150, and 2 parts by weight of sand. Age the specimens at least 48 hrs before capping them. Where the recess exceeds $\frac{1}{2}$ in. (12.7 mm), use a brick or tile slab section or metal plate as a core fill. Cap the test specimens using one of the two procedures:

Gypsum Capping: Coat the two opposite bearing surfaces of each specimen with shellac and allow to dry thoroughly. Bed one of the dry shellacked surfaces of the specimen in a thin coat of neat paste of calcined gypsum (plaster of paris) that has been spread on an oiled nonabsorbent plate, such as glass or machined metal. The casting surface plate shall be plane within 0.003 in. (0.076 mm) in 16 in. (406.4 mm) and sufficiently rigid; and so supported that it will not be measurably deflected during the capping operation. Lightly coat it with oil or other suitable material. Repeat this procedure with the other shellacked surface. Take care that the opposite bearing surfaces so formed will be approximately parallel and perpendicular to the vertical axis

of the specimen and the thickness of the caps will be approximately the same and not exceeding 1⁄8 in. (3.18 mm). Age the caps at least 24 hr before testing the specimens. A rapid-setting industrial type gypsum, such as Hydrocal or Hydrostone, is frequently used for capping.

Sulfur-Filler Capping: Use a mixture containing 40 to 60 weight % sulfur, the remainder being ground fire clay or other suitable inert material passing a No. 100 (150-$\mu$m) sieve with or without plasticizer. Place four 1-in. (25.4-mm) square steel bars on the surface plate to form a rectangular mold approximately 1⁄2 in. (12.7 mm) greater in either inside dimension than the specimen. Heat the sulfur mixture in a thermostatically controlled heating pot to a temperature sufficient to maintain fluidity for a reasonable period of time after contact with the surface being capped. Take care to prevent overheating, and stir the liquid in the pot just before use. Fill the mold to a depth of 1⁄4 in. (6.35 mm) with molten sulfur material. Place the surface of the unit to be capped quickly in the liquid, and hold the specimen so that its vertical axis is at right angles to the capping surface. The thickness of the caps shall be approximately the same. Allow the unit to remain undisturbed until solidification is complete. Allow the caps to cool for a minimum of 2 hrs before testing the specimens.

Procedure:

Step 1: Test brick specimens flatwise (that is, the load shall be applied in the direction of the depth of the brick). Test structural clay tile specimens in a position such that the load is applied in the same direction as in service. Center the specimens under the spherical upper bearing within 1⁄16 in. (1.59mm).

Step 2: The testing machine shall conform to the requirements of Practices.

Step 3: The upper bearing shall be a spherically seated, hardened metal block firmly attached at the center of the upper head of the machine. The center of the sphere shall lie at the center of the surface of the block in contact with the specimen. The block shall be closely held in its spherical seat, but shall be free to turn in any direction, and its perimeter shall have at least 1⁄4in. (6.35 mm) clearance from the head to allow for specimens whose bearing surfaces are not exactly parallel. The diameter of the bearing

surface shall be at least 5 in. (127.00 mm). Use a hardened metal bearing block beneath the specimen to minimize wear of the lower platen of the machine. The bearing block surfaces intended for contact with the specimen shall have a hardness not less than HRC60 (HB 620). These surfaces shall not depart from plane surfaces by more than 0.001 in. (0.03 mm). When the bearing area of the spherical bearing block is not sufficient to cover the area of the specimen, place a steel plate with surfaces machined to true planes within 0.001 in. (0.03 mm), and with a thickness equal to at least one third of the distance from the edge of the spherical bearing to the most distant corner between the spherical bearing block and the capped specimen.

Step 4: Speed of Testing: Apply the load, up to one half of the expected maximum load, at any convenient rate, after which, adjust the controls of the machine so that the remaining load is applied at a uniform rate in not less than 1 nor more than 2 min.

Calculation and Report:

Calculate the compressive strength of each specimen as follows:

$$\text{Compressive strength, } C = W / A \tag{16}$$

where:

$C$ = compressive strength of the specimen, (kg/cm$^2$)

$W$ = maximum load, (N), indicated by the testing machine, and

$A$ = average of the gross areas of the upper and lower bearing surfaces of the specimen, (cm$^2$).

Table 7 Compressive strength test of Masonry Unit

| Sample | Length (mm) | Width (mm) | Height (mm) | Max.load (kg.) | Compressive strength (MPa) |
|--------|-------------|------------|-------------|----------------|----------------------------|
| 1 | 163.58 | 63.63 | 39.33 | 2629 | 2.48 |
| 2 | 162.65 | 62.60 | 40.32 | 3008 | 2.91 |
| 3 | 162.45 | 63.18 | 39.88 | 2965 | 2.83 |
| 4 | 162.46 | 62.88 | 40.19 | 2710 | 2.60 |
| 5 | 162.35 | 63.31 | 41.36 | 2890 | 2.74 |
| | | | | Average | 2.71 |

3.5.2 Standard Test Method for Splitting Tensile Strength of Masonry Units (ASTM 1006-84)

This test method covers the determination of the splitting tensile strength of masonry units. Masonry units alone and within assemblages commonly fail in a tensile mode when loaded in compression to failure. These tensile stresses result from differences in modulus of elasticity and Poisson's ratio between the masonry unit and mortar. Additionally, the dissimilarity in behavior of the grout within cores of masonry units under load leads to tensile stresses in the units and results in a splitting failure. This test method produces a line load along the bed surface of the masonry unit. The compressive load applied to the unit, imposed by means of bearing rods, results in a tensile stress distributed over the height of the unit for the split length of the unit. This test method can be applied in either the longitudinal (parallel to the face) or the transverse direction. The test value provides an indicator of masonry-unit splitting tensile strength. Additionally, the presence of defects such as visible voids or impurities in masonry units may be revealed.

## Apparatus

Bearing Rods matched paired steel bearing rods with diameters within $1/8$ to $1/12$ of the specimen height, of a length greater than the length of the intended test area, and of straightness within 0.5 % of the specimen length shall be provided for each unit. Bearing rods that meet the straightness requirement can be reused.

Supplemental Bearing Bar or Plate: If the diameter or largest dimension of the upper bearing face or lower bearing block is less than the length of the specimen to be tested, a supplementary bearing bar or plate shall be used. The contact surfaces of the bar or plate shall be machined to within 0.05 % of planeness as measured on any line of contact of the bearing area. The bearing bar or plate shall have a width of at least 2 in. (50.8 mm), and a thickness not less than the distance from the edge of the spherical or rectangular bearing block to the end of the specimen. The bar or plate shall be used in such a manner that the load will be uniformly applied over the entire intended split length of the specimen.

## Testing Machine

The testing machine shall conform to the requirements, and may be of any type of sufficient capacity that will provide the rate of loading. The upper, hardened metal bearing face shall be spherically seated and attached at the center of the upper head of the machine. The center of the sphere shall lie at the center of the surface of the plate in contact with the specimen. The bearing plate shall be closely held in its spherical seat but shall be free to turn in any direction; its perimeter at the ball face shall have at least $1/4$ in. (6.4 mm) clearance from the head of the machine to allow for specimens whose test surfaces are not exactly parallel. The diameter of the bearing surface shall be at least 5 in. (127 mm). The bearing block surfaces that will contact the bearing bar or plate shall not depart from plane surfaces by more than 0.05 %.

## Sampling

Selection: For the purpose of this test, full-size masonry units shall be selected at random by the purchaser or by his authorized representative. The specimens shall be

representative of the whole lot of units from which they are selected and shall include units representative of the complete range of colors and sizes in the shipment.

Number: A minimum of five specimens shall be tested for the first 250 000 units. The minimum number of test specimens shall be increased by one unit for each 50 000 additional units or fraction thereof.

Procedure

Positioning Bearing Rods: For units less than 4 in. (101.6 mm) high, mark the intended location of the split surface on both faces, stretcher or normally exposed faces for transverse splitting, and end faces for longitudinal splitting. Spread a gypsum capping compound along the bed surface between these two marks. Place the bearing rod into the fresh compound and press until contact is made with the unit. After the compound has set, place the second bearing rod parallel to the first on the opposite bed surface using an alignment device as illustrated in Figure 28. The two rods must be within ¼ in. (6.4 mm) in 8 in. (203.2 mm) of being parallel.



Figure 28 Example of Alignment Jig for Maintaining Parallel Bearing Rods

For units ≥4 in. (101.6 mm) high, use a carpenter's square to draw a line perpendicular to the bed surface on opposite exterior faces. Spread capping compound

on the upper bed surfaces between the two lines. Align the bearing rods with the lines on the faces, and press one rod into the fresh compound until in contact with the unit. After the compound has set, invert the unit and repeat this procedure on the opposite bed surface. The two companion rods must be within $1/4$ in. (6.4mm) in 8 in. (203.2 mm) of being parallel. The bearing rods shall be positioned no closer to a free edge than one half the specimen height. Cure the capping compound for at least 2 h at 756 5°F (22 6 18°C) prior to testing.

Test Alignment: Align the rods with the centerline of the plates, and center the rods in the transverse direction. Support the specimen on compressible rods or tubes that are $1/16$ in. (1.8 mm) smaller in diameter than the bearing rods. Remove the compressible rods when the specimen is held in vertical orientation by the testing-machine platens.

Rate of Loading: Apply the load without impact and load continuously at a rate less than 8896N/min.

Measurement: Determine the height of the specimen to the nearest 0.1 in. (2.5 mm) by averaging three heights measured near the ends and the middle and on a plane perpendicular to the bed surface. Determine the split length of the specimen to the nearest 0.1 in. (2.5 mm) by averaging at least two measurements taken on the plane of the bearing rods. Measure net length for hollow units and gross length for solid units.

Calculations:

Calculate the splitting tensile strength of the specimens as follows:

$$T = 2P/\pi LH \tag{17}$$

where:

$T$ = splitting tensile strength, (kPa),

$P$ = maximum applied load indicated by the testing machine, (kN),

$L$ = split length, (m), net length for hollow units, gross length for solid units, and

$H$ = height, (m).

Table 8 Tensile Strength of masonry units

| Sample | Length (mm) | Width (mm) | Height (mm) | Max. Load (kg) | Tensile Strength (MPa) |
|--------|-------------|------------|-------------|----------------|------------------------|
| 1 | 161.5 | 61.26 | 40.66 | 173 | 0.16 |
| 2 | 160.5 | 62.84 | 41.34 | 182 | 0.17 |
| 3 | 162.2 | 60.18 | 42.58 | 151 | 0.13 |
| 4 | 162.8 | 62.30 | 40.22 | 160 | 0.15 |
| 5 | 160.6 | 61.48 | 41.28 | 165 | 0.16 |
| | | | | Average | 0.15 |

3.6 Summarized material properties and soil parameters

The materials of structural components are assumed homogeneous, isotropic and linearly elastic. The material properties are taken from previous works on material testing at the real site in Chiangmai. The permissible stresses of masonry structure are derived from the field and laboratory test in Chiangmai as shown in Table 9. Soils are considered in layers of different thickness resting on rock with decreasing damping with depth. It is assumed that the rigid bedrock is available at a depth of 17.83 m. The dynamic properties of the soil such as unit weight, Poisson's ratio, shear modulus, damping ratio, etc. that vary with the depth are given in Table 10.

Table 9 Permissible stresses on masonry

| Failure mode | Permissible stress (MPa) |
|--------------|--------------------------|
| Tensile | 0.15 |
| Compression | 2.71 |

Table 10 Properties of soil type condition

| Layer | Thickness | Unit weight | Poisson's | Max Shear modulus | Shear modulus | Damping | $V_s$ | $V_p$ |
|-------|-----------|-------------|-----------|-------------------|---------------|---------|-------|-------|
|       | (m)       | (kg/m³)     | ratio     | (MPa)             | (MPa)         | ratio   | (m/s) | (m/s) |
| 1     | 2.88      | 2200        | 0.45      | 160               | 80            | 0.04    | 270   | 890   |
| 2     | 2.24      | 2100        | 0.40      | 229               | 153           | 0.07    | 330   | 820   |
| 3     | 7.59      | 2000        | 0.35      | 174               | 87            | 0.04    | 295   | 610   |
| 4     | 5.12      | 1900        | 0.30      | 91                | 46            | 0.07    | 220   | 410   |
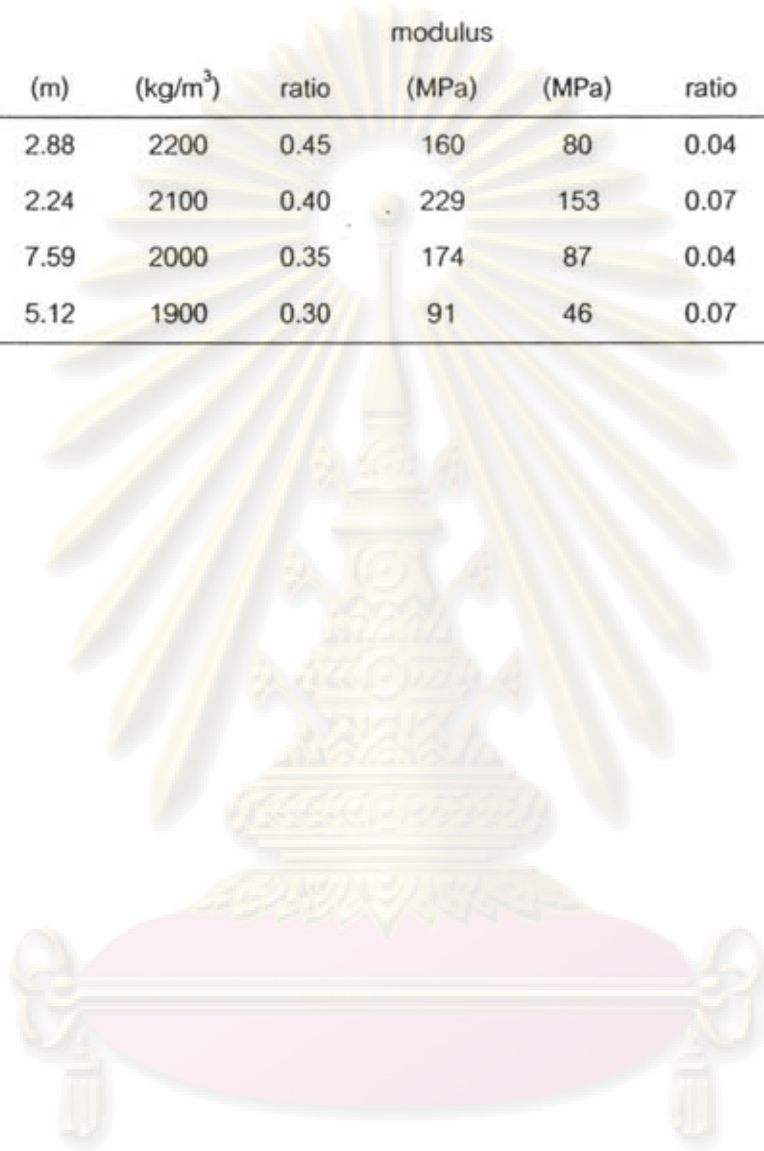
ศูนย์วิทยทรัพยากร
จุฬาลงกรณ์มหาวิทยาลัย

# CHAPTER IV
# SOIL-STRUCTURE INTERACTION

## 4.1 Dynamic analysis

For large or complex structures static methods of seismic analysis are often deemed to be not accurate enough and many authorities demand dynamic analyses for certain types and size of structure. Various methods of differing complexity have been developed for the dynamic seismic analysis of structures. They all have in common the solution of the equations of motion as well as the usual statically relationships of equilibrium and stiffness. For structures with more than three degrees of freedom such analyses are, of course, generally carried out using computers. The three main techniques currently used for dynamic analysis are;

### 4.1.1 Direct integration of the equation of motion by step-by-step procedures

Direct integration provides the most powerful and informative analysis for any given earthquake motion. A time-dependent forcing function (earthquake accelerogram) is applied and the corresponding response-history of the structure during the earthquake is computed. That is, the moment and force diagrams at each of a series of prescribed intervals throughout the applied motion can be found. Computer programs have been written for both linear elastic and nonlinear inelastic material behavior, using step-by-step integration procedures.

Linear behavior is seldom analyzed by direct integration, unless mode coupling is-involved, as normal mode techniques are easier, cheaper, and nearly as accurate. Three-dimensional non-linear analyses have been devised which can take the three orthogonal accelerogram components from a given earthquake, and apply them simultaneously to the structure. In principle, this is the most complete dynamic analysis technique so far devised, and is unfortunately correspondingly expensive to carry out.

### 4.1.2 Normal mode analysis

Normal mode analysis is a more limited technique than direct integration, as it depends on artificially separating the normal modes of vibration and combining the

forces and displacements associated with a chosen number of them by superposition. As with direct integration techniques, actual earthquake accelerograms can be applied to the structure and a stress-history determined, but because of the use of superposition the technique is limited to linear material behavior. Although modal analysis can provide and desired order of accuracy for linear behavior by incorporating all the modal responses, some approximation is usually made by using only the first few modes in order to save computation time. Problems are encountered in dealing with systems where the modes cannot be validly separated, i.e. where mode coupling occurs.

The most serious shortcoming of linear analyses is that they do not accurately indicate all the members requiring maximum ductility. In other words the pattern of highest elastic stresses is not necessarily the same as the pattern of plastic deformation in an earthquake structure. For important structures in zones of high seismic risk, non-linear dynamic analysis is sometimes called for.

### 4.1.3 Response spectrum techniques

The response spectrum technique is really a simplified special case of modal analysis. The modes of vibration are determined in period and shape in the usual way and the maximum response magnitudes corresponding to each mode are found by reference to a response spectrum. An arbitrary rule is then used for superposition of the responses in the various modes. The resultant moments and forces in the structure correspond to the envelopes of maximum values, rather than a set of simultaneously existing values. The response spectrum method has the great virtues of speed and cheapness.

Although this technique is strictly limited to linear analysis because of the use of superposition, simulations of non-linear behavior have been made using pairs of response spectra, one for deflections and one for accelerations. The expected ductility factor is chosen in advance and the appropriate spectra are used. This is clearly a fairly arbitrary procedure, and appears unlikely to be more realistic than the linear response spectrum method. Lai and Biggs have shown that Newmark and Hall's method can be unconservative and have developed an improved procedure.

4.2 Seismic response of soil-structure systems

The importance of the nature of the sub-soil for the seismic response of structures has been demonstrated in many earthquakes, but a reasonable understanding of the factors involved has only recently begun to emerge. For example, it seems clear from studies of earthquakes that the relationship between the periods of vibration of structures and the period of the supporting soil is profoundly important regarding the seismic response of the structure.

In order to evaluate the seismic response of a structure at a given site, the dynamic properties of the combined soil-structure system must be understood. The nature of the sub-soil may influence the response of the structure in three ways:

(1) The seismic excitation at bedrock is modified during transmission through the overlying soils to the foundation. This may cause attenuation or amplification effects.

(2) The fixed base dynamic properties of the structure may be significantly modified by the presence of soils overlying bedrock. This will include changes in the mode shapes and periods of vibration.

(3) A significant part of the vibration energy of the flexibly supported structure may be dissipated by material damping and radiation damping in the supporting medium.

Items (2) and (3) above are investigated under the general title of soil-structure interaction, which may be defined as the interdependent response relationship between a structure and its supporting soil. The behavior of the structure is dependent in part upon the nature of supporting soil and similarly the behavior of the stratum is modified by the presence of the structure.

It follows that soil amplification and attenuation will also be influenced by the presence of the structure, as the effect of soil-structure interaction is to produce a difference between the motion at the base of the structure and the free-field motion which would have occurred at the same point in the absence of the structure. In practice, however, this refinement in determining the soil amplification is seldom taken into account, the free-field motion generally being that which is applied to the soil-

structure model, as discussed in the following section. Because of the difficulties involved in making dynamic analytical models of soil systems, it has been common practice to ignore soil-structure interaction effects simply treating structures as if rigidly based regardless of the soil conditions. However, intensive study in recent years has produced considerable advances in our knowledge of soil-structure interaction effects and also in the analytical techniques available, as discussed below.

### 4.2.1 Dynamic analysis of soil-structure systems

Comprehensive dynamic analysis of soil-structure systems is the most demanding analytical task in earthquake engineering. The cost, complexity, and validity of such exercises are major considerations. There are two main problems to be overcome. First, the large computational effort which is generally required for the foundation analysis makes the choice of foundation model very important; five main methods of modeling the foundation are discussed in the next section. Second, there are great uncertainties in defining a design ground motion which not only represents the nature of earthquake shaking appropriate for the site but also represents a suitable level of risk.

### 4.3 Finite elements Analysis

The use of finite element for modeling the foundation of a soil-structure system is the most comprehensive (if most expensive) method available. Like the half-space model it permits radiation damping and three-dimensionality, but has the major advantage of easily allowing changes of soil stiffness both vertically and horizontally to be explicitly formulated. Embedment of footings is also readily dealt with. Although a full three-dimensional model is generally too expensive, three dimensions should be simulated. This can be achieved either by an equivalent two-dimensional model, or for structures with cylindrical symmetry an analysis in cylindrical co-ordinates can be used.

In order to simulate radiation of energy through the boundaries of the element model three main methods are available.

(1) Elementary boundaries that do not absorb energy and rely on the distance to the boundary to minimize the effect of reflection waves.

(2) Viscous boundaries which attempt to absorb the radiating waves, modeling the far field by a series of dashpots and springs, as used by Lysmer and Kuhlemeyer. The accuracy of this method is not very good for thin surface layers or for horizontal excitation, although an improved version has been developed by Ang and Newmark.

(3) Consistent boundaries are the best absorptive boundaries at present available, reproducing the far field in a way consistent with the finite element expansion used to model the core region. This method was developed by Lysmer and Waas and generalized by Kausel. The latter method, among other things, allows the lateral boundary to be placed directly at the side of the foundation, with a considerable reduction in the number of degrees of freedom.

Non-linearity of soil behavior can be modeled with non-linear finite elements, but the necessary time-domain analysis, is very expensive with most methods. Alternatively, non-linearity could theoretically be simulated in repetitive linear model analyses with adjustment of modulus and damping in each cycle as a function of strain level. In frequency-domain solutions (for example, when using consistent boundaries) non-linearity can be approximately simulated again using an iterative approach. In a study of a nuclear containment structure, Krusel showed that the iterative linear approach was adequate for structural response calculations, the costly full non-linear analysis only being warranted for detailed investigation of soil behavior at or near failure.

As in the half-space solutions, material damping may be accounted for by using a viscoelastic finite element model as used by Kausel and Roesset, or the Rayleigh damping model may be used.

A recent major development by Bayo and Wilson permits a time-domain solution with much greater computational efficiency than was previously possible, due to the use of Ritz vectors rather than exact eigenvalues for free-vibration mode shapes. Factors that may be incorporated include structural embedment, arbitrary soil profile, flexibility of the foundations, spatial variations of free field motions, interaction between two or more structures, and non-linearity of soil and structure.

## 4.4 FLUSH Program

Analyses of soil-structure interaction effects during earthquake for the structure are usually made by one of two methods. Either by means of complete interaction analysis involving consideration of the variation of methods in the structure and the adjacent soil, or by an inertial analysis in which the motions in the adjacent soil are assumed to be the same at all points above foundation depth. For surface structure, the distribution of free field motions in the underlying soil has no influence on the structure response. For embedded structures, consideration of the variation of ground motions with depth is essential if adequate evaluations of soil and structural response are to be obtained without undue conservatism. A simple structure is involved accurate evaluations of the motions at the base of the structure can be obtained using two-dimensional analytical model.

### 4.4.1 Two-dimensional Finite Element Analyses

A complete analysis of the soil-structure interaction problem would involve a determination of the response of a structure when it is subjected to earthquake ground motions which vary from point to point in the soil and rock around and underlying the structure and travel in some unknown way across the base of the structure. This admittedly complex problem is usually idealized for purposes of analysis so that motions in the vicinity of the structure are considered to be due to vertical propagation of body waves from underlying stiffer formations.

A control motion specified at some point in the free-field soil profile can be deconvolved to determine the corresponding motions at some depth such as soil-rock interface. One dimensional amplification theory can be used for this purpose (Schnabel et al, 1972). Next, the motion computed at this depth is used as input to a finite element model of the soil structure system and the response computed at points of special interest (Seed et al, 1975). Another method of approach is to compute transfer functions relating the motions and forces at desired points in the soil or structure to the control motion applied at the point on the surface of the soil well away from the structure (Kausel, 1974). In either case, the analysis should be performed iteratively to allow for the strain dependent nature of the non-linear soil characteristics (Seed and Idriss, 1967;

Schnabel et al, 1972). In each iterations the analysis is linear but the soil properties are adjusted from iteration to iteration until the computed strains are compatible with the soil properties used in the analysis.

Using this approach, different soil properties may be assigned to every element so that there is no difficulty in considering the variation of soil characteristics with depth, while the iteration procedure permits consideration of the non-linear stress-strain and damping characteristics of the soils. In order to control the damping ratio to the desired value it has been found desirable to use the complex response method of analysis.

The general method of approach in the seismic analysis of the structure is to specify a prescribed control motion in the free field, usually at the ground surface or at the depth of the base of the structure to be analyzed. If the finite element method is used for the soil-structure interaction analysis, it is necessary to determine the free field motion at a depth corresponding to the rigid base of the overall finite element model. This motion is then used as base excitation of the two-dimensional finite element system.

The rigid base motion can be computed by means of a one-dimensional wave propagation analysis of the soil column in the free field. In this research, strain compatible dynamic soil properties were obtained by using the equivalent linear method (Seed and Idriss, 1969) and the strain-soil property relationship presented by Seed and Idriss (1970).

The finite element formulation used in the analysis of both axis-symmetry and plane strain soil-structure system is based on the complex response method. This method considers frequency independent damping values for each element. The advantages of this method over more conventional methods using mode superposition or step by step integration techniques are derived by Seed. The strain dependency of the dynamic soil properties during strong earthquake is accounted for one-dimensional wave propagation analysis. The results shown in this research were obtained using the computer program FLUSH.

## 4.5 Numerical Analysis

The analytical procedure is essentially two-dimensional and the equation of motion for a finite element representation of the system can be written

$$[M]\{\ddot{u}\} + [K]\{u\} = -\{m\}\ddot{y} - \{V\} + \{F\} - \{T\}$$

(18)

where $\{u\}$ are the displacements of the nodal points relative to the rigid base, $[M]$ and $[K]$ are the usual plane strain mass and stiffness matrices respectively. A slice of unit thickness and $\{m\}$ is a vector related to [M] and the direction of the rigid base acceleration, $\ddot{y}'(t)$. Material damping can be included by forming $[K]$ from complex modulus.

The force $\{V\}$ originate from the viscous boundaries on the plannar sides of the slice. These forces are

$$\{V\} = \frac{1}{L}[C](\{\dot{u}\} - \{\dot{u}\}_f)$$

(19)

where $L$ is the thickness of the slice, $[C]$ is a simple diagonal matrix which depends on the properties of the free field, and {} are the known free field velocities.

The forces $\{F\}$ act at the ends of the slice. They are merely the forces which act on a vertical plane in the free field and they involve no horizontal transmission of wave energy. These forces are

$$\{F\} = [G]\{u\}_f$$

(20)

where $[G]$ is a simple frequency-independent stiffness matrix formed from the complex modulus in the free field. The forces related to the energy transmission are

$$\{T\} = ([R] + [L])(\{u\} - \{u\}_f)$$

(21)

where $[R]$ and $[L]$ are the frequency-dependent boundary stiffness matrices introduced by Lysmer and Drake. These matrices represent the exact dynamic effect of the semi-infinite viscoelastic soil system at both ends of the model.

The equation of motion can be solved by the complex response method which assumes that the input motion can be written as a finite sum of harmonics, i.e. truncated Fourier series

$$\ddot{y}(t) = \mathrm{Re}\sum_{s=0}^{N/2}\ddot{Y}_S \cdot \exp(i\omega_s t)$$

(22)

where $N$ is the number of digitized points in the input motion.

This implies that the response can also be written as Fourier series

$$\{u\} = \text{Re} \sum_{s=0}^{\frac{N}{2}} \{U\}_s \cdot \exp(i\omega_s t) \tag{23}$$

$$\{u\}_f = \text{Re} \sum_{s=0}^{\frac{N}{2}} \{U_f\}_s \cdot \exp(i\omega_s t) \tag{24}$$

The amplitudes $\ddot{Y}_s$ and $\{U_f\}_s$ can be found easily by the Fast Fourier Transform algorithm. Substitution of eqs 19 to 21 and corresponding terms of Eqs 22 to 24 into the equation of motion, Eq. 18, yields.

$$([K]+[R]_s+[L]_s+\frac{i\omega_s}{L}[C]-\omega_s^2[M])\{U\}_s$$
$$=-\{m\}\ddot{Y}_s+([G]+[R]_s+[L]_s+\frac{i\omega_s}{L}[C])\{U_f\}_s \tag{25}$$

which is nothing but a set of linear equations which determines the displacement amplitudes $\{U\}_s$ at each frequency $\omega_s$, $s=0, 1, ..., \frac{N}{2}$. The equations can be solved by Gaussian elimination and the displacements in the time domain follow from eq 23 by the inverse Fast Fourier Transform.

### 4.5.1 Boundary Conditions

These boundary conditions simulated the exact dynamic effects of the semi-infinite viscoelastic horizontally layered soil system beyond the finite element region. The lateral boundaries can in principle be placed right at the edges of the structures. However, if several iterations are required to account for nonlinear soil properties it might be necessary to move the transmitting boundaries further away from the structures. A distance of one to three elements will usually be sufficient. Besides the transmitting boundary conditions it is also possible to restrain nodes from moving in relation to the rigid base. This can be done separately for horizontal and vertical components of displacement and is especially useful when advantage is taken of symmetry.

### 4.5.2 Mass Distribution

The mass matrix used for solid elements in and in the free field computations is the average of the lumped and consistent mass matrix. This distribution optimizes the ability of the element to transmit high frequency.

### 4.5.3 Stiffness and Damping

All stiffness and boundary matrices in the complex equation of motion are formed using the complex shear modulus.

$$G^* = G\left(1 - 2\beta^2 + 2i\beta\sqrt{1-\beta^2}\right) \approx G \cdot \exp(2i\beta) \qquad (26)$$

Where $\beta$ is the fraction of critical damping which may vary from element to element. It can be shown, by application to a simple damped oscillator, that for a system with uniform damping and no radiation damping (transmitting and viscous boundaries) the use of the above complex modulus will lead to exactly the same amplitudes as a modal analysis with the damping ratio $\beta$. A small error will occur in the phase of each mode but this is of no importance for the analysis. A special option is provided to simulate modal analysis by using the same damping in all elements.

Poisson's ratio is assumed to be real. This implies that P- and S-waves are assumed to have the same attenuation factor. This assumption may not be physically correct but is the best which can be made with present knowledge of wave propagation in soils.

### 4.5.4 Free Field Motions

The free field motions, $\{U\}_f$, appearing in Eqs 19, 29, 21 and 24 are computed separately on the assumption that the free field consists of horizontal soil layers and that the seismic excitation consists of vertically propagation P- or S-waves. From these assumptions, it is sufficient to consider a single column of elements because all points at the same level have identical motions. The computations are performed in the frequency domain in terms of the free field amplitudes which can be expressed as

$$\{U_f\}_s = \{A_f\}_s \cdot \ddot{Y}_s, \qquad s = 0,\ 1,\ \dots \frac{N}{2} \qquad (27)$$

where the $\{A_f\}_s$ is a vector containing the amplification values from the rigid base accelerations to layer displacements.

The seismic input to the computer program FLUSH consists of a vertical or horizontal time history of acceleration digitized at $N$ points at the constant time interval, $\Delta t$. This control motion can be specified to exist at any depth in the free field, say at the top of the $j^{th}$ soil layer. The program determines the rigid base acceleration from the inverse of Eq. 27. i.e.

$$\ddot{Y}_s = U_{js} / A_{js}; \; s = 0, \, 1, \, ..., \, \frac{N}{2} \tag{28}$$

Where $U_{js}$ and $A_{js}$ are the $j^{th}$ component of $\{U_f\}_s$ and $\{A_f\}_s$, respectively. This process, which is known as deconvolution, may or may not involve iteration on the soil properties. The iteration process is controlled by the allowable difference between soil properties in successive iterations. The iterations can be suppressed by using strain-independent soil properties.

### 4.5.5 The Method of Complex Response

Substitute of Eq 27 into Eq 25 give the new equation of motion

$$[K]_s \{U\}_s = \{P\}_s \cdot \ddot{Y}_s \tag{29}$$

Where $[K]_s$ is the frequency-dependent stiffness matrix.

$$[K]_s = [K] + [R]_s + [L]_s + \frac{i\omega_s}{L}[C] - \omega_s^2[M] \tag{30}$$

and

$$\{P\}_s = \left( [G] + [R]_s + [L]_s + \frac{i\omega_s}{L}[C] \right)\{A_f\}_s - \{m\} \tag{31}$$

is the load vector corresponding to unit amplitude of the rigid base motion ($\ddot{Y}_s$ =1). In the above equations the subscript "s" indicates frequency dependence and the stiffness and damping matrices are formed from complex modulus to simulate viscous damping, see Eq 26

The linear equation of Eq 29 can be solved by Gaussian elimination. However, rather than solving Eq 29 directly, it is convenient first to find the solution of

$$[K]_s\{A\}_s = \{P\}_s \tag{32}$$

where $\{A\}_s$ is the response corresponding to unit amplitude of the rigid base motion. Since $[K]_s$ and $\{P\}_s$ are smooth functions of frequency, the components of $\{A\}_s$, here called amplification functions, will also be smooth function of $\omega$. Hence, if Eq32 is solved for a few points in the frequency domain, $\omega = \omega_s$; s= 1, 5, 9, 13, ...., the intermediate points can be obtained by interpolation. This will lead to significant saving time. Having thus determined the amplification functions the complete response follows from Eq 23.

$$\{u\} = \text{Re}\sum_{s=0}^{\frac{N}{2}}\{A\}_s\ddot{Y}_s\exp(i\omega_s t) \tag{33}$$

which can be evaluated by inverse Fast Fourier Transform algorithm. Actually, since a constant acceleration is unrealistic, the program FLUSH, neglects the first term of Eq 33.

### 4.5.6 The Frequency Domain

The frequencies, $\omega_s = 2\pi\upsilon_s$, at which the amplification functions have to be determined are defined by

$$\upsilon_s = \frac{s}{T}, s = 1,...,\frac{N}{2} \tag{34}$$

where $\upsilon_s$ is the frequency in Hz and $T = N\Delta t$ is the total duration of the control motion. In the computer program FLUSH the number, $N$, of discretized points in the control motion is limited to values which are powers of 2. This restriction is no inconvenience because it is always possible, and in fact desirable, to augment the earthquake by a string of trailing zeros. This is so because the motion defined by Eq. 22 is periodic with the period $T = N\Delta t$. Hence, in order to simulate the finite duration of actual earthquake it is necessary to introduce a "quiet zone" at the end of each cycle to allow the viscous and radiation damping of the system time to attenuate the response from one cycle before the beginning of the next cycle. Fortunately, the damping of soils is high and the quiet zone usually needs to be only a few seconds long. Furthermore, the computation time required by FLUSH is nearly independent of the duration of the control motion. This is so because the frequency step $\Delta\upsilon = \frac{1}{T}$ is inversely proportional to the duration $T$.

Hence, as $T$ is increased the amount of interpolation on the amplification functions can be increased without loss of accuracy.

A typical control motion, might contain say $N$ = 1500 points digitized at a time interval of $\Delta t$ = 0.005 sec. This might be augmented by trailing zeroes to form a motion with $N = 2^{11}$ = 2048 points. Hence, in principle, Eq. 32 would have to be solved for $N/2$ = 1024 frequencies, a formidable computational task. Fortunately, this task can be reduced considerably by interpolation and truncation of the frequency domain.

The highest frequency contained in the control motion is the "folding" or "Nyquist" frequency

$$\upsilon_{\frac{N}{2}} = \frac{1}{2\Delta t} \tag{35}$$

which for the above motion would be 1/(2x0.005) = 100 Hz. Such high frequencies are usually not of interest and can be neglected by setting the high frequency terms of Eq. 32 equal to zero. This is done in program FLUSH by the introduction of a cut-off frequency, $\upsilon_{max}$ set by the input variable STEP (I). Say $\upsilon_{max}$ = 20 Hz, then only 20x 0.005x2048 = 205 solutions of Eq. 32 are required with the control motion considered. Since many of these solutions can be obtained by the above mentioned interpolation procedure Gaussian elimination of Eq. 32 may be required for only say 26 or 52 solutions.

### 4.5.7 Interpolation

The economy of the complex response method used in FLUSH is to a large degree due to the special interpolation scheme used on the complex amplification functions. This method is based on the observation that linear interpolation on the inverse of the complex amplification function for a simple damped oscillator with the natural frequency $\upsilon_f$ and the damping ratio $\beta$ will give a maximum relative error of only

$$e_{max} = \frac{\left(\frac{\Delta \upsilon_i}{\upsilon_f}\right)^4}{128\beta^2} \tag{36}$$

where $\Delta \upsilon_i$ is the width of the interval of interpolation. The maximum error will occur at the peak and will be an under-estimate at that point. Hence if the interpolation interval is

chosen to be $\Delta v_i = 0.25 \cdot v_f$ and the damping ration happens to be 10%, which is a typical value for soils, the maximum error made by interpolation will be only 0.3%. Since the individual peaks on the amplification functions for a multi-degree-of-freedom system are similar to the single peak for a one-degree-of-freedom system the above expression is also approximately valid at each of the above peaks with the appropriate value of $v_f$. This of course assumes that the peaks are well separated which appears to be so for most soil-structure interaction problems.

### 4.5.8 The Equivalent Linear Method

The above solution procedure makes extensive use of superposition and is therefore, strictly speaking, applicable only to linear viscoelastic systems. However, the large shear deformations which occur in soils during strong earthquakes introduce significant nonlinear effects and some method must be introduced to take these into account. This problem has been solved by Seed and Idriss (1969) by the introduction of the equivalent linear method. According to this method an approximate nonlinear solution can be obtained by a linear analysis provided the stiffness and damping used in the analysis are compatible with the effective shear strain amplitudes at all points of the system. Seed and Idriss (1970) have published data on strain-compatible soil properties for typical clays and sands. This data, here called material curves have been summarized in Table 11. This or any numbers of similar curves developed for specific materials may be input to program FLUSH which proceeds as follows:

A set of shear modulus and damping values is estimated for each soil element of the finite element model. The system is analyzed using these properties and the maximum shear strain time history is computed in each element of the model. From these time histories the effective shear strain amplitudes are estimated in each element and the appropriate material curves are consulted to see if the strain level is compatible with the values of shear moduli and damping used in the response evaluation. If the soil properties are not compatible the curves are entered to provide improved values of shear moduli and damping for the next interation and the process is repeated until convergence has occurred, usually within 3 to 5 interations. The response from the last iteration is taken as being the nonlinear response. The special modular structure of

FLUSH allows the user to perform one or several iterations at each run and to restart the iterative process if the convergence is not satisfactory.

Table 11 Strain-Compatible Soil Properties

| Effective Shear Strain (%) | Log ($\gamma_{eff}$) | Shear Modulus Reduction Factor[1] | | Fraction of Critical Damping (%) | |
|---|---|---|---|---|---|
| | | clay | sand | clay | sand |
| $\leq 1.0 \times 10^{-4}$ | -4.0 | 1.000 | 1.000 | 2.50 | 0.50 |
| $3.16 \times 10^{-4}$ | -3.5 | 0.913 | 0.984 | 2.50 | 0.80 |
| $1.0 \times 10^{-3}$ | -3.0 | 0.761 | 0.934 | 2.50 | 1.70 |
| $3.16 \times 10^{-3}$ | -2.5 | 0.565 | 0.826 | 3.50 | 3.20 |
| $1.0 \times 10^{-2}$ | -2.0 | 0.400 | 0.656 | 4.75 | 5.60 |
| $3.16 \times 10^{-2}$ | -1.5 | 0.261 | 0.443 | 6.50 | 10.0 |
| $1.0 \times 10^{-1}$ | -1.0 | 0.152 | 0.246 | 9.25 | 15.5 |
| 0.316 | -0.5 | 0.076 | 0.115 | 13.8 | 21.0 |
| 1.0 | 0 | 0.037 | 0.049 | 20.0 | 24.6 |

[1] This is the factor which has to be applied to the shear modulus at low shear strain amplitudes (here define $10^{-4}$ percent) to obtain modulus at higher strain level.

### 4.5.9 Effective Shear Strain Amplitudes

The effective shear strain amplitudes used in the equivalent linear method are taken as

$$\gamma_{eff} = 0.65 x \max|\gamma_{max}| \tag{37}$$

The factor 0.65 in the above equation is purely empirical. However, due to the relatively small slope of the material curves the final motions are not sensitive to

moderate, say ±10%, variations in this factor or in the estimate of the maximum shear strain.

Two procedures are provided in program FLUSH for the evaluation of the maximum shear strain in Eq. 37. The most direct, but also most expensive option, involves the computation and transfer to the time domain of the entire time history of maximum shear strain for each element. This option is used only if specifically requested.

The above transfer of the shear strains, into the time domain and the subsequent search for the maximum value requires considerable computer time and storage. For this reason it is recommended to use the second option which estimates the maximum shear strain by a root mean square procedure in the frequency domain. The effective strains computed in the time domain will be used on entering the material curves.

## 4.6 Finite Element Mesh of the Structure

The effect of soil-structure interaction on the seismic response of the structure is often studied by two-dimensional plane strain finite element model (Anderson, 1972; Isenberg, 1972; Seed and Idriss, 1973). Because of the approximation involved in analyzing a three-dimensional system by a two-dimensional model, the seismic response obtained may differ from that obtained by a three-dimensional analysis. Three-dimensional axis-symmetry finite element analyses have been reported by several researchers. However, there is only limited information available on the comparison of the seismic response obtained from two-dimensional and three-dimensional analyses.

The structure is an axis-symmetry model of masonry structure extends 74 meters above the ground surface. The soil profile consists of 17.83 meters, divided into 4 layers, overlying bedrock. The details of finite element mesh are given in Figure 29. The layer thicknesses for the mesh were chosen to match for each layer. The model extends horizontally over a distance of 10 meters beyond the structure to ensure recovery of the free field response. The vertical degrees of freedom at the free field boundary are suppressed.
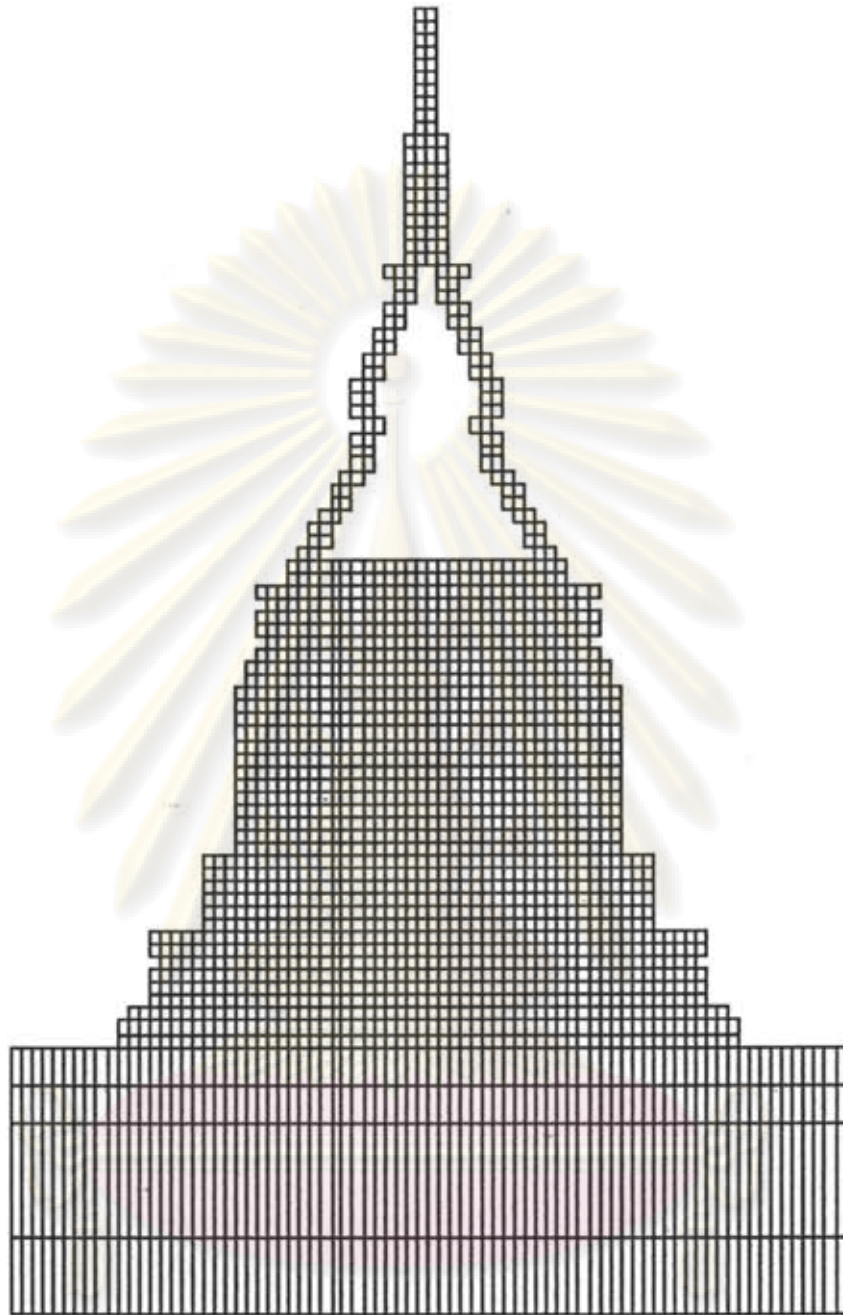
Figure 29 Detail of Chediluang finite element mesh

The plane strain finite element mesh has the same dimensions and mesh properties as those shown for the axis-symmetry model in Figure 30. This definition of the equivalent plane strain structural model is of considerable convenience because the meshes for the two analyses are identical. The adequacy of this simplifying assumption will be discussed subsequently.
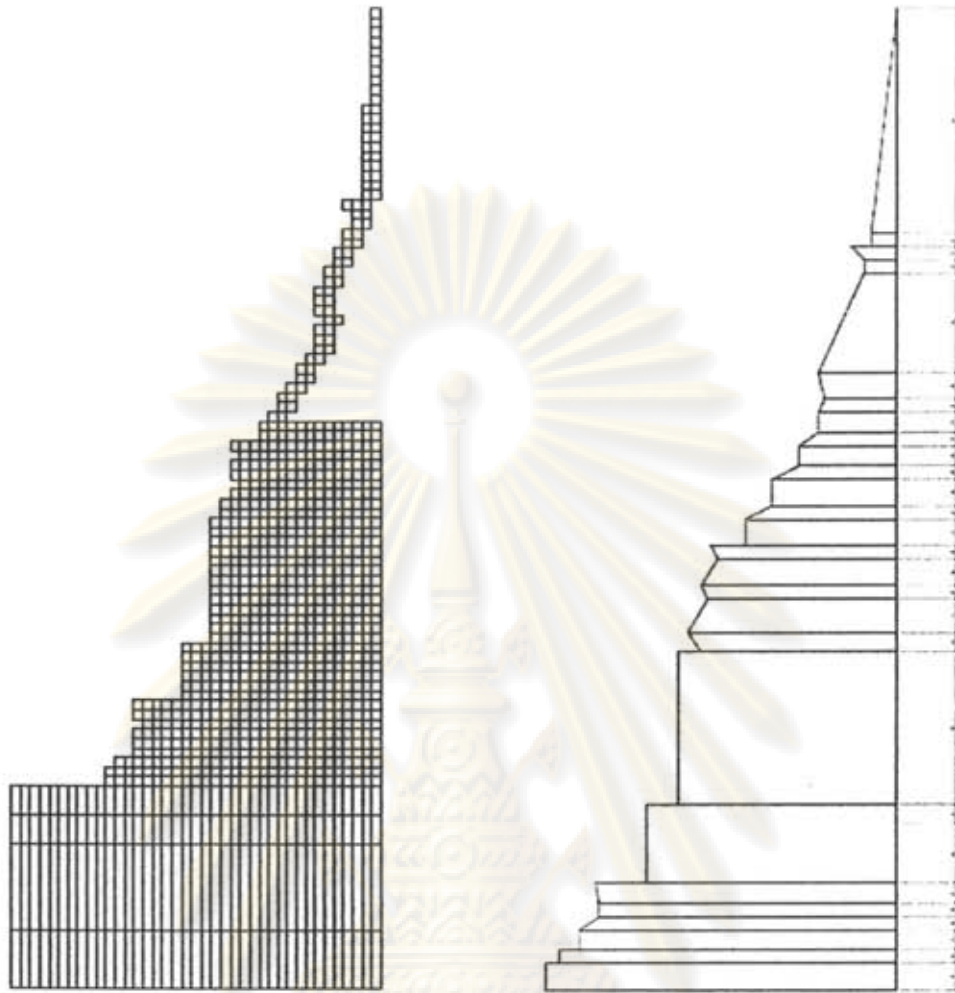
Figure 30 Mesh generation for FEM analysis

In this research, numerical results are presented which show the difference in seismic response as obtained from an axis-symmetry and an equivalent plane strain finite element analysis of a soil structure system. A finite element model used is shown conceptually in Figure 30. A comparison of the structure response computed by the two methods shows that there is good agreement for point below the ground surface, while pronounce are observed in the structure above the ground surface. Using a simplified substructure approach, it is shown that these differences are largely due to the different bending characteristics of the axis-symmetry and plane strain models of the structure above the ground surface.

# CHAPTER V
# RESULT AND DISCUSSION

## Determination of ground motion

The method for simulating ground motion is to combine parametric or functional descriptions of the ground motion's amplitude spectrum with a random phase spectrum modified such that the motion is distributed over a duration related to the earthquake magnitude and to the distance from the source. It is widely used to predict ground motions for the regions of the world in which recording of motion from potentially damaging earthquakes are not available. One of the essential characteristics of the method is that it distills what is known about the various factors affecting ground motion (source, path and site) into simple function forms Boore. The parameters for generating small ground motion for Maerim fault are summarized in Table 12 and 13.

In the analysis, waveforms of earthquakes having moment magnitude of 5, 6 and 7 are generated for Maerim and Maetha faults. Based on these two small earthquake records, the strong ground motion waveforms from both active faults are generated by Stochastic method. The synthetic wave forms of Maerim fault M5, M6 and M7 are shown in Figure 31-33, whereas the synthetic wave forms of Maetha fault M5, M6 and M7 on Richter scale are shown in Figure 34-36. Durations of vibration are less than 20 seconds. The peak accelerations (for outcrop motion) are about 66 gals (0.066g) for Maerim M7 and 37 gals (0.037g) for Maetha M7. By adopting the maximum magnitude of earthquake that can be produced from the faults of M7, waveforms of strong ground motion at the proposed site will be generated. Table 14 summarizes the maximum acceleration of the strong ground motion at the proposed site due to earthquake magnitude of M5 to M7 induced from Maerim faults and Maetha fault. Ground motions associated with peak accelerations of 66 gals (0.066g) can be expected at the proposed site due to earthquakes induced Maerim fault. The acceleration time histories expected at the proposed site is shown.

Table 12 Summary of parameters used for ground motion generation for Maerim Fault

| Data | Maerim M5 | Maerim M6 | Maerim M7 |
|---|---|---|---|
| Time step (sec) | 0.01 | 0.01 | 0.01 |
| Radiation coefficient | 0.63 | 0.63 | 0.63 |
| Influence of ground surface | 2.0 | 2.0 | 2.0 |
| Cut off frequency in high frequency region (Hz) | 10.5 | 10.5 | 10.5 |
| Rock density (g/cm$^3$) | 2.7 | 2.7 | 2.7 |
| Shear wave velocity (m/s) | 3500 | 3500 | 3500 |
| Stress drop (bar) | 50 | 50 | 50 |
| Focal distance (km) | 23 | 23 | 23 |
| Seismic moment of small earthquake, $M_o$ (dyne-cm) | $4.94 \times 10^{23}$ | $7.21 \times 10^{24}$ | $1.05 \times 10^{26}$ |
| Moment Magnitude of small earthquake, $M_w$ | 5.0 | 6.0 | 7.0 |
| $Q_v$ (Q value) switch | 5 | 5 | 5 |
| $T_w$ (Earthquake duration time) switch | 2 | 2 | 2 |
| $F_c$ (Corner frequency) switch | 1 | 1 | 1 |

Table 13 Summary of parameters used for ground motion generation for Maetha Fault

| Data | Maetha5 M5 | Maetha M6 | Maetha M7 |
|---|---|---|---|
| Time step (sec) | 0.01 | 0.01 | 0.01 |
| Radiation coefficient | 0.63 | 0.63 | 0.63 |
| Influence of ground surface | 2.0 | 2.0 | 2.0 |
| Cut off frequency in high frequency region (Hz) | 10.5 | 10.5 | 10.5 |
| Rock density (g/cm$^3$) | 2.7 | 2.7 | 2.7 |
| Shear wave velocity (m/s) | 3500 | 3500 | 3500 |
| Stress drop (bar) | 50 | 50 | 50 |
| Focal distance (km) | 23 | 38 | 38 |
| Seismic moment of small earthquake, $M_o$ (dyne-cm) | $4.94 \times 10^{23}$ | $7.21 \times 10^{24}$ | $1.05 \times 10^{26}$ |
| Moment Magnitude of small earthquake, $M_w$ | 5.0 | 6.0 | 7.0 |
| $Q_v$ (Q value) switch | 5 | 5 | 5 |
| $T_w$ (Earthquake duration time) switch | 2 | 2 | 2 |
| $F_c$ (Corner frequency) switch | 1 | 1 | 1 |

Figure 31 Maerim, M5.0, synthetic wave form generated by stochastic method
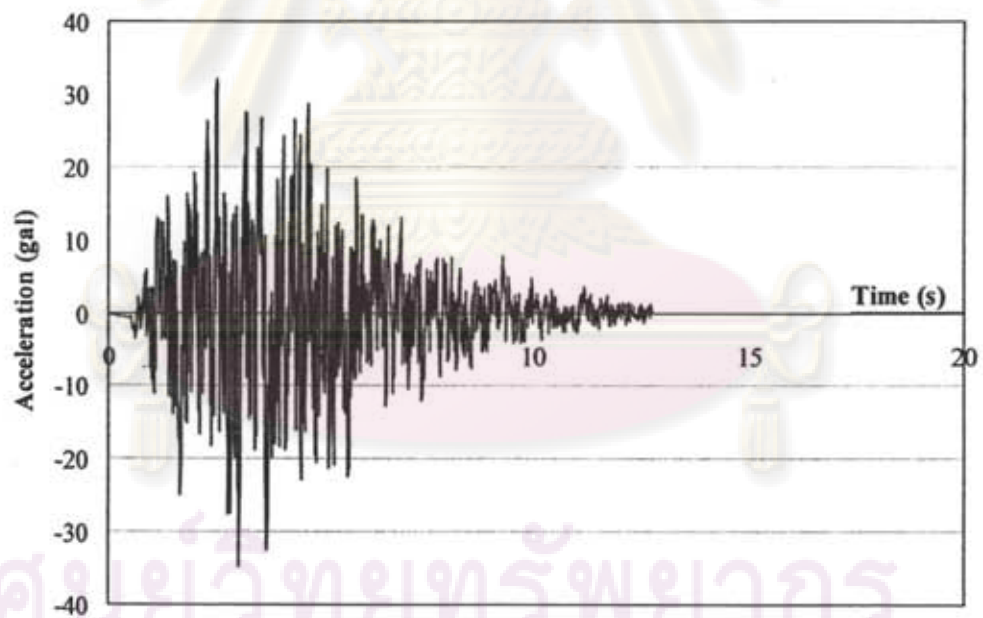


Figure 32 Maerim, M6.0, synthetic wave form generated by stochastic method
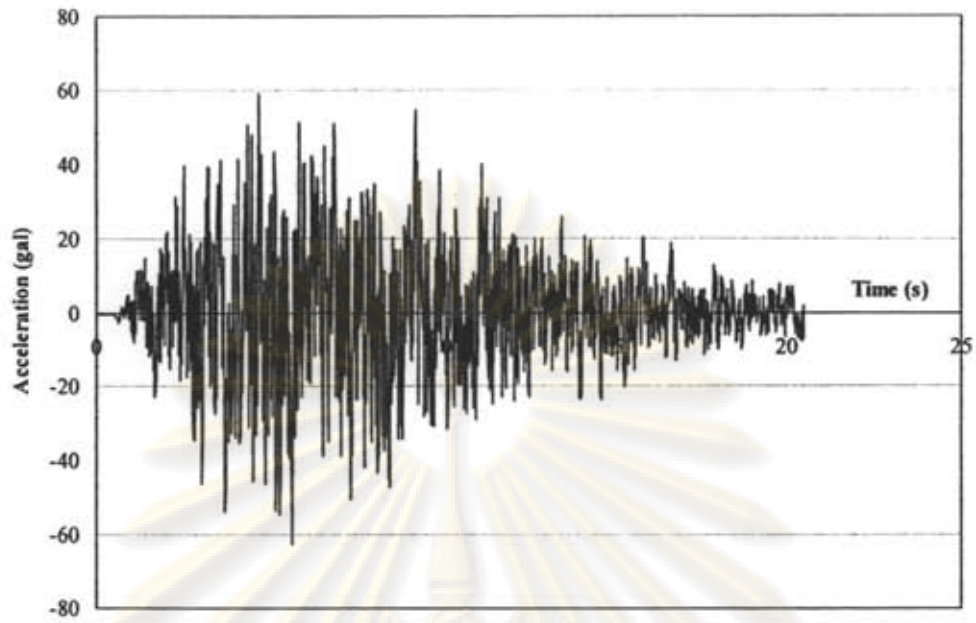
Figure 33 Maerim, M7.0, synthetic wave form generated by stochastic method
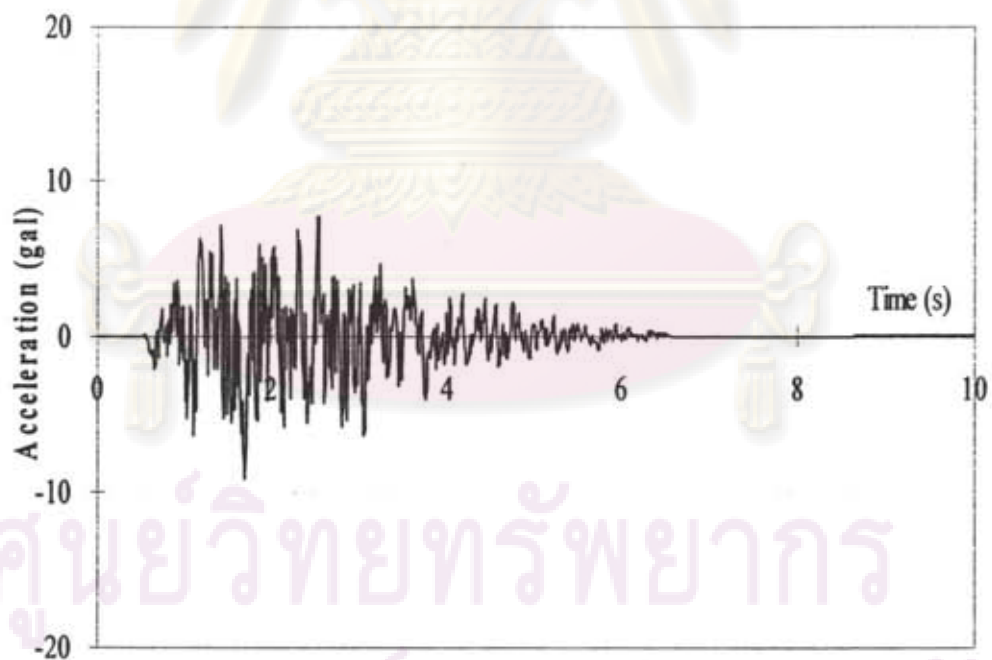


Figure 34 Maetha, M5.0, synthetic wave form generated by stochastic method
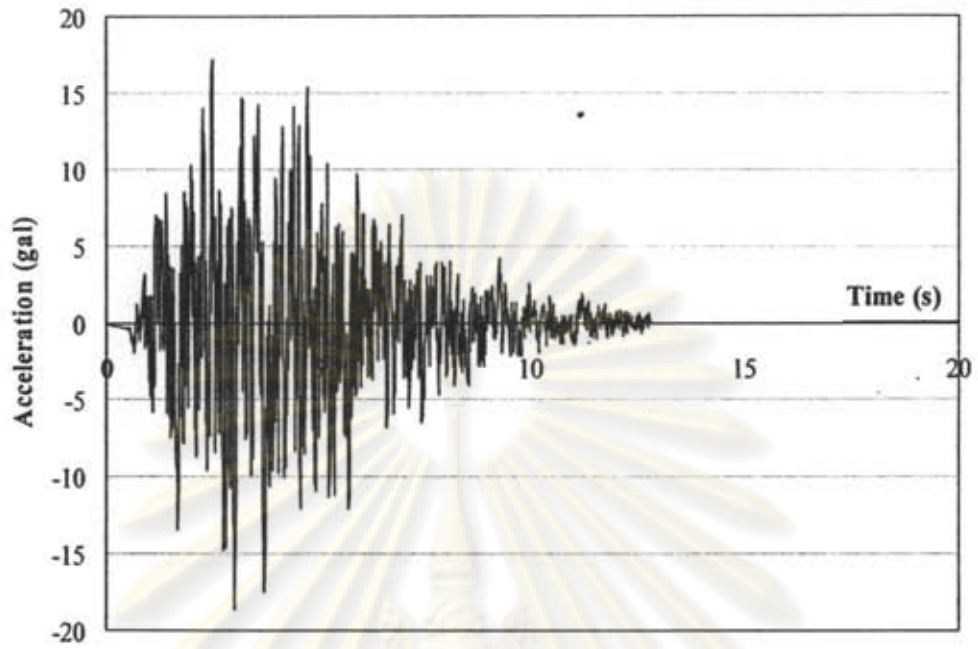
Figure 35 Maetha, M6.0, synthetic wave form generated by stochastic method
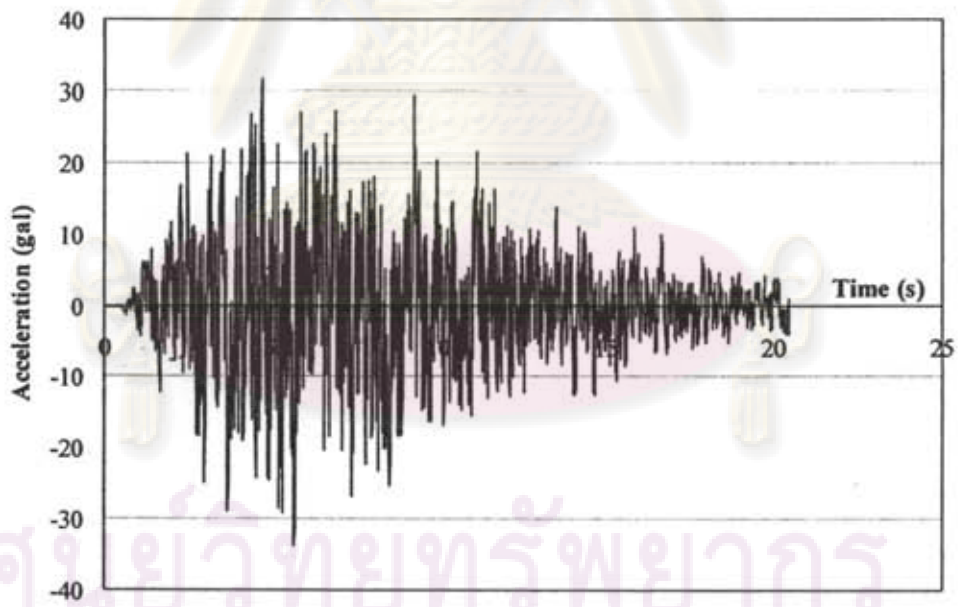


Figure 36 Maetha, M7.0, synthetic wave form generated by stochastic method
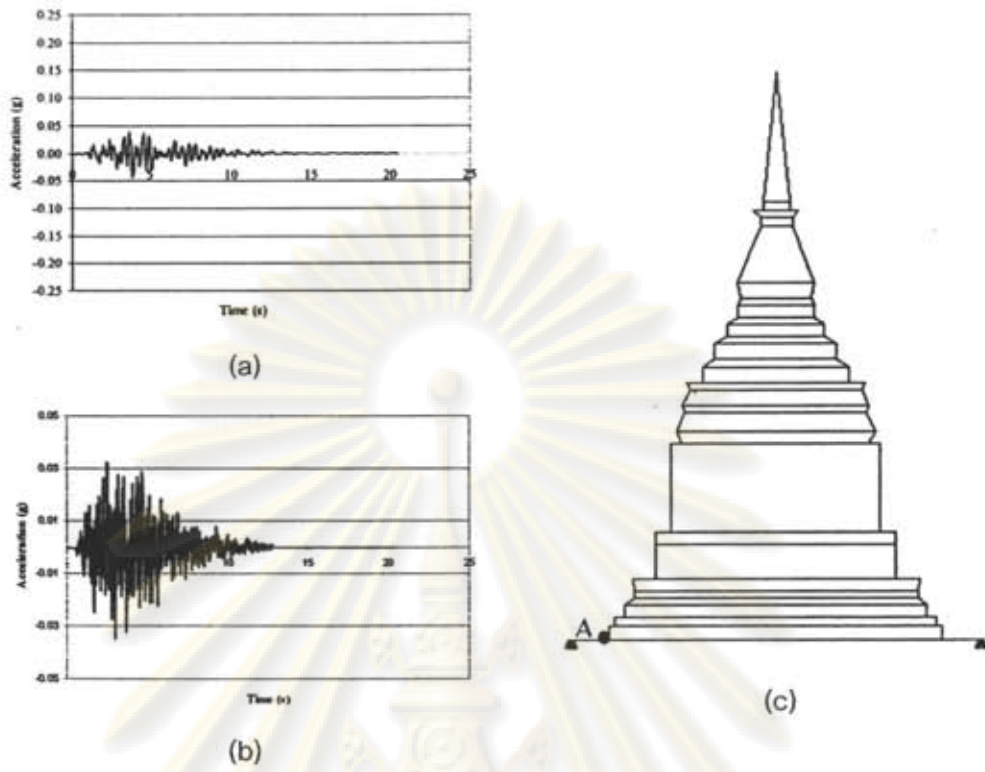
Figure 37 Acceleration-Time history for Maerim M5 at Point A
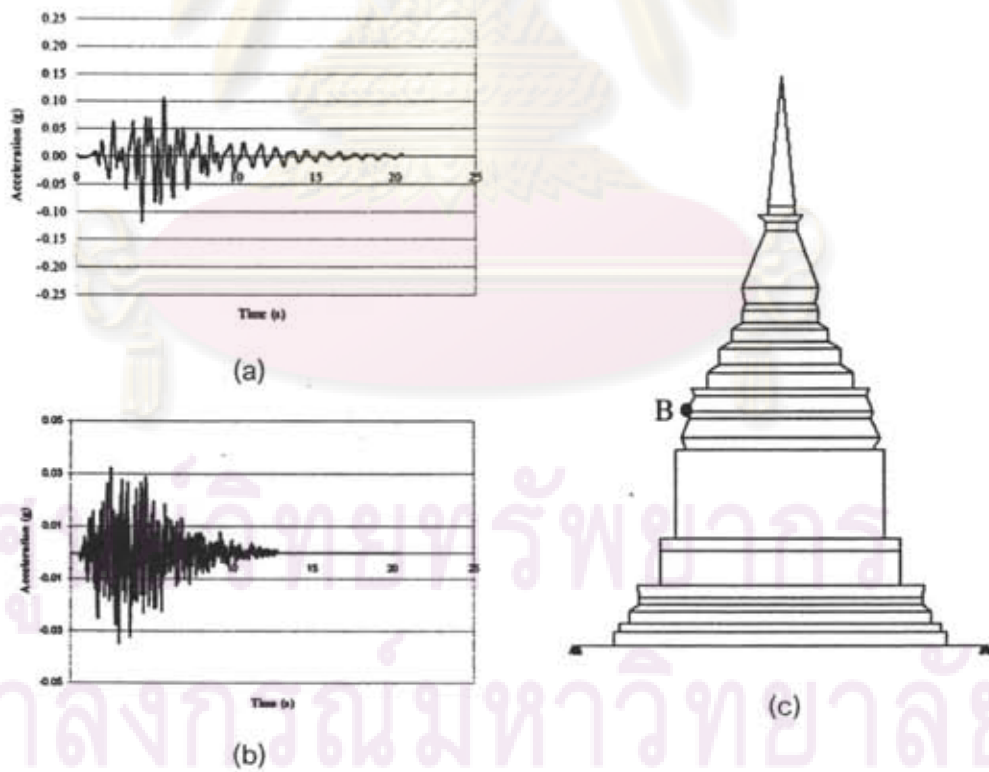


Figure 38 Acceleration-Time history for Maerim M5 at Point B
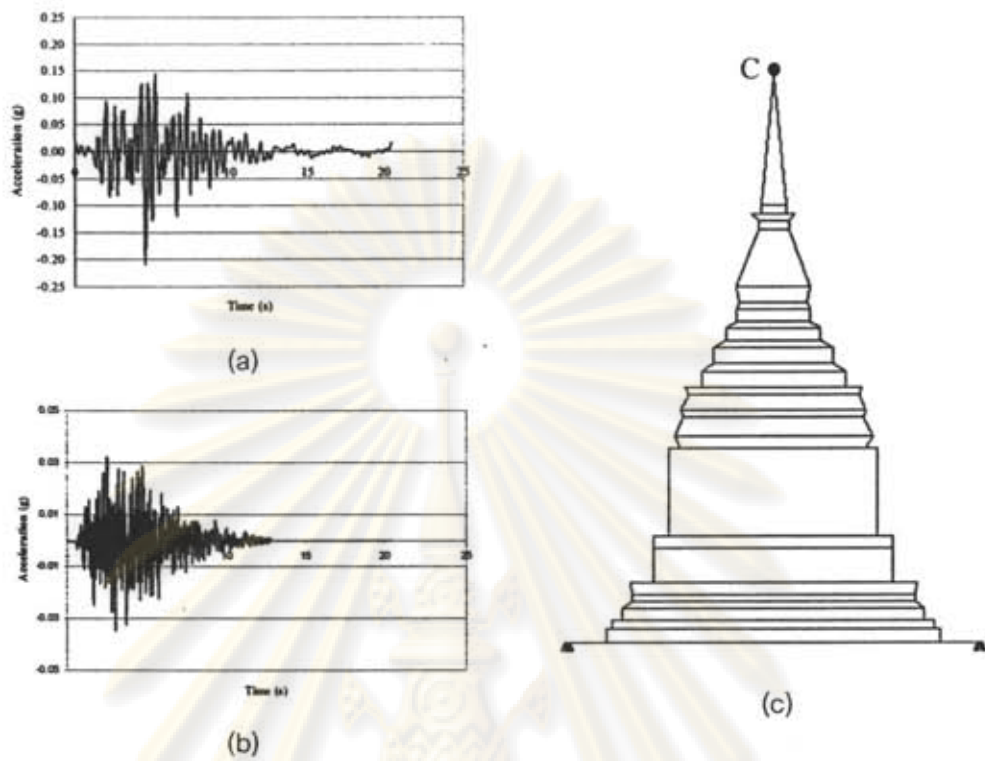
Figure 39 Acceleration-Time history for Maerim M5 at Point C
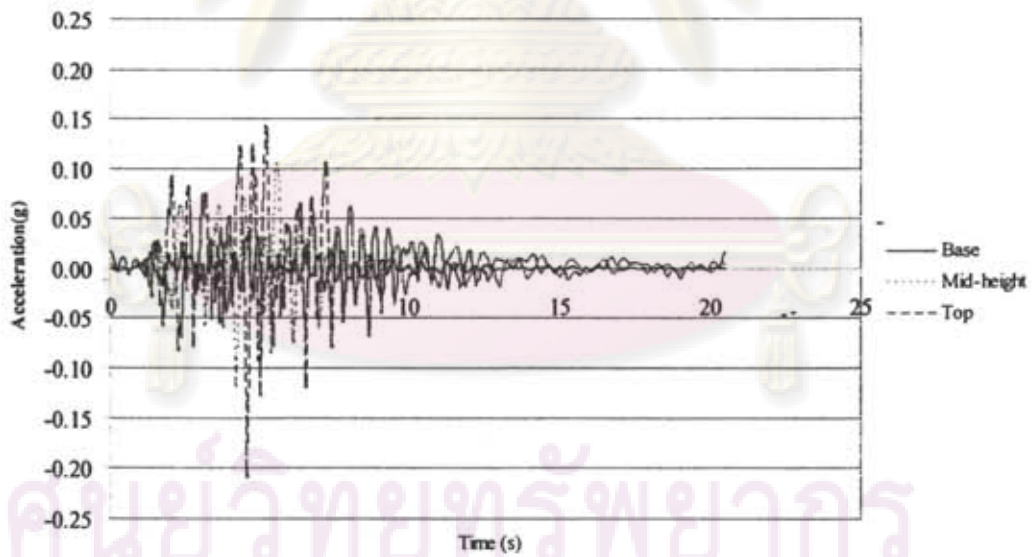


Figure 40 Comparison Acceleration-time history for Maerim M5 at each level
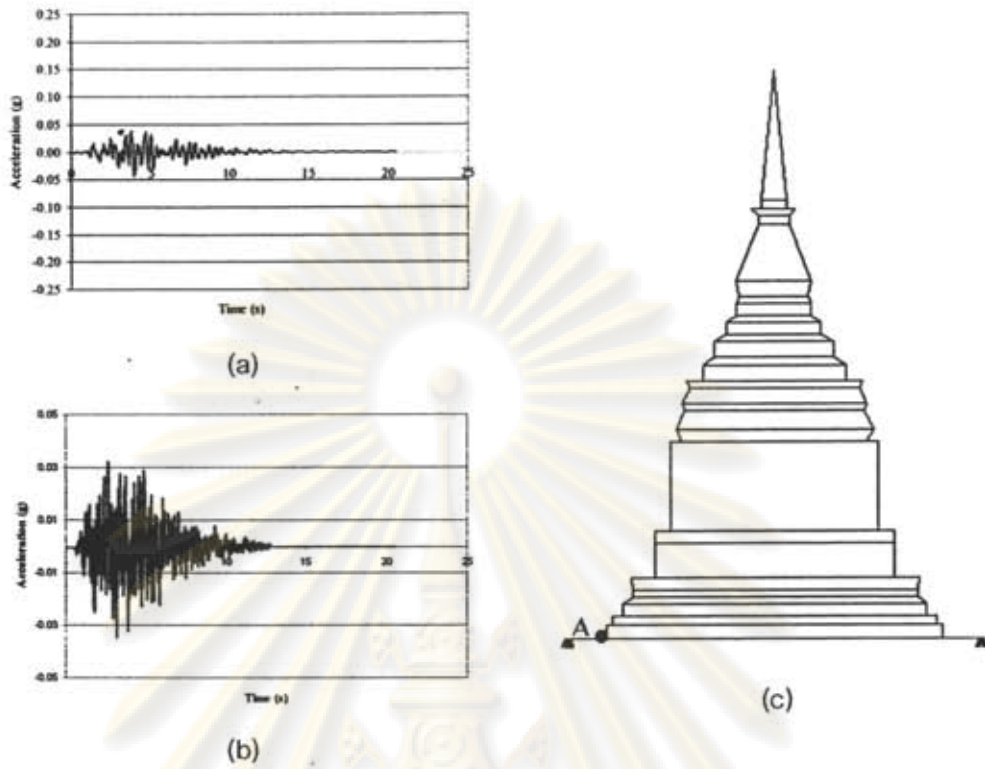
Figure 41 Acceleration-Time history for Maerim M6 at Point A
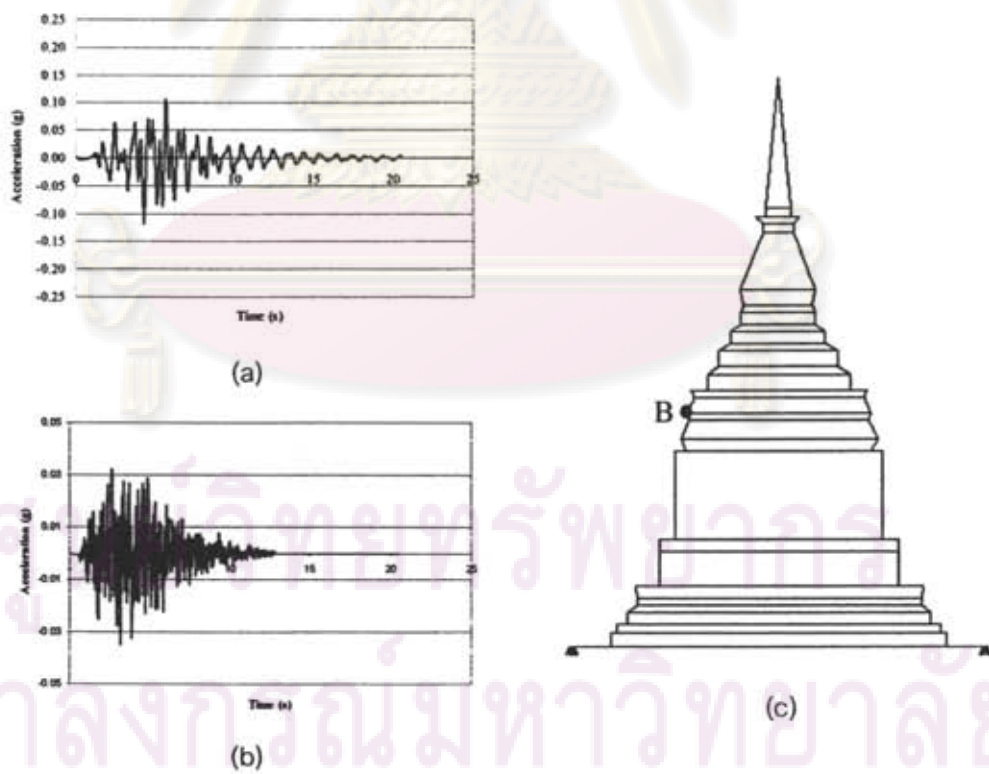


Figure 42 Acceleration-Time history for Maerim M6 at Point B
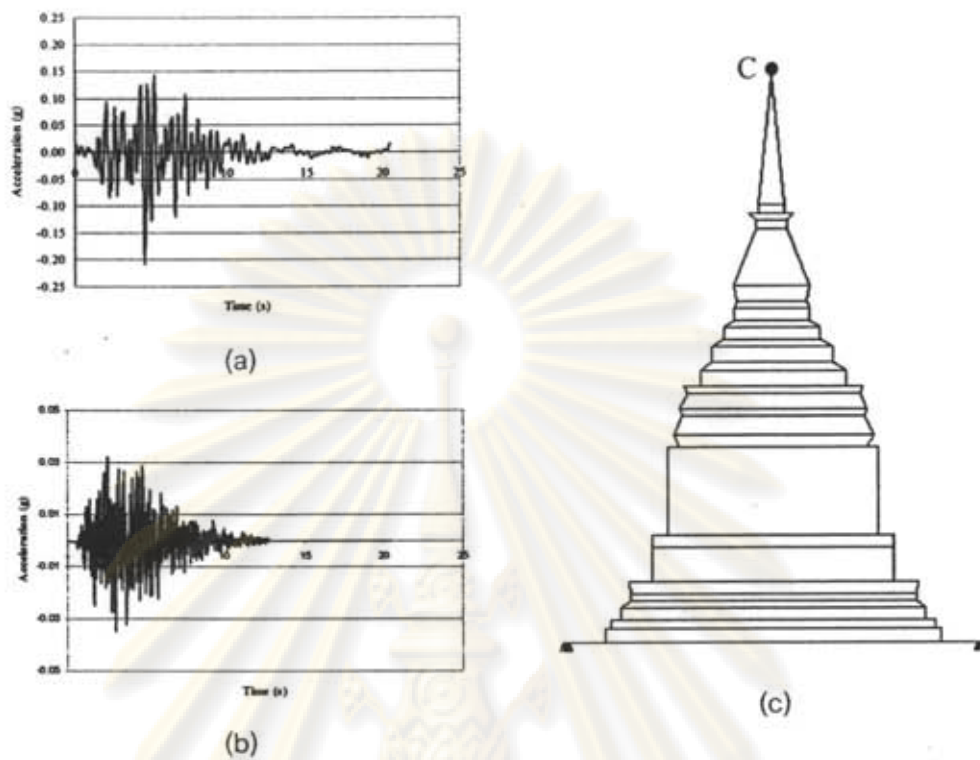
Figure 43 Acceleration-Time history for Maerim M6 at Point C
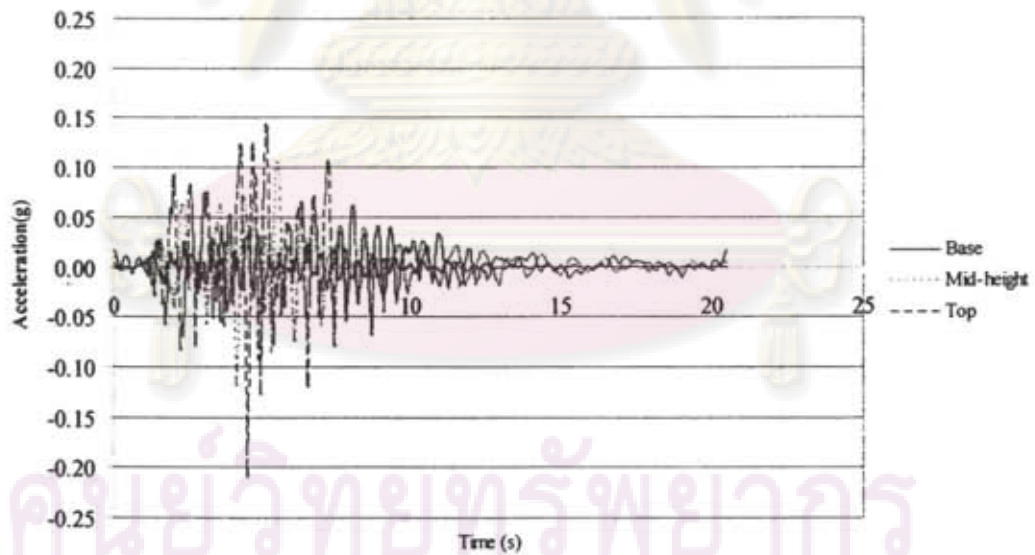


Figure 44 Comparison Acceleration-time history for Maerim M6 at each level
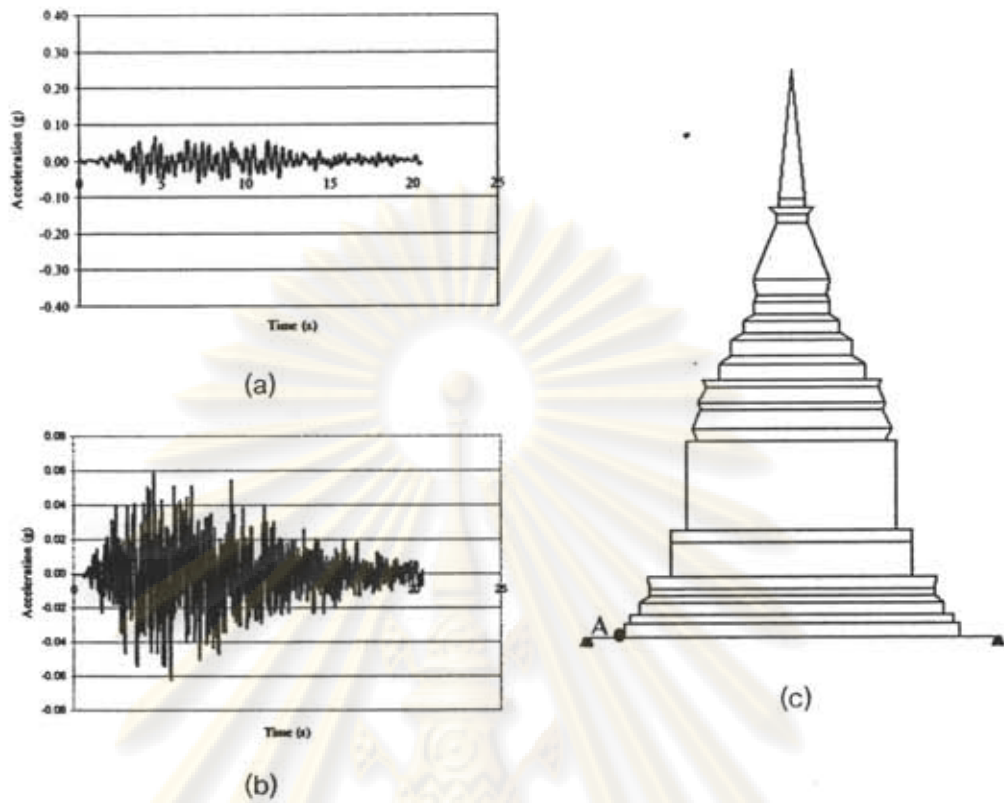
Figure 45 Acceleration-Time history for Maerim M7 at Point A
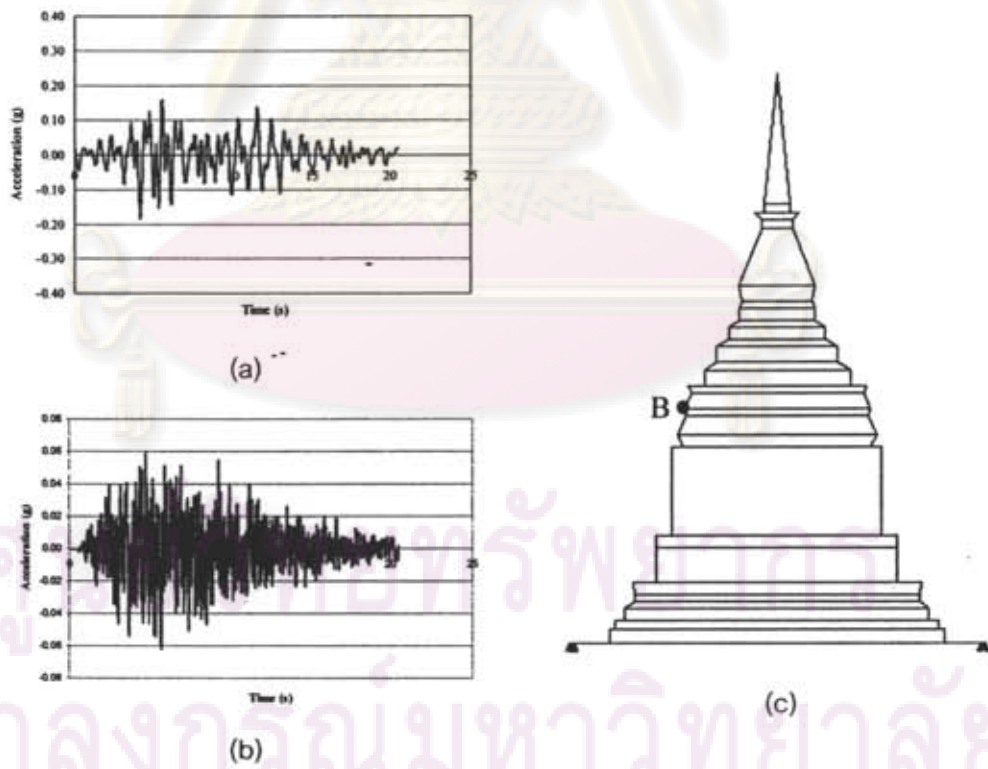


Figure 46 Acceleration-Time history for Maerim M7 at Point B

(a)

(b)

(c)
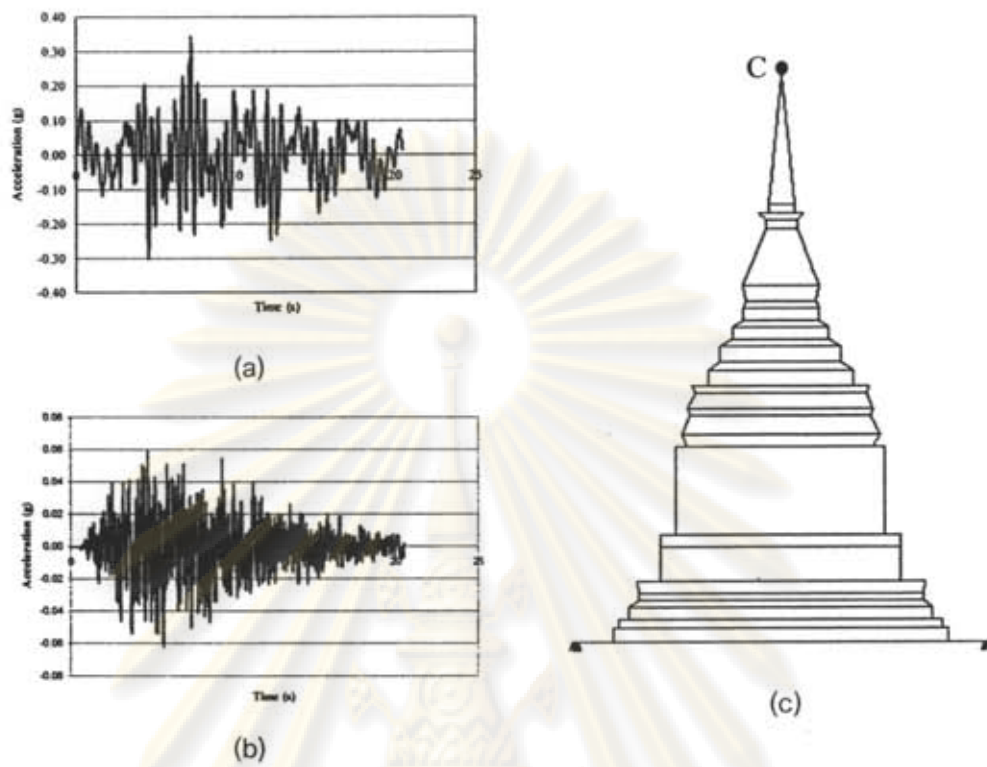
Figure 47 Acceleration-Time history for Maerim M7 at Point C
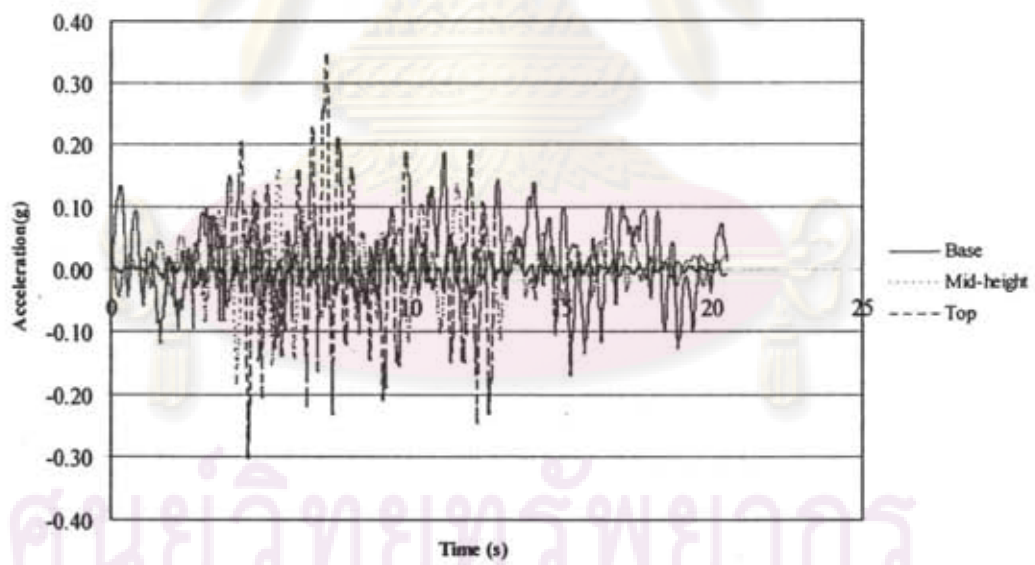


Figure 48 Comparison Acceleration-time history for Maerim M7 at each level
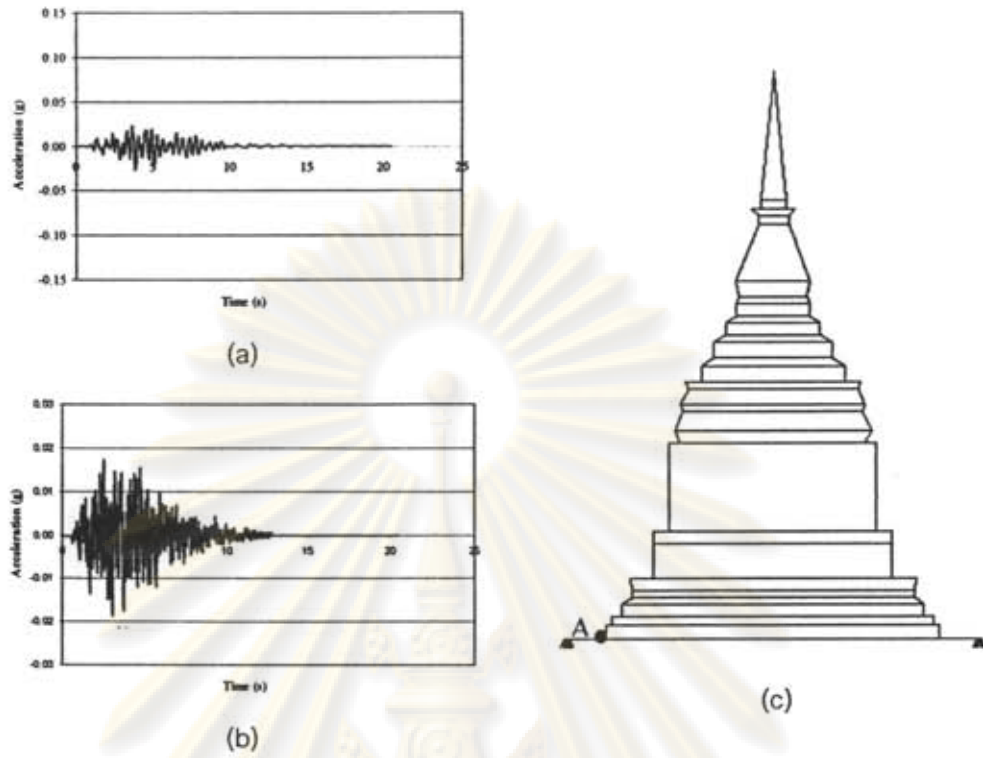
Figure 49 Acceleration-Time history for Maetha M5 at Point A
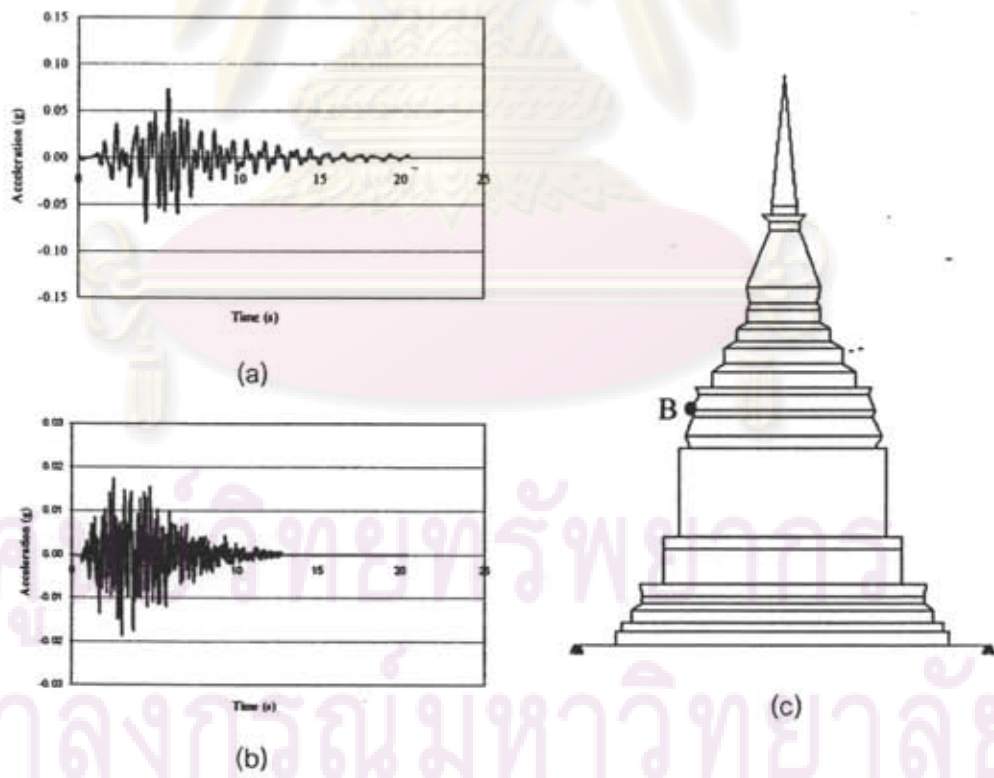


Figure 50 Acceleration-Time history for Maetha M5 at Point B
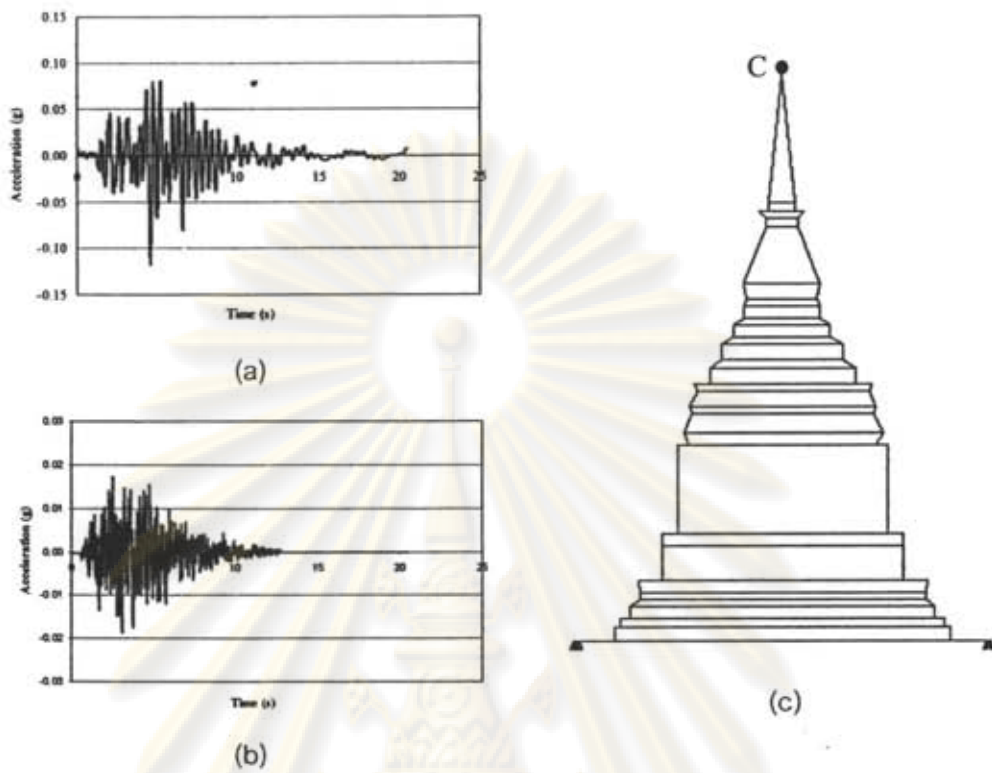
Figure 51 Acceleration-Time history for Maetha M5 at Point C
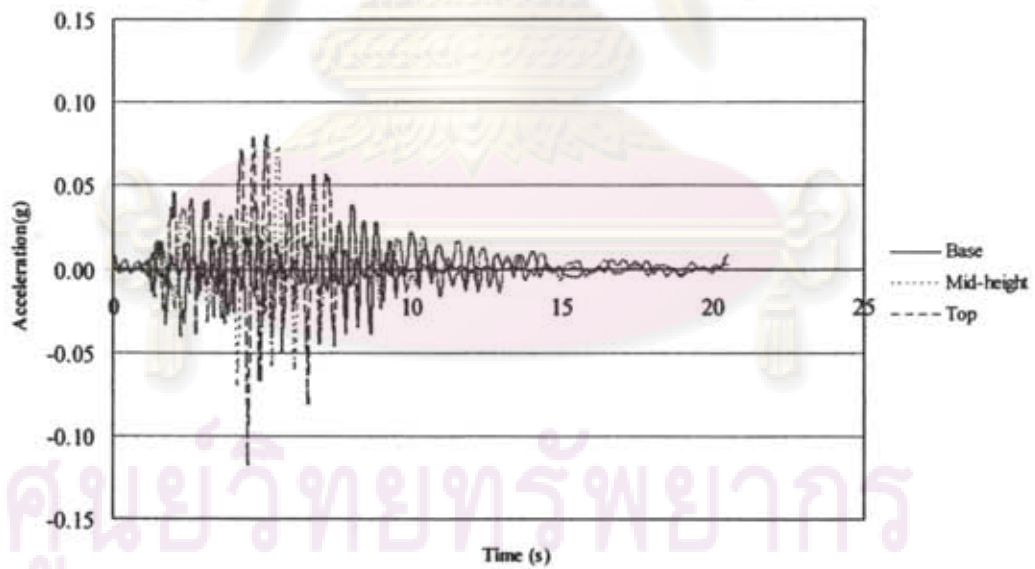


Figure 52 Comparison Acceleration-time history for Maetha M5 at each level
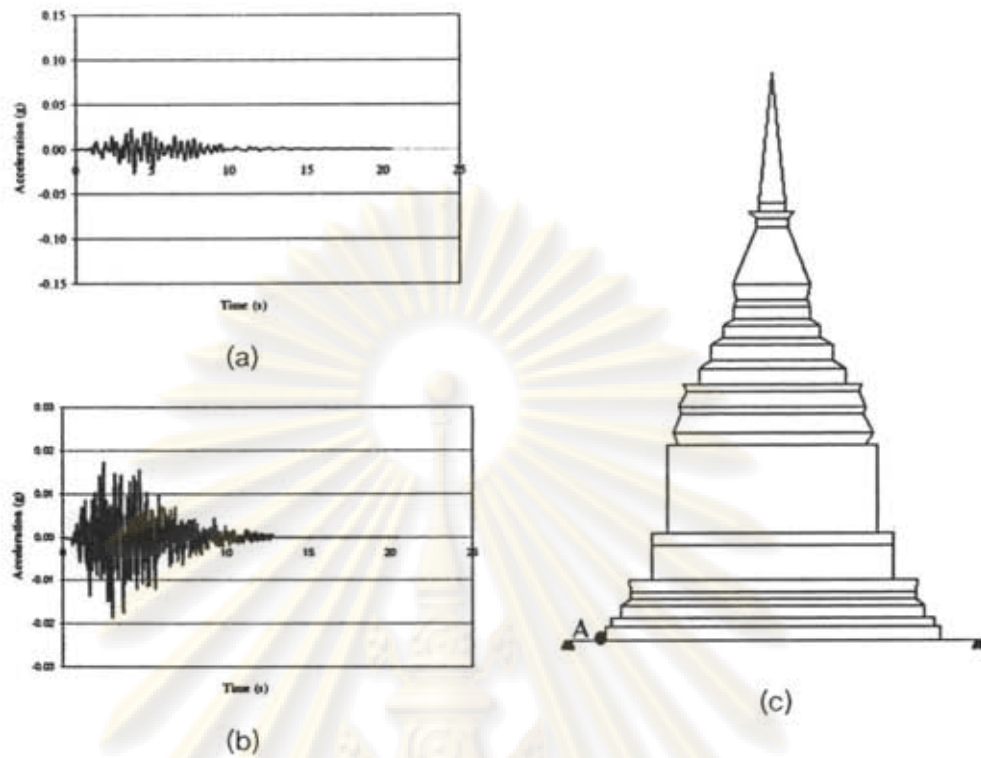
Figure 53 Acceleration-Time history for Maetha M6 at Point A
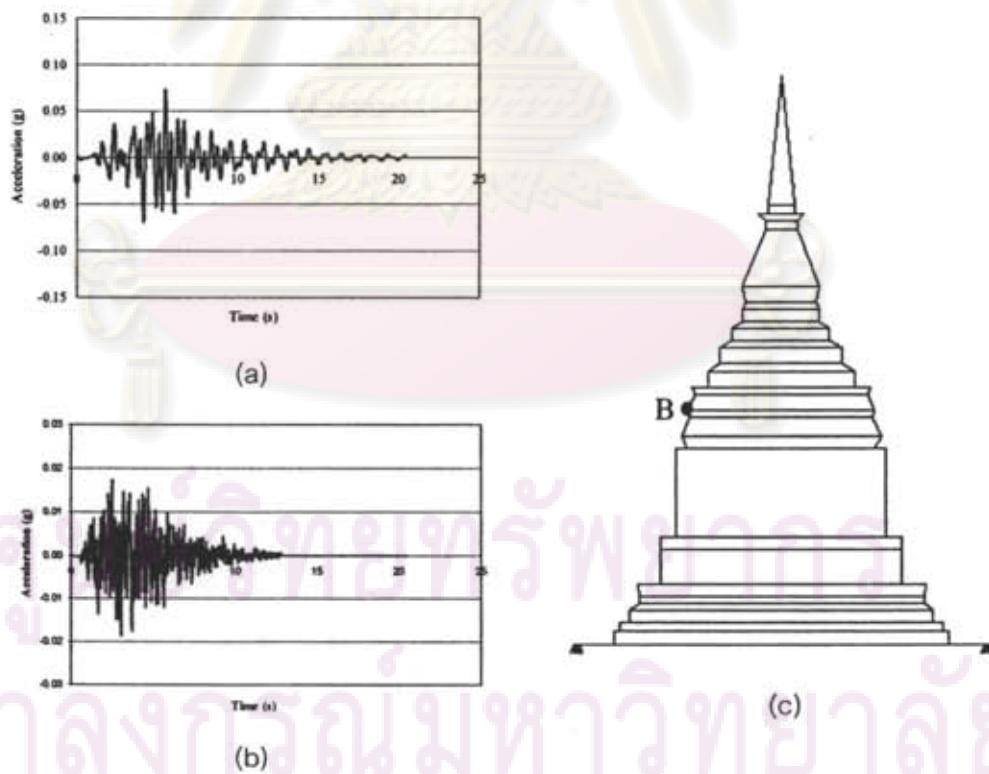


Figure 54 Acceleration-Time history for Maetha M6 at Point B
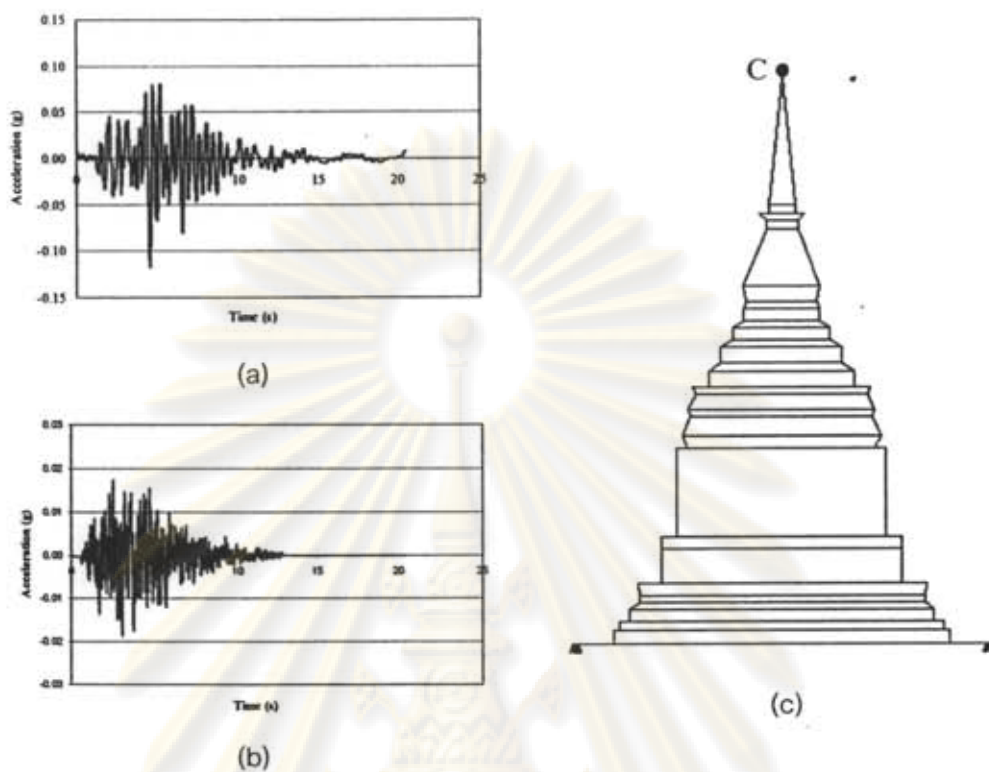
Figure 55 Acceleration-Time history for Maetha M6 at Point C
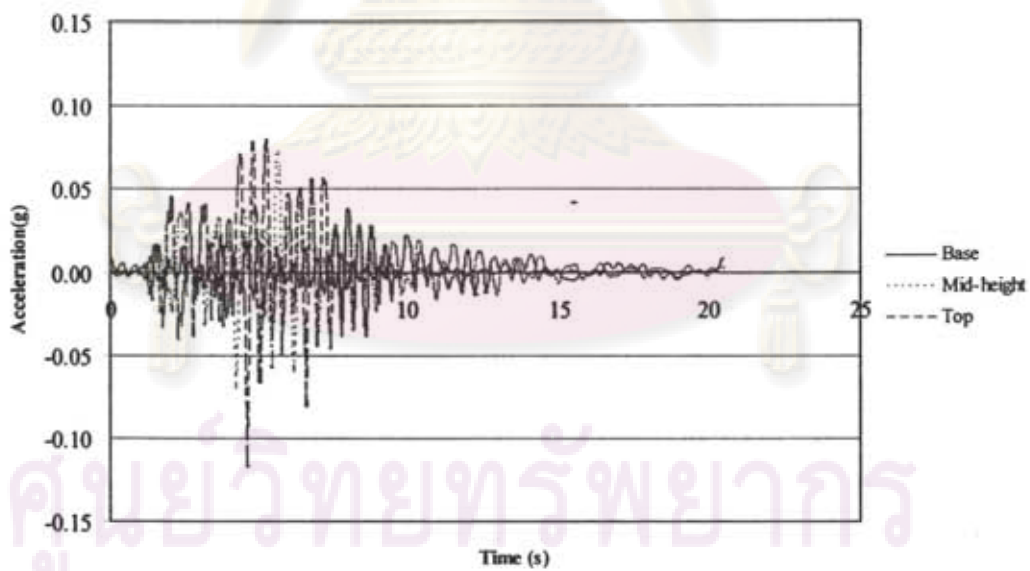


Figure 56 Comparison Acceleration-time history for Maetha M6 at each level
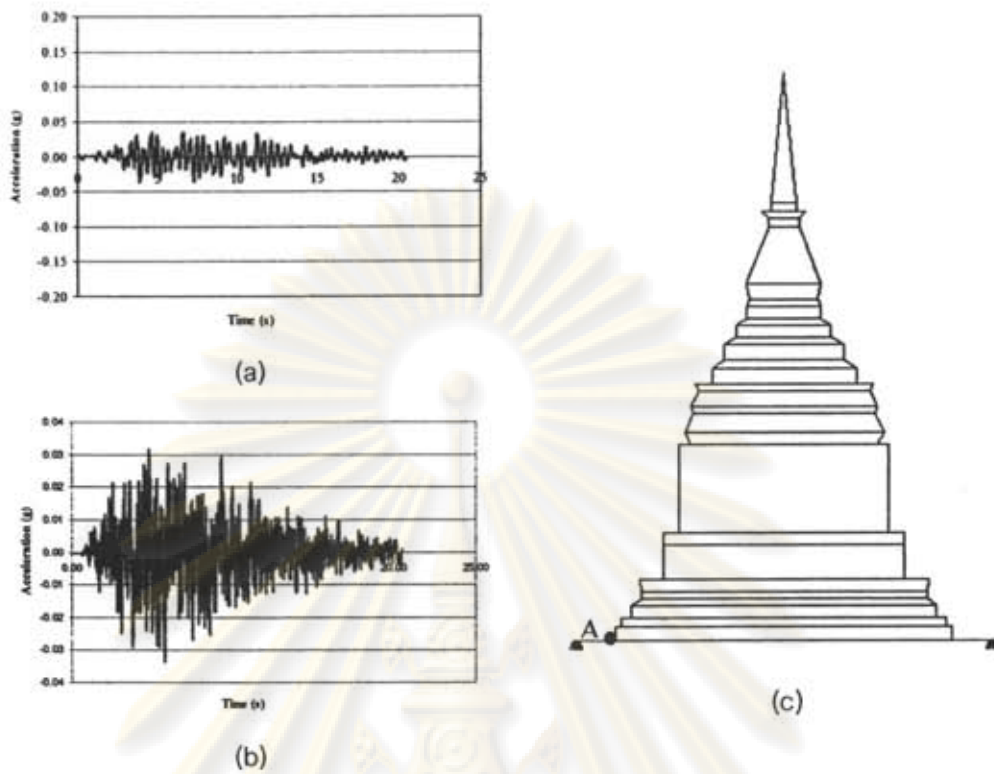
Figure 57 Acceleration-Time history for Maetha M7 at Point A
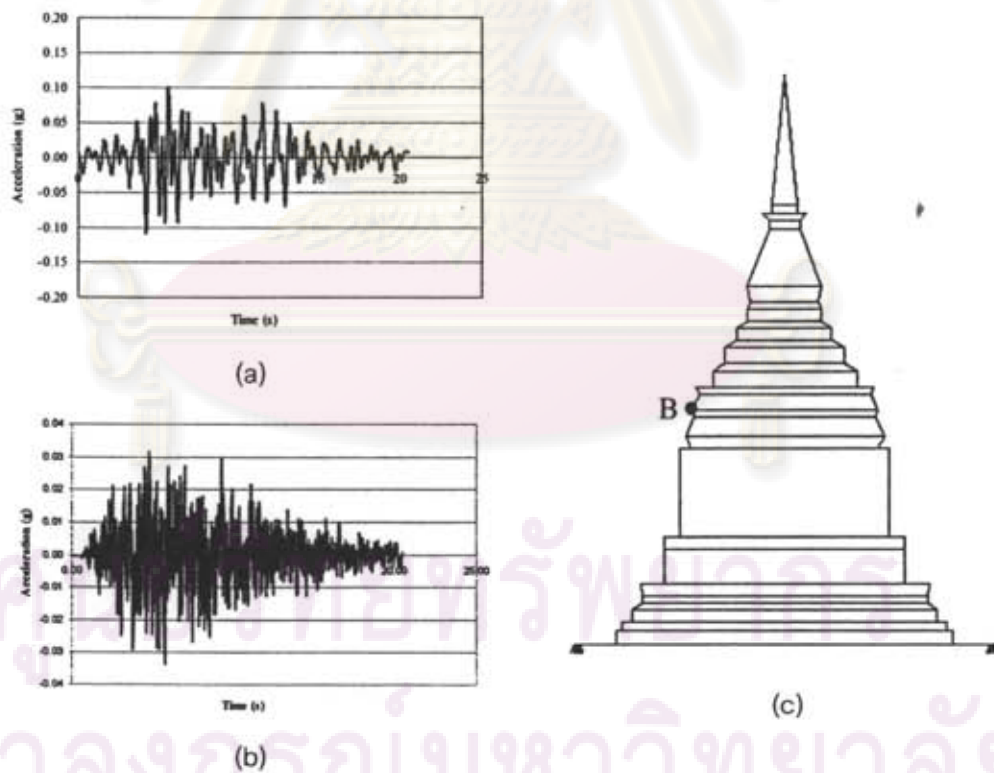


Figure 58 Acceleration-Time history for Maetha M7 at Point B

(a)

(b)

(c)
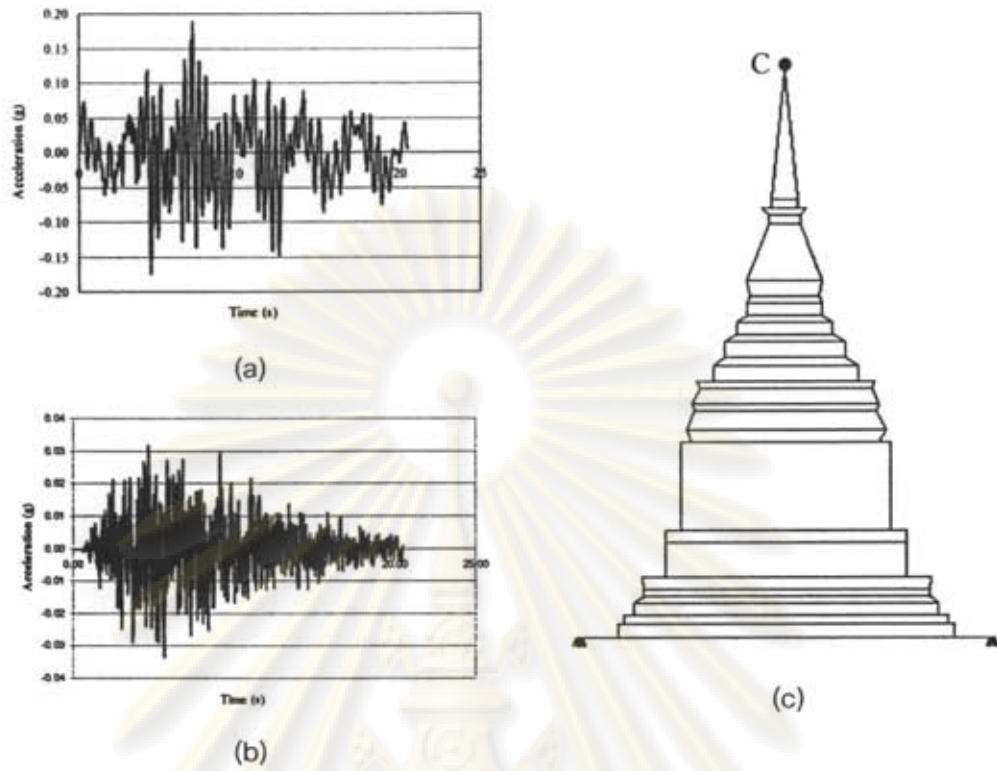
Figure 59 Acceleration-Time history for Maetha M7 at Point C
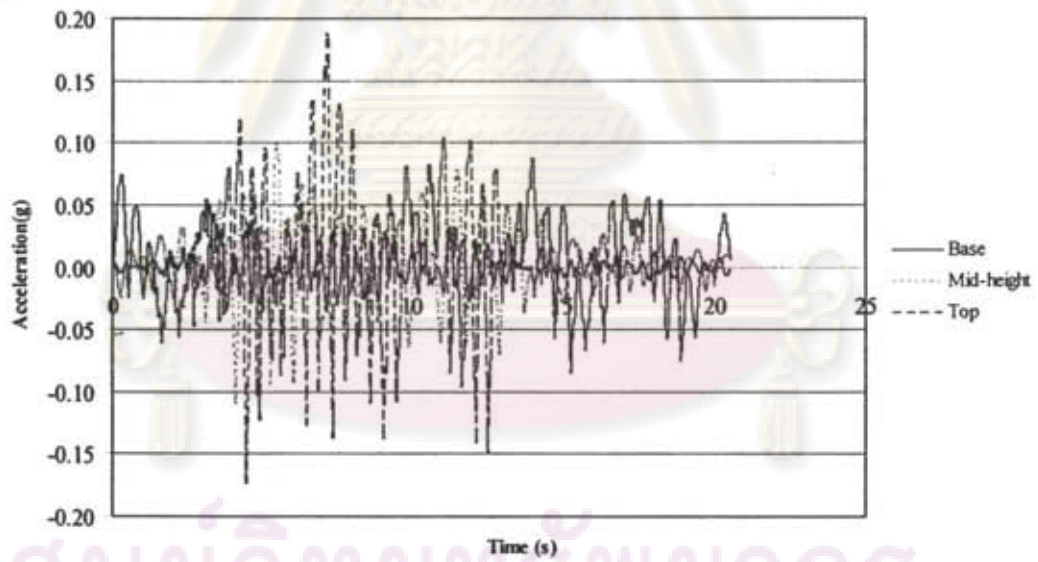


Figure 60 Comparison Acceleration-time history for Maetha M7 at each level

Table 14 peak acceleration time history analyses under earthquake ground motion along longitudinal direction of Maerim and Maetha fault

| Maximum Acceleration (g) | Maerim M5 | Maerim M6 | Maerim M7 | Maetha M5 | Maetha M6 | Maetha M7 |
|---|---|---|---|---|---|---|
| Acceleration (g), point A, Base, At time (s) | 0.05 | 0.044 | 0.066 | 0.02 | 0.027 | 0.037 |
| | 1.52 | 3.85 | 4.17 | 1.44 | 4.85 | 3.36 |
| Acceleration (g), Point B, Mid-Height, At time (s) | 0.09 | 0.119 | 0.185 | 0.04 | 0.073 | 0.109 |
| | 1.83 | 4.17 | 4.60 | 1.53 | 5.23 | 3.57 |
| Acceleration (g), Point C, Top, At time (s) | 0.17 | 0.209 | 0.345 | 0.07 | 0.122 | 0.189 |
| | 1.97 | 4.54 | 7.21 | 1.64 | 5.54 | 4.21 |

Normalize base acceleration with acceleration at any height of the structure in comparison with M5 to M7 of Maerim and Maetha are shown in Figure 61 and Figure 62.
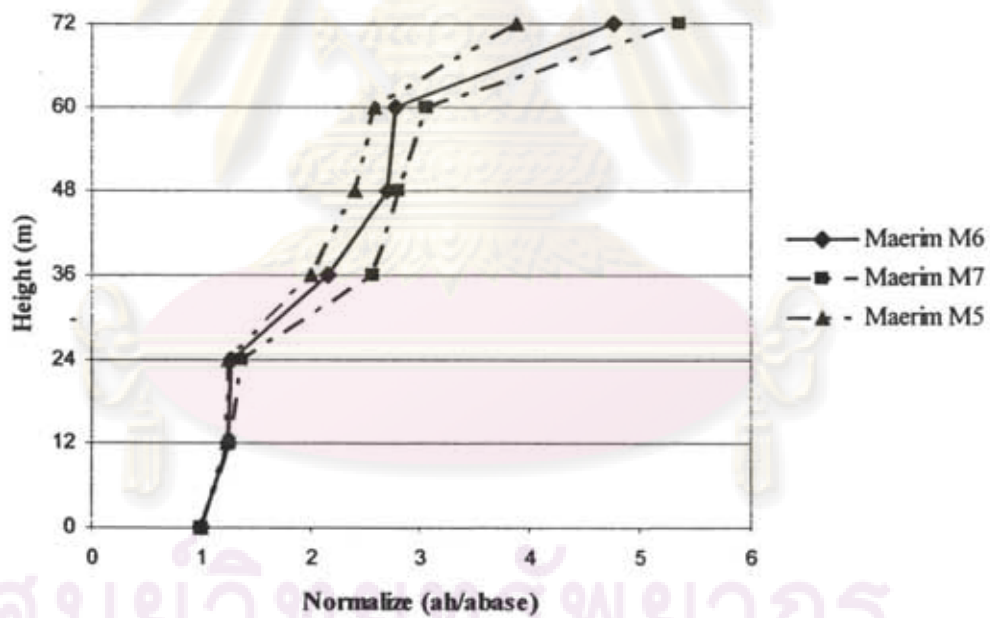


Figure 61 Normalize base acceleration with any height acceleration for Maerim
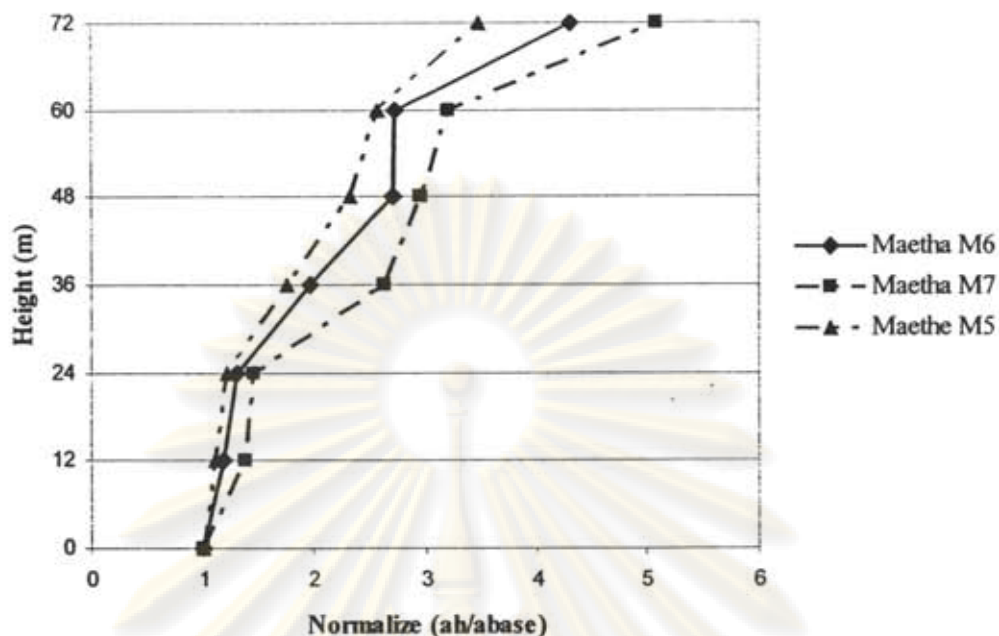
Figure 62 Normalize base acceleration with any height acceleration for Maetha

In this study, the interest has naturally focused primarily on the response of masonry structure during severe earthquakes. For masonry structures, the shear strength provided must exceed the actual flexural strength to ensure that shear deformation associated with large deterioration of stiffness and strength, which could lead to failure, cannot occur. During strong motion, the result in severe reduction in strength often occurred in conjunction with shear failure and tensile failure of masonry elements, damage or collapse were common. It became apparent that in many cases, seismic design to existing lateral force was inadequate to ensure that the structural strength provided was not exceeded by the demands of strong ground shaking. Numerous cases illustrate applications including recommended of reinforcement at failure zone is required.

From FLUSH program, maximum shear strain computed from its time history with maximum stress of each element as shown in Figure 63.

Figure 63 maximum shear strain computed from its time history

The stresses were plotted on the plane and Mohr's circle (Figure 64) is applied to locate the center of circle.
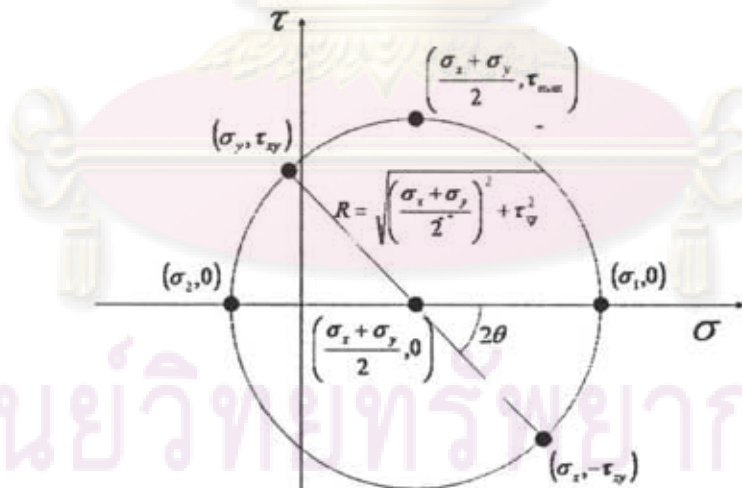


Figure 64 Mohr's circle

The maximum stress on principle plane of each element is shown in Figure 65 and those permissible stresses on each mode is compared with the stress on each element as shown in Figure 66.



Figure 65 Maximum stresses on principle plane of each element



Figure 66 Comparison of permissible stress with maximum stress for each element.

Failure zones of the structure from Maerim fault with magnitude M5 to M7 is shown in Figure 67 (a) through (c), whereas failure zones of the structure bfrom Maetha fault is with magnitude M5 to M7 is shown in Figure 68 (a) through (c). Because of symmetrical structure with anti-symmetry earthquake loading about vertical axis of symmetry, the results at the symmetrical nodes of the structure are found similar in magnitude and direction. Result of the response quantities are presented for left half part of the structure. As expected, the mode of failure in this structure is of tensile failures.

Although their tensile strength cannot be relied on as a primary source of resistance, masonry is eminently suited to carry compression stress. However, the maximum strains developed in compression are rather limited unless special precautions are taken. The primary aim of detailing of composite structures consisting of masonry and steel is to combine these materials in such a way as to produce ductile members, which are capable of meeting the deformation demands imposed by severe earthquake.
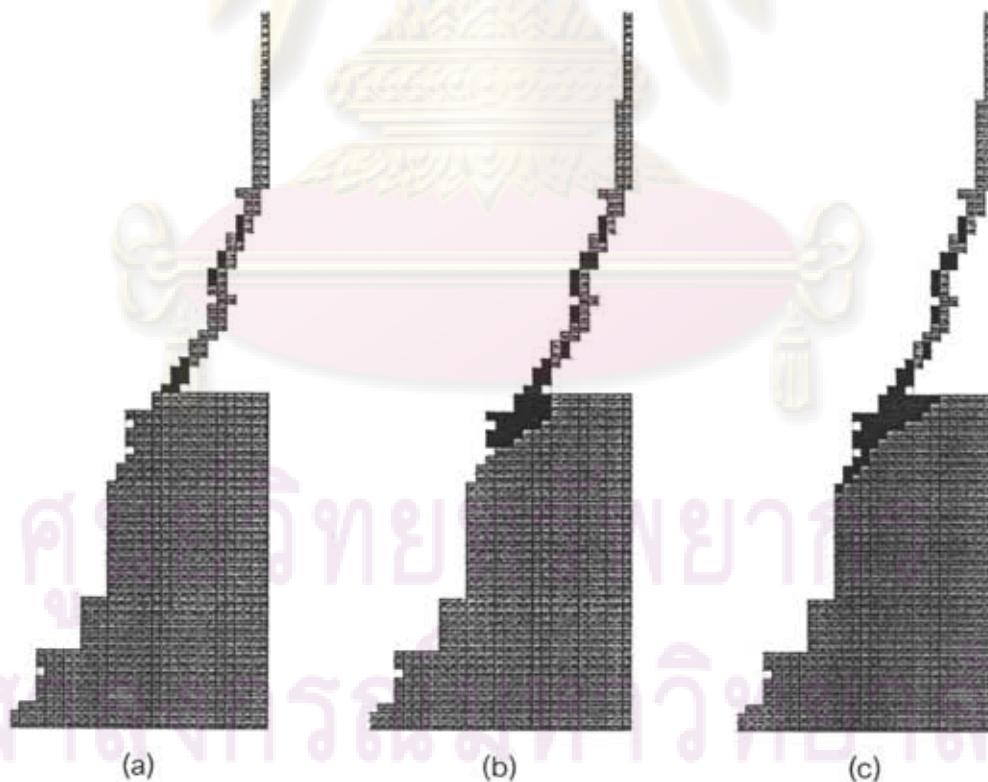


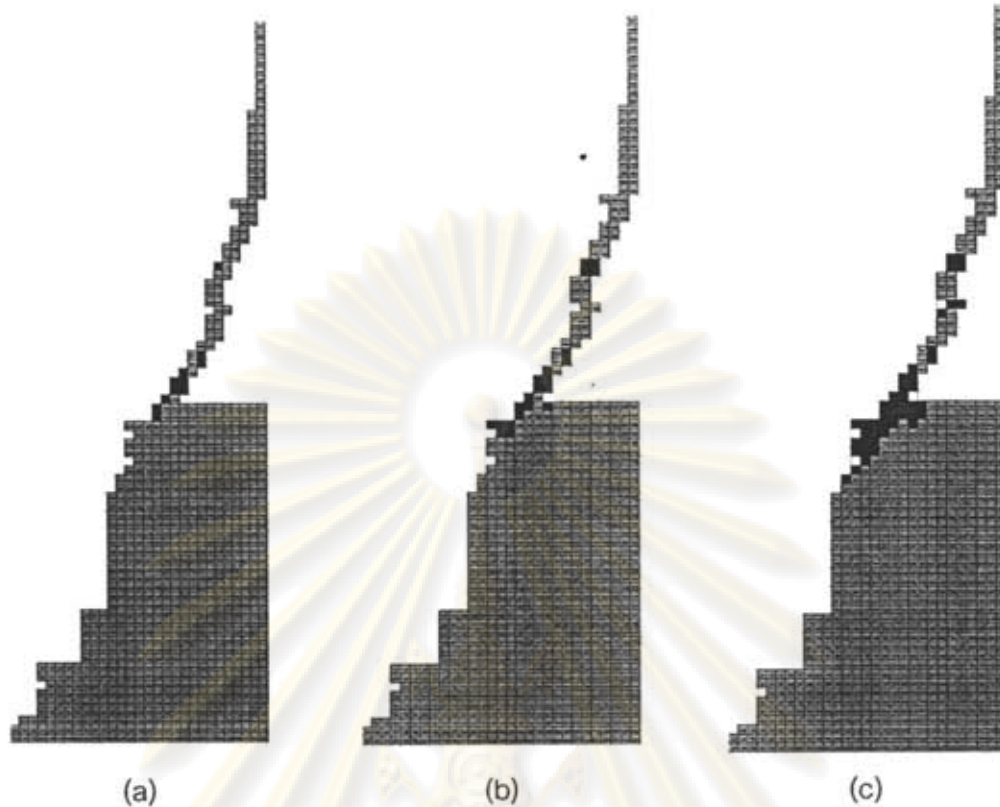Figure 67 Damage pattern of (a) Maerim M5 (b) Maerim M6 (c) Maerim M7

Figure 68 Damage pattern of (a) Maetha M5 (b) Maetha M6 (c) Maetha M7

Major deviations from a continuous variation with height of both stiffness and strength are likely to invite poor and often dangerous structure response. Reduced stiffness is likely to be accompanied by reduce strength, and this may result in the concentration of extremely large deformation. Constant or gradually reducing stiffness and strength with height reduce the concentration of plastic deformations during severe seismic events beyond the capacities of affected members.

If masonry structure is to be protected against damage during seismic excitation, the structure must have adequate strength to resist internal actions generated during the elastic dynamic response of the structure. Therefore, the appropriate technique for the evaluation of earthquake induced actions is an elastic analysis based on stiffness properties.

To minimize major damage and to ensure the survival of structure with moderate resistance with respect to lateral forces, structures must be capable of sustain a high proportion of their initial strength when an earthquake imposed large deformation. These

deformations may be well beyond elastic limit. It includes the ability to sustain large deformations and a capability to absorb energy by hysteretic behavior.

# CHAPTER VI

## CONCLUSION

It is generally accepted that soft soils modify the characteristics of strong ground motion transmitted to the surface from the underlying bedrock. Amplification of long-period components occurs, and generally peak accelerations in short-period range are reduced, as a result of strength limitations of the soil. It also appears that amplification of ground motion is dependent on the intensity of ground shaking.

As dynamic loading varies with time, the response of the structure also varies with time. A full dynamic analysis involves determining the responses at each of a series of time intervals throughout the motion induced by the loading. The primary purpose of all structures is to support gravity loads. However, structures may also be subjected to lateral forces due to wind or earthquakes. The taller structure, the more significant the effect of lateral forces will be. When subjected to lateral forces only, a structure will act as a vertical cantilever. The resulting total horizontal force and the overturning moment will be transmitted at the level of the foundation. During an earthquake, acceleration-induced inertia forces will be generated at each level.

The reinforcement of masonry is recommended into high tensile stress zone. The reinforcement of masonry depends for its effectiveness on transfer of stress from steel to masonry. In order to ensure adequate standard of retrofit and construction more supervision is required for reinforcement. The points in particular need watching such as reinforcement should be placed centrally or properly spaced from the masonry, reinforcement should be properly lapped, the grouting procedure should be properly carried out and the grout mix should conform to the specification

# REFERENCE

Ang, A. H., and Newmark, N. M. (1971). Development of a transmitting boundary for numerical wave motion calculations. Washington, DC: Defence Atomic Support Agency.

Bayo, E., and Wilson, E. L. (1983). Numerical techniques for the evaluation of soil-structure interaction effects in the time domain. Berkeley, CA: Earthquake Engineering Research Center, University of California.

Bayo, E.; and Wilson, E. L. Solution of the three dimensional soil-structure interaction problem in the time domain. Proceedings 8th World Conference on Earthquake Engineering (1984): 961-968.

Boore, D. M. 2003. Simulation of ground motion using the stochastic method. Pure Appl Geophys 160: 635-676.

Bull, J. W., ed. (1994). Soil-structure interaction: Numerical analysis and modeling. London: E & Fn Spon.

Bycroft, G. N. 1956. Forced vibrations of a rigid circular plate on a semi-infinite Elastic space and on an elastic stratum. Phil. Trans. Roy. Soc 248: 327-368.

Chan, W. – F., and Scawthorn, C., eds. (2003). Earthquake engineering handbook. Boca Raton: CRC Press.

Comgrit M, Chedsada A, Eakaphop T. (1997). Behavior of a masonry
structure without considering the soil-structure interaction during earthquake by
using STRAP Program. Chiang Mai: Department of Civil Engineering,
Faculty of Engineering, Chiang Mai University.

Danay, A. 1977. Vibrations of rigid foundations. The Arup Journal, London 12: 19-27.

De Luca, A., Giordano, A., and Mele, E. 2004. A simplified procedure for assessing
the seismic capacity of masonry arches. Engineering Structures 26: 1915-1929.

Dowrick, D. J. (1987). Earthquake resistant design: For engineers and architects.
2nd ed. Chichester: John Wiley & Sons.

Fenton, C. H., Charusiri, P., and Wood, S. H. 2003. Recent paleoseismic investigations
in Northern and Western Thailand. Annals of Geophysics 46: 957-981.

Gazetas, G., and Dobry, R. 1984. Simple radiation damping model for piles and footings.
Journal of Engineering Mechanics 110: 937-956.

Jaishi, B., Ren, W. –X., Zong, Z. –H., and Maskey, P. N. 2003. Dynamic and seismic
Performance of old multi-tiered temples in Nepal. Engineering Structures
25: 1827-1839.

Juhasova, E., Hurak, M., and Zembaty, Z. 2002. Assessment of seismic resistance of
masonry structures including boundary conditions. Soil Dynamics and
Earthquake Engineering 22: 1193-1197.

Kausel, E. (1974). Forced vibrations of circular foundations on layered media.
Department of Civil Engineering, Massachusetts Institute of Technology.

Kausel, E., and Roesset, J. M. 1975. Dynamic stiffness of circular foundations Journal Engineering Mechanics 101: 771-785.

Kramer, S. L. (1996). Geotechnical earthquake engineering. Upper Saddle River, NJ: Prentice-Hall.

Livaoglu, R., and Dogangun, A. 2007. Effect of foundation embedment on seismic behavior of elevated tanks considering fluid-structure-soil interaction. Soil Dynamics and Earthquake Engineering 27:855-863.

Luco, J. E. 1974. Impedance functions for a grid foundation on a layered medium. Nuclear Engineering and Design 31: 204-217.

Luco, J. E., and Westmann, R. A. 1971. Dynamic response of circular footings. Journal Engineering Mechanics 97: 1381-1395.

Lysmer, J., Udaka, T., Tsai, C. – F., and Seed H. B. (1975). Flush: A computer program for approximate 3-D analysis of soil-structure interaction problems. Berkeley, CA: College of Engineering, University of California.

Lysmer, J., and Waas, G. 1972. Shear waves in plane infinite structures. Journal Engineering Mechanics 98: 85-105.

Newmark, N. M., and Rosenblueth, E. (1971). Fundamentals of earthquake engineering. Englewood Cliffs, NJ: Prentice-Hall.

Paulay T., and Priestley M. J. N. (1992). Seismic design of reinforced concrete and masonry buildings. New York: John Wiley & Sons.

Penzien, J.; and Tseng, W. S. Seismic analysis of gravity platforms including
soil-structure interaction effects. Proceedings Offshore Technology Conference
2674 (1976).

Poulos, H. G., and Davis, E. H. (1974). Elastic solutions for soil and rock mechanics.
New York: John Wiley & Sons.

Seed, H. B., Lysmer, J., and Hwang, R. 1975. Soil-structure interaction analysis for
Seismic response. Journal Geotechnical Engineering 101: 439-457.

Seed, H. B., Tokimatsu, K., Harder, L., and Chung, R. (1984). The influence of SPT
procedures in soil liquefaction resistence evalutions. Berkeley, CA:
Earthquake Engineering Research Center, University of California.

Soneji, B. B., and Jangid, R. S. 2007. Influence of soil-structure interaction on the
response of seismically isolated cable-stayed bridge. Soil Dynamics and
Earthquake Engineering 28: 245-257.

Teachavorasinskun, S. (2006). Behavior of soil in dynamics. Bangkok: Chulalongkorn
University Press.

Vaish, A. K., and Chopra, A. K. 1974. Earthquake finite element analysis of structure
Foundations systems. Journal Engineering Mechanics 100: 1101-1116.

Veletsos, A. S., and Nair, V. V. D. 1975. Seismic interaction of structures on hysteretic
foundations. Journal Structural 101: 109-129.

Veletsos, A. S., and Verbic, B. 1973. Vibrations of viscoelastic foundations.
Earthquake Engineering and Structural Dynamics 2: 87-102.

Veletsos, A. S., and Wei, Y. T. 1971. Lateral and rocking vibrations of footings. Journal Soil Mechanics and Foundations 97: 1227-1248.

Watt, B. J.; Boaz, I. B.; Ruhl, J. A.; Shipley, S. A.; Dowrick, D. J.; and Ghose, A. Earthquake survivability of concrete platforms. Proceedings Offshore Technology Conference 3159 (1978): 957-973.

Werkle, H.; and Waas, G. Dynamic stiffness of foundations in inhomogeneous soils. Proceedings 8th European Conference on Earthquake Engineering (1986).
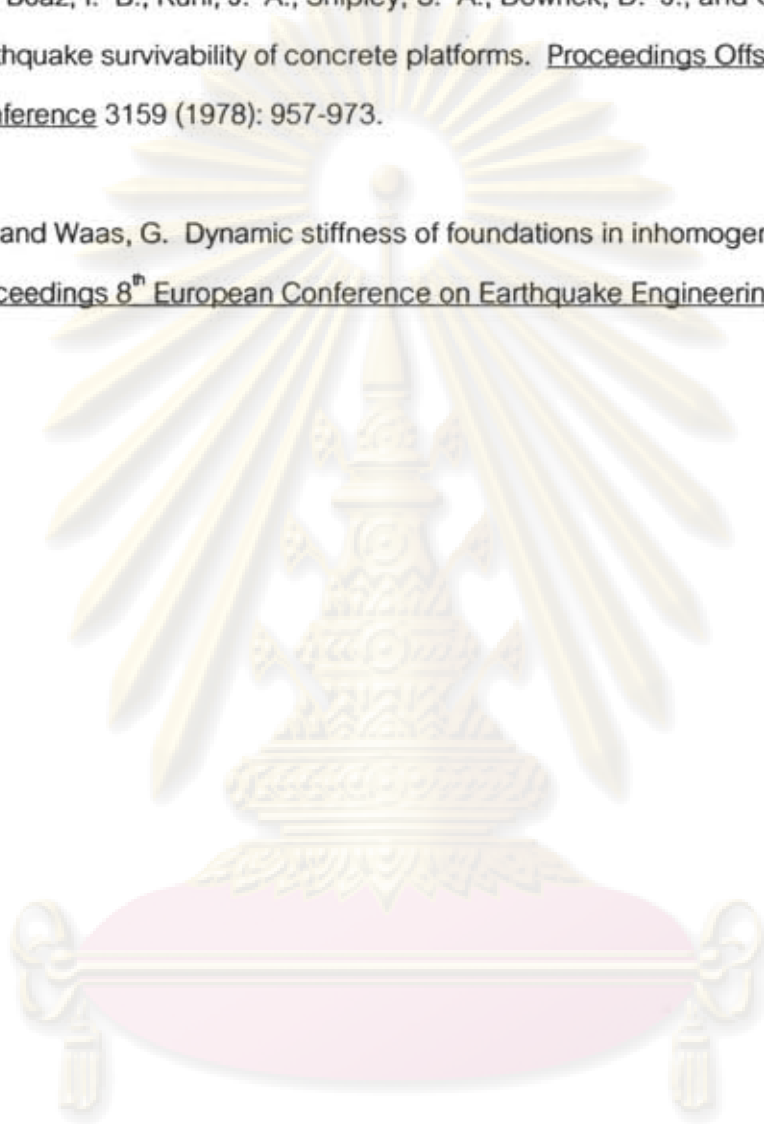
# BIOGRAPHY

### Ronnapa Photchana

I was born in Bangkok, Thailand, on September 11, 1975. I studied elementary at Udomsuksa School. Then, I continued studying secondary school at Bondindecha School. After graduated from secondary school, I continued my study Bachelor of Civil Engineering at Sirindhorn International Institute of Technology, Thammasat University. Then, I studied Master of Civil Engineering at Kasetsart University before studying Doctor of Philosophy Program in Civil Engineering at Chulalongkorn University.